

Extrapolated cross-validation for randomized ensembles

Jin-Hong Du[†] Pratik Patil[‡] Kathryn Roeder[†] Arun Kumar Kuchibhotla[†]

June 16, 2023

Abstract

Ensemble methods such as bagging and random forests are ubiquitous in various fields, from finance to genomics. Despite their prevalence, the question of the efficient tuning of ensemble parameters has received relatively little attention. This paper introduces a cross-validation method, ECV (Extrapolated Cross-Validation), for tuning the ensemble and subsample sizes in randomized ensembles. Our method builds on two primary ingredients: initial estimators for small ensemble sizes using out-of-bag errors and a novel risk extrapolation technique that leverages the structure of prediction risk decomposition. By establishing uniform consistency of our risk extrapolation technique over ensemble and subsample sizes, we show that ECV yields δ -optimal (with respect to the oracle-tuned risk) ensembles for squared prediction risk. Our theory accommodates general ensemble predictors, only requires mild moment assumptions, and allows for high-dimensional regimes where the feature dimension grows with the sample size. As a practical case study, we employ ECV to predict surface protein abundances from gene expressions in single-cell multiomics using random forests. In comparison to sample-split cross-validation and K -fold cross-validation, ECV achieves higher accuracy avoiding sample splitting. At the same time, its computational cost is considerably lower owing to the use of the risk extrapolation technique. Additional numerical results validate the finite-sample accuracy of ECV for several common ensemble predictors under a computational constraint on the maximum ensemble size.

Keywords: Ensemble learning; Bagging; Random forest; Risk extrapolation; Tuning and model selection; Distributed learning.

[†]Department of Statistics and Data Science, Carnegie Mellon University, Pittsburgh, PA 15213, USA.

[‡]Department of Statistics, University of California, Berkeley, CA 94720, USA.

1 Introduction

Bagging and its variants are popular randomized ensemble methods in statistics and machine learning. These methods combine multiple models, each fitted on different bootstrapped or subsampled datasets, to improve prediction accuracy and stability (Breiman, 1996; Pugh, 2002). The success of these methods lies in the careful tuning of key parameters: the *ensemble size* M and the *subsample size* k (Hastie et al., 2009). As M grows, the predictive accuracy improves while prediction variance decreases and stabilizes, a concept known as algorithmic convergence (Lopes, 2019; Lopes et al., 2020). However, in the era of big data (Politis, 2023), achieving a precise approximation in the infinity ensemble is challenging due to computational costs. Thus, it necessitates selecting a suitable M value to balance data-dependent considerations and budget constraints, without necessarily requiring it to scale with the sample size. Further, the number of subsampled/bootstrapped observations, k , used for each predictor plays a crucial role in ensemble learning. In low-dimensional scenarios, a smaller k can yield consistent results (Politis and Romano, 1994; Bickel et al., 1997); however, in high-dimensional scenarios, the prediction risk may not have a straightforward monotonic relationship with subsample size, exhibiting instead multiple descent behaviors (Patil et al., 2022b,a). Selecting the right subsample size is thus also of paramount importance for optimal predictive performance.

Several approaches have been proposed to tune either the ensemble size M or the subsample size k . For instance, to choose an ensemble size M , Lopes (2019) and Lopes et al. (2020) propose a heuristic variance stabilization strategy. This approach is driven by the convergence rate of variance or quantile estimates, using these metrics to gauge the point at which the ensemble’s performance stabilizes as M approaches infinity, thereby mitigating computational expense. On the other hand, determining the optimal subsample size k is somewhat more difficult. Towards this end, generic cross-validation (CV) methods are commonly used to tune k . The most basic CV method, sample-split CV, estimates the predictive risk of every predictor associated with a configuration of parameters using independent hold-out observations. However, when the overall sample size is small, it suffers from finite-sample effects because of sample splitting, especially in overparameterized scenarios, as observed in Patil et al. (2022a). Another commonly used cross-validation method, K -fold CV, repeatedly fits each candidate predictor on K different subsets of the data and uses their average to obtain the prediction risk estimates.

These methods have several drawbacks. In terms of turning over the ensemble size M , the specialized method proposed by Lopes (2019); Lopes et al. (2020) involves tracking the variability of the test errors as a function of M . Because this approach only tracks the *variance of the risk* rather than the *prediction risk* itself, the method does not provide any suboptimality guarantee compared to the optimal risk of an infinite ensemble (Patil et al., 2022a). Furthermore, the method does not provide any estimators for the prediction risks for any finite ensemble size M . In terms of tuning the subsample size k , the traditional CV methods can significantly suffer from finite-sample effects due to sample splitting, especially in high-dimensional scenarios (Wang et al., 2018; Rad and Maleki, 2020). Additionally, these generic CV methods must evaluate every possible ensemble and subsample size within an arbitrarily chosen search space, which often requires exploring larger ensemble sizes, thus demanding more computing power. Even then, it is not generally possible to certify any optimality outside this predefined search.

This paper seeks to address both the theoretical and practical challenges associated with ensemble parameter tuning. Specially, we aim to design a cross-validation method that can efficiently and consistently tune both the ensemble and subsample sizes. We focus primarily on randomized ensembles such as bagging and subbagging (Breiman, 1996; Bühlmann and Yu, 2002) and rely on out-of-bag observations to estimate the conditional prediction risk. Theoretically, we first demonstrate uniform consistency of extrapolated risk estimation for general predictors and data distributions in Section 2 (see Proposition 3.3). Based on the consistent risk estimates, a practical algorithm ECV (Extrapolated Cross-Validation) is designed in Section 4 (see Algorithm 1) for a broad set of base predictors to tune the ensemble and subsample sizes without sample splitting and without requiring an exhaustive search over all possible tuning parameters. Under a mild moment condition, we prove that the resulting tuned ensemble obtains the best possible ensemble risk over all ensemble and subsample sizes up to a specified tolerance of δ (see Theorem 4.1). This general result is then specialized for subbagged ridge predictors under proportional asymptotics (see Proposition 4.3). Through simulations and applications in Sections 5 and 6, we illustrate the utility of ECV under a computational budget for the maximum ensemble size.

Our proposed method, ECV, enjoys several advantages over the previously mentioned approaches. We highlight two of those next: (1) *Statistical consistency*: ECV is applicable for general ensemble predictors and is model-agnostic. It provides uniform consistency in estimating the actual prediction risk of ensembles over all ensemble and subsample sizes under mild conditions. It also notably outperforms standard cross-validation methods, especially in high-dimensional settings. (2) *Computational efficiency*: ECV operates by estimating the risk of ensembles with small ensemble sizes ($M = 1, 2$) using out-of-bag observations and then extrapolates the risk estimates to arbitrary ensemble sizes. Hence, in contrast to sample-split and K -fold CV, our method does not require fitting an ensemble for every ensemble size and explicitly estimating prediction risks for every ensemble size. As a result, the computational cost of ECV is significantly reduced. To showcase these points, we apply ECV on four single-cell datasets and aim to select a δ -optimal random forest in Section 6. Compared to other CV methods, ECV controls the out-of-sample error within $\delta = 0.05$ away from the optimal random forest with 50 trees while reducing the computational time substantially with larger sample sizes.

Paper outline. In Section 2, we describe the randomized ensemble learning procedure and the ensemble tuning problem setup. We also review related work on cross-validation and tuning and contrast our method to earlier work. In Section 3, we motivate our proposed method by building theoretical ingredients that constitute to our main algorithm. Section 4 presents our main algorithm along with its theoretical properties and discusses various practical considerations. In Section 5, we examine ECV’s generality and effectiveness with various types of predictors. Comparisons in Section 6 with sample-split and K -fold CV in the protein prediction problem highlight the statistical and computational benefits of ECV on low- and high-dimensional datasets. Section 7 concludes the paper with a brief discussion. The programs to replicate all our experiments can be obtained from <https://github.com/jaydu1/ECV>.

2 Randomized ensembles

We consider a supervised regression setup. Suppose $\mathcal{D}_n = \{(\mathbf{x}_1, y_1), \dots, (\mathbf{x}_n, y_n)\}$ represents a dataset with independent and identically distributed random vectors from $\mathbb{R}^p \times \mathbb{R}$. We will not assume any specific data model, only that the second moment of the response is finite, i.e., $\mathbb{E}[y_1^2] < \infty$. A prediction procedure $\hat{f}(\cdot; \cdot)$ is defined as a map from $\mathbb{R}^p \times \mathcal{P}(\mathcal{D}_n) \rightarrow \mathbb{R}$, where $\mathcal{P}(A)$, for any set A , represents the power set of A .

Randomized ensembles. Bagging (as in **bootstrap-aggregating**) traditionally refers to computing predictors multiple times based on bootstrapped data (Breiman, 1996), which can involve repeated observations. There is another version of bagging called subagging (as in **subsample-aggregating**) in Bühlmann and Yu (2002, Section 3.2) where we sample observations without replacement. Our method and analysis apply to both of these sampling strategies. Formally, these can be understood as simple random samples from a finite set, commonly used in survey sampling. Fix any $k \in [n]$, we define the indices $\{I_\ell\}_{\ell=1}^M$ to be M independent samples with replacement from \mathcal{I}_k (denoted by $\{I_\ell\}_{\ell=1}^M \stackrel{\text{SRS}}{\sim} \mathcal{I}_k$). Here \mathcal{I}_k is defined for bagging and subagging as

$$\mathcal{I}_k := \begin{cases} \{\{i_1, i_2, \dots, i_k\} : 1 \leq i_1 \leq i_2 \leq \dots \leq i_k \leq n\}, & \text{(bagging)} \\ \{\{i_1, i_2, \dots, i_k\} : 1 \leq i_1 < i_2 < \dots < i_k \leq n\}. & \text{(subagging)} \end{cases} \quad (2.1)$$

For bagging, \mathcal{I}_k represents the set of all possible independent draws from $[n]$ with replacement, and there are n^k many of them. For subagging, \mathcal{I}_k represents the set of all k subset choices from $[n]$, and there are $\binom{n}{k}$ many of them. Throughout the paper, we mainly focus on subagging but the results apply equally well to bagging. For this reason, we do not distinguish different choices of \mathcal{I}_k .

For any $I \in \mathcal{I}_k$, let \mathcal{D}_I and the corresponding subsampled predictor be defined as $\mathcal{D}_I = \{(\mathbf{x}_j, y_j) : j \in I\}$ and $\hat{f}(\mathbf{x}; \mathcal{D}_I) = \hat{f}(\mathbf{x}; \{(\mathbf{x}_j, y_j) : j \in I\})$. Then the randomized ensemble using either bootstrap or subsampling is defined as follows:

$$\tilde{f}_{M,k}(\mathbf{x}; \{\mathcal{D}_{I_\ell}\}_{\ell=1}^M) = \frac{1}{M} \sum_{\ell=1}^M \hat{f}(\mathbf{x}; \mathcal{D}_{I_\ell}) \quad \text{with } I_1, \dots, I_M \stackrel{\text{SRS}}{\sim} \mathcal{I}_k. \quad (2.2)$$

In the context where we want to highlight the size of bootstrap/subsample, k , we write $I_{k,1}, \dots, I_{k,M}$ instead of I_1, \dots, I_M .

Prediction risk. We are interested in the performance of our predictors (computed on \mathcal{D}_n) on future data from the same distribution P . We consider the behavior of the predictors conditional on \mathcal{D}_n and $\{I_\ell\}_{\ell=1}^M$. More specifically, for a predictor \hat{f} fitted on \mathcal{D}_n and its bagged predictor $\tilde{f}_{M,k}$ fitted on $\{\mathcal{D}_{I_\ell}\}_{\ell=1}^M$, with $\{I_\ell\}_{\ell=1}^M \stackrel{\text{SRS}}{\sim} \mathcal{I}_k$, the (subsample) conditional risks:

$$\begin{aligned} R(\hat{f}; \mathcal{D}_n) &:= \int (y - \hat{f}(\mathbf{x}; \mathcal{D}_n))^2 dP(\mathbf{x}, y), \\ R(\tilde{f}_{M,k}; \mathcal{D}_n, \{I_\ell\}_{\ell=1}^M) &:= \int \left(y - \tilde{f}_{M,k}(\mathbf{x}; \{\mathcal{D}_{I_\ell}\}_{\ell=1}^M) \right)^2 dP(\mathbf{x}, y). \end{aligned} \quad (2.3)$$

The two critical quantities for ensemble learning are the ensemble size M and the subsample size k . Different values of M trade-off model stability and computational burden. As M increases, the bagged predictors get more stabilized while requiring more time to fit them. On the other hand, the subsample size trades off the bias and variance of the bagged predictors. A smaller subsample size has considerable bias but may reduce the variance. For example, in the context of subbagging the minimum norm least square predictor with $M = \infty$, a properly chosen subsample size k strictly less than n can have higher variance reduction compared to the inflation of bias. This raises the question: how to efficiently choose both the ensemble size (M) and the subsample size (k) to minimize prediction risk (2.3) for general predictors. We address this question in the following sections. Before that, we review some related work on cross-validation and situate our work in the context of other related work.

Related work. Different cross-validation (CV) approaches have been proposed for parameter tuning and model selection (Allen, 1974; Stone, 1974, 1977; Geisser, 1975). We refer readers to Arlot and Celisse (2010); Zhang and Yang (2015) for a review of different CV variants used in practice. The simplest version of CV is the sample-split CV (Hastie et al., 2009), which holds out a specific portion of the data to evaluate models with different parameters. By repeated fitting of each candidate model on multiple subsets of the data, K -fold CV extends the idea of the sample splitting and reduces the estimation uncertainty. When K is small, the risk estimate may inherit more uncertainty; however, it can be computationally prohibitive when K is large. Asymptotic distributions of suitably normalized K -fold CV are obtained in Austern and Zhou (2020), under some stability conditions on the predictors.

In a high-dimensional regime where the number of variables is comparable to the number of observations, the commonly-used small values of K such as 5 or 10 suffer from bias issues in risk estimation (Rad and Maleki, 2020). Leave-one-out cross-validation (LOOCV), i.e., the case when $K = n$, alleviates the bias issues in risk estimation, whose theoretical properties have been analyzed in recent years by Kale et al. (2011); Kumar et al. (2013); Rad et al. (2020). However, LOOCV, in general, is computationally expensive to evaluate, and there has been some work on approximate LOOCV to address the computational issues (Wang et al., 2018; Stephenson and Broderick, 2020; Wilson et al., 2020; Rad and Maleki, 2020). Another line of research about CV is on statistical inference; see, for example, Wager et al. (2014); Lei (2020); Bates et al. (2021). Central limit theorems for CV error and a consistent estimator of its variance are derived in Bayle et al. (2020), which assumes certain stability assumptions, similar to Kumar et al. (2013); Celisse and Guedj (2016). Their results yield asymptotic confidence intervals for the prediction error and apply to K -fold CV and LOOCV. A naive application of these traditional CV methods for ensemble learning to tune M and k requires fitting the ensembles of arbitrary sizes M , leading to a higher computational cost.

In the context of bagging and subbagging, Liu et al. (2019) study parameters selection for bagging in sparse regression based on the derived error bound. The other line of research uses the out-of-bag (OOB) observations to estimate the prediction risk without sample splitting (Breiman, 2001). For example, Oshiro et al. (2012); Wager et al. (2014) study the algorithmic variance of ensemble regression functions at a fixed test point; Lopes (2019); Lopes et al. (2020) extrapolates the algorithmic variance and quantile of random forests for classification and regression problems, respectively. Their extrapolated estimators based on the heuristic scaling improve computation empirically, but the statistical property is still unclear theoretically. Politis (2023) discuss scalable subbagging estimator when the subsample size k and the ensemble size M

scale with the sample size n . The current paper differs in three crucial ways in relation to these works. First, these papers utilize the convergence rate of variance to extrapolate the fluctuations estimates, while ECV directly and consistently estimates the extrapolated risk (not just variance or quantiles). Second, we focus on tuning both the ensemble and the subsample sizes. The tuning of the subsample is crucial to minimizing the predictive risks. Further, our proposed method applies to a broader range of general predictors and asymptotic regimes covering both low-dimensional and high-dimensional scenarios.

3 Preliminaries and method motivation

In this section, we derive preliminary results that form the basis for our extrapolated cross-validation method in Section 4, which is based on OOB observations for tuning both the ensemble size M and the subsample size k . Below, we describe the four components.

(1) Risk decomposition. We will first fix k and consider tuning over $M \in \mathbb{N}$. Recall the conditional risk $R(\tilde{f}_{M,k}; \mathcal{D}_n, \{I_\ell\}_{\ell=1}^M)$ for a M -bagged predictor $\tilde{f}_{M,k}$ defined in (2.3). The following proposition shows that $R(\tilde{f}_{M,k}; \mathcal{D}_n, \{I_\ell\}_{\ell=1}^M)$ can be decomposed as a linear combination of the conditional risks of $M = 1$ and $M = 2$.

Proposition 3.1 (Squared conditional risk decomposition). *The conditional prediction risk defined in (2.3) for a bagged predictor $\tilde{f}_{M,k}$ decomposes into*

$$R(\tilde{f}_{M,k}; \mathcal{D}_n, \{I_\ell\}_{\ell=1}^M) = -\left(1 - \frac{2}{M}\right) a_{1,M} + 2\left(1 - \frac{1}{M}\right) a_{2,M}, \quad (3.1)$$

where

$$a_{1,M} = \frac{1}{M} \sum_{\ell=1}^M R(\tilde{f}_{1,k}; \mathcal{D}_n, \{I_\ell\}), \quad a_{2,M} = \frac{1}{M(M-1)} \sum_{\substack{\ell, m \in [M] \\ \ell \neq m}} R(\tilde{f}_{2,k}; \mathcal{D}_n, \{I_\ell, I_m\}).$$

Conditioning on \mathcal{D}_n , note that $a_{1,M}$ and $a_{2,M}$ are average and U -statistic based on i.i.d. elements $\{I_\ell\}_{\ell=1}^M$ sampled from \mathcal{I}_k . To explain our ECV method, suppose there exist constants $\mathfrak{R}_{1,k}$ and $\mathfrak{R}_{2,k}$ such that as $n \rightarrow \infty$, $a_{1,M} - \mathfrak{R}_{1,k}$ and $a_{2,M} - \mathfrak{R}_{2,k}$ converge almost surely to 0. Then Proposition 3.1 implies that the conditional prediction risk of $\tilde{f}_{M,k}$ can be approximated asymptotically by $-(1 - 2/M)\mathfrak{R}_{1,k} + 2(1 - 1/M)\mathfrak{R}_{2,k}$. This motivates the idea of ECV that a consistent estimation of $\mathfrak{R}_{1,k}$ and $\mathfrak{R}_{2,k}$ yields a consistent estimator for risk of $\tilde{f}_{M,k}$ for every $M \in \mathbb{N}$ and hence the name ‘‘extrapolated’’ cross-validation. The next step is to consistently estimate $\mathfrak{R}_{1,k}$ and $\mathfrak{R}_{2,k}$, for which we leverage the OOB observations.

(2) OOB component risk estimation. To consistently estimate the basic components in (3.1), we first define the OOB risk estimator for an arbitrary predictor \hat{f} fitted on \mathcal{D}_I based on the OOB test dataset $\mathcal{D}_{I^c} = \mathcal{D}_n \setminus \mathcal{D}_I$. One can simply consider the average of the squared loss (MEAN) on OOB observations in \mathcal{D}_{I^c} as a risk estimator. This choice, however, is not suitable for heavy-tailed data and hence we also consider a median-of-means (MOM) estimator:

$$\hat{R}(\hat{f}, \mathcal{D}_{I^c}) := \begin{cases} \frac{1}{|I^c|} \sum_{i \in I^c} (y_i - \hat{f}(\mathbf{x}_i))^2, & \text{if EST = MEAN,} \\ \text{median} \left\{ \frac{1}{|I^{(b)}|} \sum_{i \in I^{(b)}} (y_i - \hat{f}(\mathbf{x}_i))^2, b \in [B] \right\}, & \text{if EST = MOM,} \end{cases} \quad (3.2)$$

with $B = \lceil 8 \log(1/\eta) \rceil$ and $I^{(1)}, \dots, I^{(B)}$ being $B = \lceil 8 \log(1/\eta) \rceil$ random splits of I^c for some $\eta > 0$. The median-of-means estimator was developed for heavy-tailed mean estimation and is commonly used in robust statistics (Lugosi and Mendelson, 2019).

We will provide a condition to certify the pointwise consistency of risk estimates \widehat{R} under certain assumptions on the data distribution. Towards that end, for any non-negative loss function \mathcal{L} and a given test observation (\mathbf{x}_0, y_0) from P , define the conditional ψ_1 -Orlicz norm of $\mathcal{L}(y_0, \widehat{f}(\mathbf{x}_0))$ given \mathcal{D}_I as $\|\mathcal{L}(y_0, \widehat{f}(\mathbf{x}_0))\|_{\psi_1|\mathcal{D}_I} := \inf \{C > 0 : \mathbb{E}[\exp(\mathcal{L}(y_0, \widehat{f}(\mathbf{x}_0))C^{-1}) \mid \mathcal{D}_I] \leq 2\}$. Similarly, for $r \geq 1$, define the conditional L_r -norm as $\|\mathcal{L}(y_0, \widehat{f}(\mathbf{x}_0))\|_{L_r|\mathcal{D}_I} := (\mathbb{E}[\mathcal{L}(y_0, \widehat{f}(\mathbf{x}_0))^r \mid \mathcal{D}_I])^{1/r}$. See [Vershynin \(2018, Chapter 2\)](#) for more details. The following proposition provides the condition for consistency.

Proposition 3.2 (Consistent risk estimators). *Let $\widehat{f}(\cdot; \mathcal{D}_I)$ be any predictor trained on $\mathcal{D}_I \subset \mathcal{D}_n$, and EST = MEAN or EST = MOM with $\eta = n^{-A}$, where $A \in (0, \infty)$ is a fixed constant. Define $\widehat{\sigma}_I := \|(y_0 - \widehat{f}(\mathbf{x}_0; \mathcal{D}_I))^2\|_{\psi_1|\mathcal{D}_I}$. Then the following holds: If $\widehat{\sigma}_I/\sqrt{|I^c|/\log n} \xrightarrow{P} 0$, then $|\widehat{R}(\widehat{f}, \mathcal{D}_{I^c}) - R(\widehat{f}; \mathcal{D}_I)| \xrightarrow{P} 0$. The conclusion remains true for EST = MOM even when the conditional ψ_1 -Orlicz norm in the definition of $\widehat{\sigma}_I$ is replaced with $\|\cdot\|_{L_2|\mathcal{D}_I}$.*

Recall from (2.2) that $\widetilde{f}_{1,k}$ is computed from one dataset \mathcal{D}_{I_1} and $\widetilde{f}_{2,k}$ is computed from two datasets \mathcal{D}_{I_1} and \mathcal{D}_{I_2} or equivalently that $\widetilde{f}_{2,k}$ is computed on $\mathcal{D}_{I_1 \cup I_2}$. Hence, Proposition 3.2 can be applied to $\widetilde{f}_{1,k}$ with $I = I_1$ and to $\widetilde{f}_{2,k}$ with $I = I_1 \cup I_2$ to consistently estimate the conditional prediction risks of $\widetilde{f}_{1,k}$ and $\widetilde{f}_{2,k}$. To obtain consistency, we need to ensure that the assumption on $\widehat{\sigma}_I$ becomes reasonable if $|I^c|/\log n \rightarrow \infty$ as $n \rightarrow \infty$. For subbagging predictors $\widetilde{f}_{1,k}$ and $\widetilde{f}_{2,k}$, we have $|I_1^c| = n(1 - k/n)$ and by Lemma S3.2, $|(I_1 \cup I_2)^c| \approx n(1 - k/n)^2$, asymptotically. On the other hand, for bagging predictors $\widetilde{f}_{1,k}$ and $\widetilde{f}_{2,k}$, we have $|I_1^c| \approx n \exp(-k/n)$ and $|(I_1 \cup I_2)^c| \approx n \exp(-2k/n)$, asymptotically. Hence, collectively, assuming $k \leq n(1 - 1/\log n)$ implies that $|I^c| \gtrsim n/\log^2 n$, asymptotically.

Under the assumption $k \leq n(1 - 1/\log n)$, the risks of $\widetilde{f}_{1,k}$ and $\widetilde{f}_{2,k}$ computed on \mathcal{D}_{I_1} and $\mathcal{D}_{I_1 \cup I_2}$, respectively, can be estimated consistently. Further, if we assume that the limiting conditional risks ($\mathfrak{R}_{1,k}$ and $\mathfrak{R}_{2,k}$) of $\widetilde{f}_{1,k}$ and $\widetilde{f}_{2,k}$ do not depend on the particular subsets I_1, I_2 , then $\widehat{R}(\widetilde{f}_{1,k}, \mathcal{D}_{I_1^c})$ and $\widehat{R}(\widetilde{f}_{2,k}, \mathcal{D}_{(I_1 \cup I_2)^c})$ consistently estimate $\mathfrak{R}_{1,k}$ and $\mathfrak{R}_{2,k}$, as $n \rightarrow \infty$. Note, however, that because the limiting conditional risks do not depend on specific subsets I_1, I_2 , we can reduce the variance in our estimates of $\mathfrak{R}_{1,k}$ and $\mathfrak{R}_{2,k}$ by averaging the estimated risks over several subsets I_ℓ 's. This observation suggests the following definition of the out-of-bag risk estimates for $M = 1, 2$ as:

$$\widehat{R}_{M,k}^{\text{ECV}} := \begin{cases} \frac{1}{M_0} \sum_{\ell=1}^{M_0} \widehat{R}(\widetilde{f}_{1,k}(\cdot; \mathcal{D}_n, \{I_\ell\}), \mathcal{D}_{I_\ell^c}), & M = 1, \\ \frac{1}{M_0(M_0 - 1)} \sum_{\substack{\ell, m \in [M_0] \\ \ell \neq m}} \widehat{R}(\widetilde{f}_{2,k}(\cdot; \mathcal{D}_n, \{I_\ell, I_m\}), \mathcal{D}_{(I_\ell \cup I_m)^c}), & M = 2, \end{cases} \quad (3.3)$$

where I_1, \dots, I_{M_0} are i.i.d. samples from \mathcal{I}_k and $M_0 \geq 2$ is a pre-specified natural number. Increasing M_0 improves estimates but also increases computation.

(3) Risk extrapolation. As hinted above, the risk decomposition (3.1), along with the component risk estimation (3.3), suggests a natural estimator for the M -ensemble risk:

$$\widehat{R}_{M,k}^{\text{ECV}} := - \left(1 - \frac{2}{M}\right) \widehat{R}_{1,k}^{\text{ECV}} + 2 \left(1 - \frac{1}{M}\right) \widehat{R}_{2,k}^{\text{ECV}}, \quad M > 2. \quad (3.4)$$

We call this ‘‘extrapolated’’ risk estimation according to (3.1) because the M -ensemble risk is *extrapolated* from the risks of the 1- and 2-ensemble risks. For a fixed k , if the prediction risk of $M = 1, 2$ can be consistently estimated, then the extrapolated risk estimates (3.4) are also consistent over all $M \in \mathbb{N}$. The next step is then to tune both M and k .

(4) Uniform risk consistency over (M, k) . To tune k , we define $\mathcal{K}_n \subset [n]$ to be a grid of subsample sizes. In practice, we would like \mathcal{K}_n to cover the full range of n asymptotically (in the sense that $\mathcal{K}_n/n \approx [0, 1]$), and one simple choice is to set $\mathcal{K}_n = \{0, k_0, 2k_0, \dots, \lfloor n(1 - (\log n)^{-1})/k_0 \rfloor k_0\}$ where the minimum subsample size is $k_0 = \lfloor n^\nu \rfloor$ for some $\nu \in (0, 1)$. Here we adopt the convention that when $k = 0$, the

ensemble predictor reduces to the *null predictor* that always outputs zero. To facilitate our theoretical results for general predictors, we make the following two assumptions. The results are stated asymptotically as n tends to infinity, where we view both k and p as sequences $\{k_n\}$ and $\{p_n\}$ indexed by n , and assume k diverges with the sample size n (except when $k \equiv 0$), but the feature dimension p may or may not diverge.

Assumption 1 (Variance proxy). For $k \in \mathcal{K}_n$, assume for all $\{I_1, I_2\} \stackrel{\text{SRS}}{\sim} \mathcal{I}_k$, as $n \rightarrow \infty$,

$$\frac{\log n}{\sqrt{n}} \widehat{\sigma}_{I_1} \xrightarrow{\mathbb{P}} 0, \quad \text{and} \quad \frac{(\log n)^{3/2}}{\sqrt{n}} \widehat{\sigma}_{I_1 \cup I_2} \xrightarrow{\mathbb{P}} 0,$$

where the variance proxies $\widehat{\sigma}_{I_1}$ and $\widehat{\sigma}_{I_1 \cup I_2}$ are defined in Proposition 3.2.

Assumption 2 (Convergence of asymptotic risks). For $k \in \mathcal{K}_n$, assume for all $\{I_1, I_2\} \stackrel{\text{SRS}}{\sim} \mathcal{I}_k$ and for $M = 1, 2$, there exist constants $\epsilon \in (0, 1)$, $C_0 > 0$, $\eta_0 \geq 1$, $\gamma_{M,n} = o(n^{-\epsilon})$, and $\mathfrak{R}_{M,k} \geq 0$, such that the following holds:

$$\limsup_{n \rightarrow \infty} \sup_{\eta \geq \eta_0} \eta^{1/\epsilon} \mathbb{P}(\gamma_{M,n}^{-1} |R_{M,k}(\widetilde{f}_{M,k}; \mathcal{D}_n, \{I_\ell\}_{\ell=1}^M) - \mathfrak{R}_{M,k}| \leq \eta) \leq C_0. \quad (3.5)$$

Assumption 1 is used to show consistent risk estimation with $M = 1, 2$ in Appendix S1.2. Assumption 2 formalizes the assumption that the limiting values of the conditional risks $R_{M,k}(\widetilde{f}_{M,k}; \mathcal{D}_n, \{I_\ell\}_{\ell=1}^M)$ do not depend on $\{I_\ell\}_{\ell=1}^M$. This assumption also requires certain rate and tail assumptions, which are used to provide rate of consistency of our ECV procedure. In Assumption 2, $\gamma_{M,n}$ for $M = 1, 2$ represent the lower bounds of the rates of convergence over $k \in \mathcal{K}_n$, which are typically on a scale of $n^{-\alpha}$ for some constant $\alpha > 0$. The weak moment norm condition (3.5) is a tail assumption (Rio, 2017; Guo and Peterson, 2019), which ensures that the expected differences between the risks and the limits also converge to zero in certain rates. Under classical linear models with fixed- X design and Gaussian noises, the risk of linear predictor concentrates around its mean and satisfies (3.5); see, e.g., Bellec (2018, Lemma 3.1). Another sufficient condition for (3.5) is the strong moment condition that $\mathbb{E}[\gamma_{M,n}^{-1/\epsilon} |R_{M,k}(\widetilde{f}_{M,k}; \mathcal{D}_n, \{I_\ell\}_{\ell=1}^M) - \mathfrak{R}_{M,k}|^{1/\epsilon}]$ is bounded.

From now on, we shall write $R_{M,k} = R(\widetilde{f}_{M,k}; \mathcal{D}_n, \{I_\ell\}_{\ell=1}^M)$ to indicate the dependency only on M and k and to simplify the notations in what follows. In Section 4.1, we will consider an example of ridge regression where the convergence is under the proportional asymptotics (i.e., both the *data aspect ratio* p/n and the *subsample aspect ratio* p/k converge to fixed constants), where Assumptions 1-2 are satisfied. The following lemma guarantees uniform consistency over both M and k .

Proposition 3.3 (Uniform consistency of risk extrapolation). *Suppose Assumptions 1 and 2 hold for all $k \in \mathcal{K}_n$, then the ECV estimates defined in (3.4) satisfy that*

$$\sup_{M \in \mathbb{N}, k \in \mathcal{K}_n} \left| \widehat{R}_{M,k}^{\text{ECV}} - R_{M,k} \right| = \mathcal{O}_p(\zeta_n),$$

where $\zeta_n = \widehat{\sigma}_n \log n / n^{1/2} + n^\epsilon (\gamma_{1,n} + \gamma_{2,n})$ and $\widehat{\sigma}_n = \max_{m, \ell \in [M_0], k \in \mathcal{K}_n} \widehat{\sigma}_{I_{k,\ell} \cup I_{k,m}}$.

Proposition 3.3 states that the convergence rate of the extrapolated error depends on three factors: the cross-validation error and the rate for $M = 1, 2$. The rate of the out-of-bag CV error is governed by $\mathcal{O}_p(\widehat{\sigma}_n \log n / n^{1/2})$ where $\widehat{\sigma}_n$ is a variance proxy of the risk estimates, while the convergence rate of asymptotic risks for $M = 1, 2$ typically depends on the predictor.

Proposition 3.3 completes the study of the consistency of ECV risk estimator for ensemble predictors. Now, we proceed to discuss the use of ECV risk estimator for tuning an ensemble predictor by choosing the “best” ensemble size M and the subsample/bootstrapped size k .

4 Main proposal: Extrapolated cross-validation

Based on the previous discussion in Section 3, we present the proposed cross-validation algorithm for tuning the ensemble parameters without sample splitting in Algorithm 1. The proposed algorithm’s theoretical guarantees and practical considerations are presented in Section 4.1 and Section 4.2, respectively.

Algorithm 1 Tuning of ensemble and subsample sizes without sample splitting

Input: A dataset $\mathcal{D}_n = \{(\mathbf{x}_i, y_i) \in \mathbb{R}^p \times \mathbb{R} : 1 \leq i \leq n\}$, a base prediction procedure \widehat{f} , a real number $\nu \in (0, 1)$ (subsample size unit parameter), a natural number $M_0 \geq 2$ (ensemble size for risk estimation), a centering procedure $\text{EST} \in \{\text{MEAN}, \text{MOM}\}$, a real number A used to compute η when $\text{EST} = \text{MOM}$, and optimality tolerance parameter δ .

- 1: **Subsample sizes grid construction:** Let $k_0 = \lfloor n^\nu \rfloor$ and $\mathcal{K}_n = \{0, k_0, 2k_0, \dots, \lfloor n(1 - 1/\log n)/k_0 \rfloor k_0\}$.
- 2: **Building ensembles:** For each $k \in \mathcal{K}_n$, define $\widetilde{f}_{M_0, k}$ trained on \mathcal{D}_n as: $\widetilde{f}_{M_0, k}(\cdot) = \widetilde{f}_{M_0}(\cdot; \{\mathcal{D}_{I_{k, \ell}}\}_{\ell=1}^{M_0})$ the ensemble (2.2) with M_0 base predictors, where $I_{k, 1}, \dots, I_{k, M_0} \stackrel{\text{SRS}}{\sim} \mathcal{I}_k$.
- 3: **Risk estimation for $M = 1, 2$:** For each $k \in \mathcal{K}_n$, estimate the conditional prediction risk on OOB observations of $\widetilde{f}_{M_0, k}$ with $\widehat{R}_{M, k}^{\text{ECV}}$ defined in (3.3) for $M = 1, 2$.
- 4: **Risk extrapolation for $M > 2$:** Extrapolate the estimations $\widehat{R}_{M, k}^{\text{ECV}}$ using (3.4).
- 5: **Tuning subsample size:** Set $\widehat{k} \in \mathcal{K}_n$ to be the subsample size that minimizes the extrapolated estimates using

$$\widehat{k} \in \underset{k \in \mathcal{K}_n}{\operatorname{argmin}} 2\widehat{R}_{2, k}^{\text{ECV}} - \widehat{R}_{1, k}^{\text{ECV}}.$$

- 6: **Tuning ensemble size:** Choose $\widehat{M} \in \mathbb{N}$ for the δ -optimal risk with a plug-in estimator:

$$\widehat{M} = \left\lceil \frac{2}{\max\{\delta, n^{-1/2}\}} (\widehat{R}_{1, \widehat{k}}^{\text{ECV}} - \widehat{R}_{2, \widehat{k}}^{\text{ECV}}) \right\rceil.$$

- 7: **Fitting:** If $M > M_0$, fit a M -bagged predictor $\widetilde{f}_{\widehat{M}, \widehat{k}} := \widetilde{f}_{\widehat{M}, \widehat{k}}(\cdot; \{\mathcal{D}_{I_{\widehat{k}, \ell}}\}_{\ell=1}^{\widehat{M}})$.

Output: Return the ECV-tuned predictor $\widetilde{f}_{\widehat{M}, \widehat{k}}$, and the risk estimators $\widehat{R}_{M, k}^{\text{ECV}}$ for all M, k .

The procedure requires a dataset \mathcal{D}_n of n observations, a base prediction procedure \widehat{f} , a natural number M_0 for risk estimation, and some other parameters. It first constructs the grid of subsample sizes \mathcal{K}_n and fits only M_0 base predictors accordingly. Then, the prediction risk for M -bagged predictors can be estimated based on the OOB observations through (3.3) and (3.4). Observe that the optimal risk of (3.4) for any k is obtained at $\widehat{R}_{\infty, k}^{\text{ECV}} = 2\widehat{R}_{2, k}^{\text{ECV}} - \widehat{R}_{1, k}^{\text{ECV}}$ when $M = \infty$. Thus, to tune k , it suffices to perform a grid search to minimize $\widehat{R}_{\infty, k}^{\text{ECV}}$ over $k \in \mathcal{K}_n$. Though we know from the previous results (Lopes, 2019; Patil et al., 2022a) that the optimal ensemble size happens to be infinity, calculating it is prohibitive in practice. Thus, we pick the smallest \widehat{M} such that $\widehat{R}_{\widehat{M}, \widehat{k}}^{\text{ECV}}$ is close to $\widehat{R}_{\infty, \widehat{k}}^{\text{ECV}}$ within δ error, where δ is the suboptimality parameter. Finally, Algorithm 1 returns a \widehat{M} -bagged predictor using subsample size \widehat{k} . Note that Algorithm 1 naturally applies to other randomized ensemble methods, such as random forests, when keeping other hyperparameters fixed.

As a byproduct, Algorithm 1 also gives the ECV risk estimates $\widehat{R}_{M, k}^{\text{ECV}}$ for all $M \in \mathbb{N}$ and $k \in \mathcal{K}_n$. This risk profile in (M, k) is helpful for users to investigate whether the given base predictor \widehat{f} well fits the dataset \mathcal{D}_n or not. For instance, one can estimate the amount of improvement due to subsampling for a given ensemble size M , the one due to aggregation for a given subsample size k , and compare them with the estimated risk of the null predictor. This gives rise to practical considerations presented later in Section 4.2.

4.1 Theoretical guarantees

The following theorem states that Algorithm 1 yields an ensemble predictor whose risk is at most δ away from the best ensemble predictor. Further, it provides an estimator of the risk of the selected ensemble predictor.

Theorem 4.1 (Optimality of OOB estimate and ECV-tuned risk). *Under the assumed conditions in Proposition 3.3, for any $\delta > 0$, the OOB estimate and the ECV-tuned risk output by Algorithm 1 satisfy the*

following properties respectively

$$\left| \widehat{R}_{\widehat{M}, \widehat{k}}^{\text{ECV}} - R_{\widehat{M}, \widehat{k}} \right| = \mathcal{O}_p(\zeta_n), \quad \left| R_{\widehat{M}, \widehat{k}} - \inf_{M \in \mathbb{N}, k \in \mathcal{K}_n} R_{M, k} \right| = \delta + \mathcal{O}_p(\zeta_n), \quad (4.1)$$

where ζ_n is the quantity defined in Proposition 3.3.

Theorem 4.1 implies that the OOB estimate is close to the true risk because of the uniform consistency from Proposition 3.3. Furthermore, the ECV-tuned ensemble parameters \widehat{M} and \widehat{k} produce a bagged predictor with a risk δ -close to the optimal predictor. The optimality is model-agnostic because it does not directly depend on the feature and response models.

Remark 4.2 (From additive to multiplicative optimality). Theorem 4.1 provides a guarantee of additive optimality for tuned predictor returned by Algorithm 1, while it is also useful to consider the multiplicative optimality. Towards that end, with the choice of \widehat{k} in Step 5 of Algorithm 1 and change the choice of \widehat{M} in Step 6 to

$$\widehat{M} = \left\lceil \frac{2}{\max\{\delta, n^{-1/2}\}} \frac{\widehat{R}_{1, \widehat{k}}^{\text{ECV}} - \widehat{R}_{2, \widehat{k}}^{\text{ECV}}}{2\widehat{R}_{2, \widehat{k}}^{\text{ECV}} - \widehat{R}_{1, \widehat{k}}^{\text{ECV}}} \right\rceil,$$

then, under the assumption that the irreducible risk $\int (y - \mathbb{E}[y | \mathbf{x}])^2 dP(\mathbf{x}, y)$ is strictly positive, Proposition S2.1 guarantees

$$R_{\widehat{M}, \widehat{k}} = (1 + \delta) \inf_{M \in \mathbb{N}, k \in \mathcal{K}_n} R_{M, k} (1 + \mathcal{O}_p(\zeta_n)). \quad (4.2)$$

Compared to (4.1), the optimality upper bound in the right hand side of (4.2) depends on the scale of the optimal prediction risk.

Application of Theorem 4.1 to a specific data model and a base predictor requires verification of Assumptions 1 and 2. As an illustration, we verify all the conditions for Theorem 4.1 hold for ridge predictors, as shown below.

Example: bagged ridge predictors. Consider a dataset $\mathcal{D}_n = \{(\mathbf{x}_1, y_1), \dots, (\mathbf{x}_n, y_n)\}$ consisting of random vectors in $\mathbb{R}^p \times \mathbb{R}$. Let $\mathbf{X} \in \mathbb{R}^{n \times p}$ denote the corresponding feature matrix whose j -th row contains \mathbf{x}_j^\top , and let $\mathbf{y} \in \mathbb{R}^n$ denote the corresponding response vector whose j -th entry contains y_j . Recall that the ridge estimator with regularization parameter $\lambda > 0$ fitted on \mathcal{D}_I for $I \subseteq [n]$ is defined as

$$\widehat{\boldsymbol{\beta}}_\lambda(\mathcal{D}_I) = \underset{\boldsymbol{\beta} \in \mathbb{R}^p}{\operatorname{argmin}} \frac{1}{|I|} \sum_{j \in I} (y_j - \mathbf{x}_j^\top \boldsymbol{\beta})^2 + \lambda \|\boldsymbol{\beta}\|_2^2. \quad (4.3)$$

The associated ridge base predictor and the subagged predictor are given by $\widehat{f}_\lambda(\mathbf{x}; \mathcal{D}_I) = \mathbf{x}^\top \widehat{\boldsymbol{\beta}}_\lambda(\mathcal{D}_I)$ and $\widetilde{f}_{M, k}(\mathbf{x}; \mathcal{D}_n) = \mathbf{x}^\top \widetilde{\boldsymbol{\beta}}_{\lambda, M}(\{\mathcal{D}_{I_\ell}\}_{\ell=1}^M)$, where $I \in \mathcal{I}_k$ and $\{I_\ell\}_{\ell=1}^M \stackrel{\text{SRS}}{\sim} \mathcal{I}_k$. Under standard assumptions in the overparameterized learning literature, the following proposition shows that the ridge predictors satisfy all the required conditions of Theorem 4.1.

Proposition 4.3 (ECV for ridge predictors). *Suppose Assumptions A1-A2 in Appendix S2.3 hold. Then, the ridge predictors with $\lambda > 0$ using subagging satisfy Assumption 1 with $\widehat{\sigma}_n = \mathcal{O}_p(1)$ for MOM and Assumption 2 for any $\psi \in (0, 1)$ such that $p/n \rightarrow \phi \in [\psi, \psi^{-1}]$ and $p/k \rightarrow \phi_s \in [\phi, \psi^{-1}]$ as $k, n, p \rightarrow \infty$. Consequently, the conclusions in Theorem 4.1 hold.*

In Proposition 4.3, Assumptions A1-A2 assume a linear model $y_i = \mathbf{x}_i^\top \boldsymbol{\beta}_0 + \epsilon_i$ for observation i , where the feature vector is generated by $\mathbf{x}_i = \boldsymbol{\Sigma}^{\frac{1}{2}} \mathbf{z}_i$, $\boldsymbol{\Sigma}$ is the covariance matrix and \mathbf{z}_i contains i.i.d. entries with zero mean and unit variance. We make mild assumptions about such a data-generating process: (1) the noise ϵ_i and the entries of \mathbf{z}_i have bounded moments, and (2) the covariance and signal-weighted spectrums converge weakly to some distributions as $n, p \rightarrow \infty$. These assumptions are commonly used in the literature

of overparameterized learning; see, for example, [Hastie et al. \(2022\)](#); [Patil et al. \(2022b,a\)](#). We remark that Proposition 4.3 verifies Theorem 4.1 for EST =MOM, but one can also verify for EST =MEAN under slightly different assumptions; see Appendix S2.3 for more details.

It is worth mentioning that Assumption 2 only requires the conditional risks for the ridge ensemble with $M = 1, 2$ converge to their respective conditional (on \mathcal{D}_n) limits, while the limiting forms of them are not required. In this regard, Assumptions A1-A2 can be further relaxed with some efforts, but we do not pursue fine-tuning of assumptions as our intent is only to illustrate the end-to-end applicability of Theorem 4.1.

4.2 Practical considerations

Algorithm 1 estimates the ensemble parameters \hat{k} and \hat{M} to derive a δ -optimal bagged predictor. Here, we discuss some considerations when the proposed method is used in practice.

- (1) **Maximum ensemble size:** Algorithm 1 determines \hat{k} and \hat{M} by minimizing the estimated risk (3.4) with the infinite ensemble. However, it may still be computationally infeasible if \hat{M} is too large. In such cases, based on the extrapolated risk estimation in line 4 of Algorithm 1, we can also derive the δ -optimal bagged predictor whose ensemble size is no more than a pre-specified number M_{\max} , which we call the restricted oracle. That is, we choose subsample and ensemble size to restrict the computational cost.

$$\hat{k} \in \operatorname{argmin}_{k \in \mathcal{K}_n} \widehat{R}_{M_{\max}, k}^{\text{ECV}}, \quad \text{and} \quad \widehat{M} = \left\lceil 2(\delta + \widehat{R}_{M_{\max}, \hat{k}}^{\text{ECV}} - \widehat{R}_{\infty, \hat{k}}^{\text{ECV}})^{-1} (\widehat{R}_{1, \hat{k}}^{\text{ECV}} - \widehat{R}_{2, \hat{k}}^{\text{ECV}}) \right\rceil.$$

On the other hand, it also controls the suboptimality to the oracle:

$$\underbrace{R_{\widehat{M}, \widehat{k}} - \min_{k \in \mathcal{K}_n} R_{\infty, k}}_{\text{suboptimality to the oracle}} = \underbrace{R_{\widehat{M}, \widehat{k}} - \min_{k \in \mathcal{K}_n} R_{M_{\max}, k}}_{\text{suboptimality to the restricted oracle}} + \underbrace{\min_{k \in \mathcal{K}_n} R_{M_{\max}, k} - \min_{k \in \mathcal{K}_n} R_{\infty, k}}_{\text{unavoidable budget error}}.$$

When $\delta = 0$, the suboptimality to the restricted oracle vanishes, and the tuned ensemble simply tracks the optimal M_{\max} -ensemble.

- (2) **To bag or not to bag:** The benefit of ensemble learning may be slight in some cases. For instance, when the number of samples is much larger than the feature dimensions and the signal-noise ratio is large, ensemble learning can only provide minor improvements over the non-ensemble predictor. Suppose that $\widehat{R}_0^{\text{ECV}}$ is the estimated risk of the null predictor, $\min_{k \in \mathcal{K}_n} \widehat{R}_{1, k}^{\text{ECV}}$ is the optimal estimated risk due to subsampling when $M = 1$, and $\min_{k \in \mathcal{K}_n} \widehat{R}_{M_{\max}, k}^{\text{ECV}}$ is the optimal ECV estimate with maximum ensemble size M_{\max} . Let $\zeta > 0$ be a user-specified improvement factor that encodes the desired excess risk improvement in a multiplicative sense. Then we can decide to bag if either the null risk is smaller in the sense that $\widehat{R}_0^{\text{ECV}} < \min_{k \in \mathcal{K}_n} \widehat{R}_{1, k}^{\text{ECV}}$, or the improvement due to ensemble exceeds ζ times the improvement due to subsampling:

$$\underbrace{\min_{k \in \mathcal{K}_n} \widehat{R}_{1, k}^{\text{ECV}} - \min_{k \in \mathcal{K}_n} \widehat{R}_{M_{\max}, k}^{\text{ECV}}}_{\text{improvement due to ensemble}} > \underbrace{\zeta}_{\text{improvement factor}} \times \underbrace{\widehat{R}_0^{\text{ECV}} - \min_{k \in \mathcal{K}_n} \widehat{R}_{1, k}^{\text{ECV}}}_{\text{improvement due to subsampling}}. \quad (4.4)$$

- (3) **Absolute versus normalized tolerances:** The choice of the tolerance threshold δ is for controlling the absolute suboptimality, but the scale of the prediction risk may be different for different predictors and datasets. One can normalize the estimated risk by the null predictor's estimated risk to make the tolerance threshold comparable across different predictors and datasets, or tune based on the multiplicative guarantee (4.2).

5 Numerical illustrations

In this section, we evaluate Algorithm 1 on synthetic data. In Section 5.1, we inspect whether the extrapolated risk estimates $\widehat{R}_{M, k}^{\text{ECV}}$ serve as reasonable proxies for the actual out-of-sample prediction errors for various base predictors on uncorrelated features. In Section 5.2, we further evaluate the risk minimization performance with tuned ensemble parameters $(\widehat{M}, \widehat{k})$. Finally, in Section 5.3, we consider tuning M for random forests on correlated features.

5.1 Validating extrapolated risk estimates

In this simulation, we examine whether our risk extrapolation strategy provides reasonable risk estimates for specific values of ensemble size M and subsample size k based on only the risk estimates for $M = 1$ and $M = 2$. We evaluate six base predictors (as summarized in Figure 1) on data generated from a linear regression model:

$$y_i = \mathbf{x}_i^\top \boldsymbol{\beta}_0 + \epsilon_i, \quad \mathbf{x}_i \sim \mathcal{N}(0, \mathbf{I}_p), \quad \boldsymbol{\beta}_0 \sim \mathcal{N}(0, p^{-1} \rho^2 \mathbf{I}_p), \quad \epsilon_i \sim \mathcal{N}(0, \sigma^2), \quad (\text{M-ISO-LI})$$

with $n = 1,000$ samples and feature dimensions $p = \lfloor n\phi \rfloor$. Here the data aspect ratio ϕ varies from 0.1 (low-dimensional regime) to 1.1 (high-dimensional regime). The response for logistic predictors is binarized by thresholding at the median of y_i 's. For each ϕ , we evaluate on the subsample sizes $k = \lfloor p/\phi_s \rfloor$ with ϕ_s varying from ϕ to 10. The *null risk*, the risk of the null predictor that always outputs zero, can also be estimated at each ϕ . For ridgeless and lassoless predictors, we exclude k whose estimated risk is more than ten times the estimated null risk following the practical consideration for exploding risks in Section 4.2.

The ECV estimated values and the corresponding prediction errors for different ensemble size M and subsample aspect ratio ϕ_s are then summarized in Figure 2 for bagged and subbagged ridge predictors and in Appendix S5.1 for other predictors. As k decreases, the ensemble with subsample size k behaves more like the null predictor. As a result, the risk curves approach a particular value as the subsample aspect ratio p/k increases. From Figure 2, we observe a good match between the ECV estimates and the theoretical prediction risk curves obtained from Patil et al. (2022a). The theoretical risks may be unavailable for other predictors in Appendix S5.1. However, their ECV estimates and out-of-sample prediction errors still have a good match. This suggests that Theorem 4.1 potentially applies to various types of predictors. Comparing the results of bagging and subbagging, the risk estimates are very similar, especially in the over-parameterized regime when $p > n$. Thus, we will only present the results using subbagging for illustration purposes and leave those using bagging in Appendix S5.

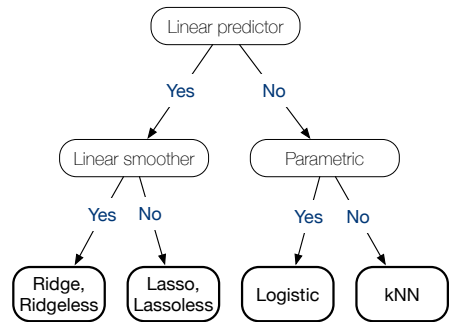


Figure 1: Predictors for regression tasks evaluated in Sections 5.1 and 5.2.

5.2 Tuning ensemble and subsample sizes

Next, we examine the performance of ECV on predictive risk minimization. More specifically, we apply Algorithm 1 to tune an ensemble that is close to the optimal M_{\max} -ensemble up to additive error δ , where the maximum ensemble size M_{\max} is 50 and optimality threshold δ ranges from 0.01 to 1. With the same predictors and data used in Section 5.1, their out-of-sample mean squared errors are evaluated on the same test set. The results are summarized in Figures 3 and S24 where the former uses the rule (4.4) with $\zeta = 5$.

In Figure 3, the blue dashed lines represent the non-ensemble prediction risk, and the darkest purple lines represent the prediction risk of optimal 50-ensemble predictors using a finer grid. Note that the former may be non-monotonic in the data aspect ratio ϕ , but the latter is increasing in ϕ . The finite-sample prediction errors of the ECV-tuned predictor are shown as solid points. As we can see, when δ decreases, the prediction errors of ECV get closer to those of the optimal 50-ensemble predictor. The slight discrepancy between the ECV-tuned risks with the least δ and the oracle risks comes from the fact that a coarser grid \mathcal{K}_n is used for ECV tuning. Overall, these results suggest that the ECV choices of the ensemble parameters (\hat{M}, \hat{k}) give risks close to the oracle choices for various predictors within the desired optimality threshold δ in finite samples.

5.3 Tuning ensemble sizes of random forests

When the original sample size n is too small, tuning both the subsample size k and the ensemble size M may be unnecessary. In such cases, tuning the ensemble size M (in the sense that how large M is sufficient to have good performance) is a more substantial and practical consideration. The paper by Lopes (2019) has a way to do this for random forests on the classification tasks by estimating the conditional variance of the

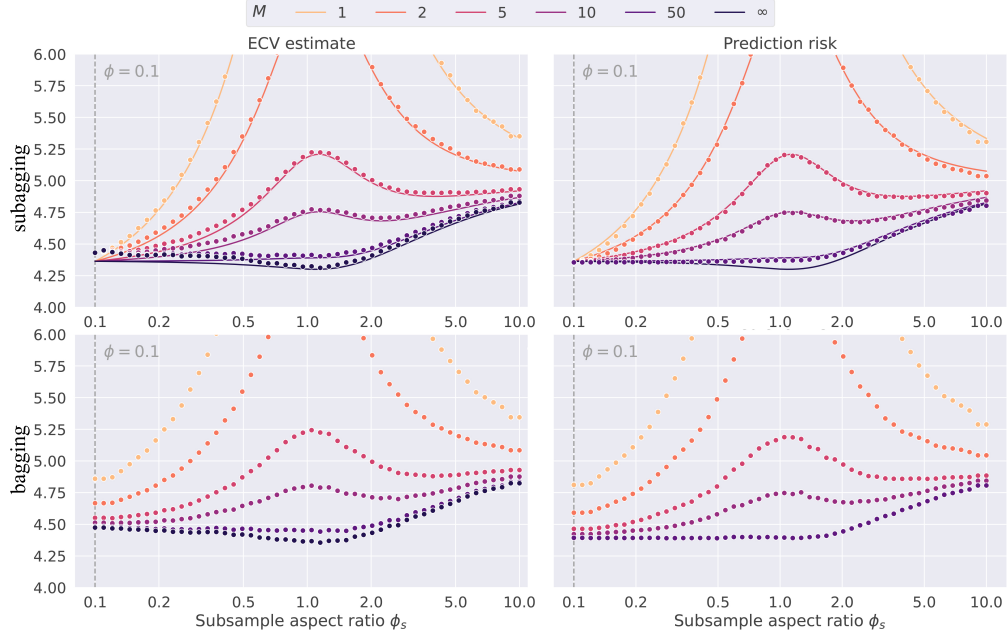


Figure 2: Finite-sample ECV estimate (left panel) and prediction risk (right panel) for ridge predictors ($\lambda = 0.1$) using subbagging (first row) and bagging (second row), under model (M-ISO-LI) when $\rho^2 = 1$ and $\sigma^2 = 0.01$ for varying subsample size $k = \lfloor p/\phi_s \rfloor$, and the ensemble size M . For each value of M , the points denote the finite-sample ECV cross-validation estimates (3.4) computed on $M_0 = 10$ base predictors or the out-of-sample prediction error computed on $n_{te} = 1,000$ samples, averaged over 100 dataset repetitions, with $n = 1,000$ and $p = \lfloor n\phi \rfloor$, and $\phi = 0.1$ ($p < n$).

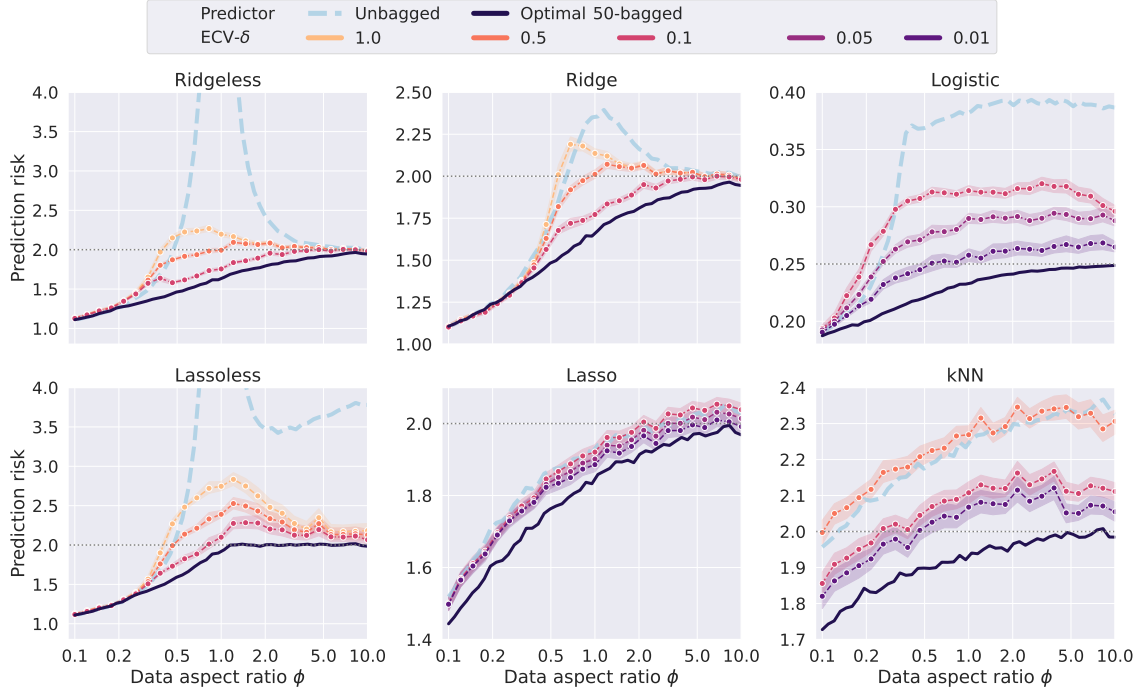


Figure 3: Prediction risk for different subbagged predictors by ECV, under model (M-ISO-LI) with $\sigma^2 = 1$, $\rho^2 = 1$, $M_0 = 10$, and $M_{\max} = 50$, for varying ϕ and tolerance threshold δ . An ensemble is fitted when (4.4) is satisfied with $\zeta = 5$. The null risks and the risks for the non-ensemble predictors are marked as gray dotted lines and blue dashed lines, respectively. The points denote finite-sample risks averaged over 100 dataset repetitions, and the shaded regions denote the values within one standard deviation, with $n = 1,000$ and $p = \lfloor n\phi \rfloor$.

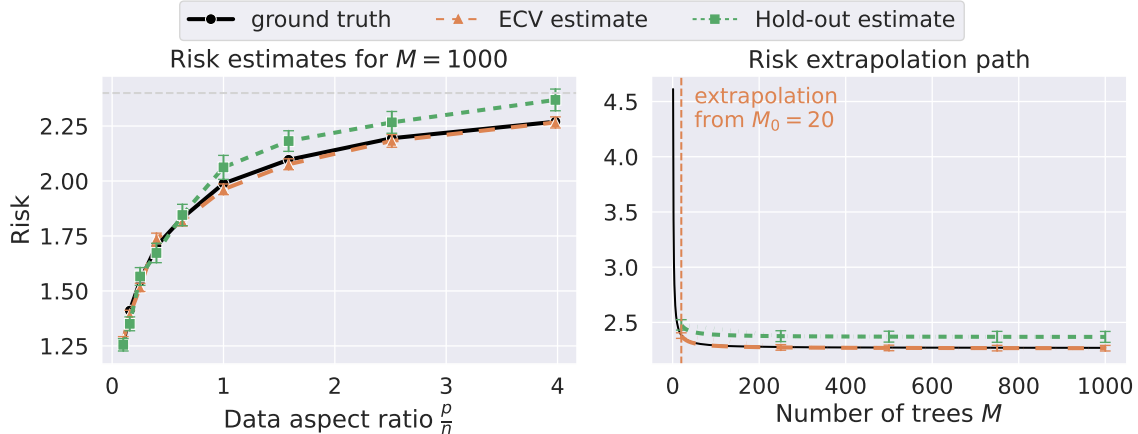


Figure 4: Risk extrapolation for random forest based on the first $M_0 = 20$ trees, under model (M-AR1-LI) with $\sigma^2 = 1$ and $\rho_{\text{ar1}} = 0.75$. The left panel shows the risk estimates for random forests with $M = 1,000$ trees and varying data aspect ratios, and the gray dash line $y = 2.4$ denotes the risk of the null predictor; the right panel shows the full risk extrapolation path in M when $p/n = 4$. The error bar denotes one standard deviation across 100 simulations, and the ground truth is estimated from 5,000 test observations, with $n = 1,000$.

test error via the bootstrap. Still, ECV is designed for regression tasks, which is more general and accurate because the estimation of the prediction risk is our direct target. In this experiment, we apply Algorithm 1 to tune only the ensemble size of random forests.

Since the most crucial advantage of the random forest model is its flexibility to incorporate highly correlated variables while avoiding multi-collinearity issues, we consider a non-isotropic AR(1) covariate model where adjacent features have the highest correlations. Let Σ_{ar1} be the covariance matrix of an autoregressive process of order 1 (AR(1)), where $(\Sigma_{\text{ar1}})_{ij} = \rho_{\text{ar1}}^{|i-j|}$ for some parameter $\rho_{\text{ar1}} \in (0, 1)$. Then the data model is defined as

$$y_i = \mathbf{x}_i^\top \boldsymbol{\beta}_0 + \epsilon_i, \quad \mathbf{x}_i \sim \mathcal{N}(0, \Sigma_{\text{ar1}}), \quad \boldsymbol{\beta}_0 = \frac{1}{5} \sum_{j=1}^5 \mathbf{w}_{(j)}, \quad \epsilon_i \sim \mathcal{N}(0, \sigma^2), \quad (\text{M-AR1-LI})$$

where $\mathbf{w}_{(j)}$ is the eigenvector of Σ_{ar1} associated with the top j th eigenvalue $r_{(j)}$. From Grenander and Szegö (1958, pp. 69-70), the top j -th eigenvalue can be written as $r_{(j)} = (1 - \rho_{\text{ar1}}^2) / (1 - 2\rho_{\text{ar1}} \cos \theta_{jp} + \rho_{\text{ar1}}^2)$ for some $\theta_{jp} \in ((j-1)\pi/(p+1), j\pi/(p+1))$.

For a given dataset, we examine two strategies to estimate the conditional prediction risks. The first utilizes the OOB observations according to Algorithm 1, while the other uses a hold-out subset to estimate the risks. Similar to Lopes (2019), $\lfloor n/6 \rfloor$ observations are randomly selected as the evaluation set for the hold-out estimates. As suggested by Hastie et al. (2009), each decision tree uses $\lfloor p/3 \rfloor$ randomly selected features with a minimum node size of 5 as the default without pruning. To build each tree, we fix the subsample size $k = n(1 - 1/\log n)$ observations for subsampling. The results are shown in Figure 4, where the standard deviation of the estimates are also visualized as error bars.

As shown in the left panel of Figure 4, in the underparameterized regime when $n > p$, we observe that ECV and hold-out estimates have similar performance. Both of them are close to the out-of-sample errors in this case. However, in the overparameterized regime when $n < p$, the hold-out estimates suffer from biases due to sample splitting. On the contrary, the ECV estimates are still accurate and have smaller variability compared to the hold-out estimates. In the right panel of Figure 4, we see that ECV estimates provide a valid extrapolation path from $M = 20$ to $M = 1000$ in the ultrahigh-dimensional scenarios.

6 Applications to single-cell multiomics

In genomics, cell surface proteins act as primary targets for therapeutic intervention and universal indicators of particular cellular processes. More importantly, immunophenotyping of cell surface proteins has become

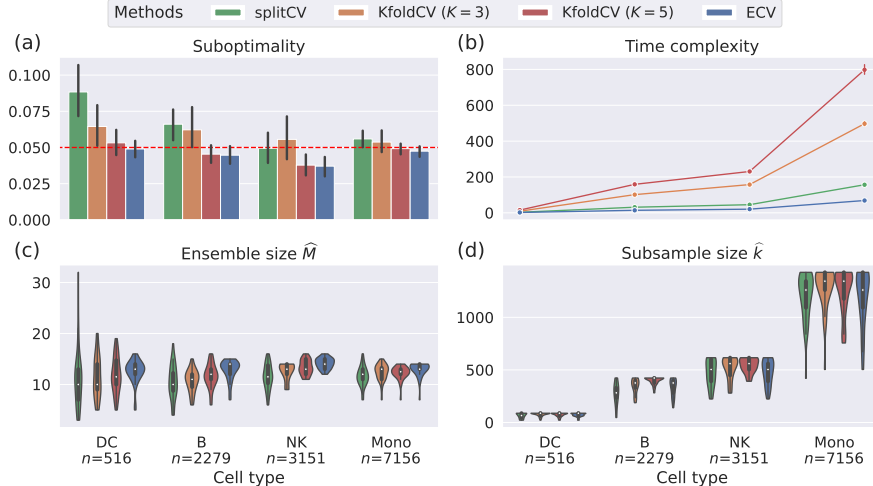


Figure 5: Overview of different cross-validation methods for predicting 50 surface proteins based on 5,000 genes in the single-cell sequencing multiomic datasets from Hao et al. (2021) using random forests. The proposed ECV method estimates the prediction risks based on 20 trees. Each panel shows cell types DC, B, NK, and Mono. (a) The out-of-sample suboptimality compared to the optimal random forest with 50 trees. The CV predictors are tuned to be δ -optimal in terms of normalized mean squared errors. The error bars show the standard deviations over 50 proteins, and the red dashed line indicates the optimality threshold $\delta = 0.05$. (b) The time consumption in seconds. (c) The cross-validated ensemble size \widehat{M} . (d) The cross-validated subsample size \widehat{k} .

an essential tool in hematopoiesis, immunology, and cancer research over the past 30 years (Hao et al., 2021). However, most single-cell investigations only quantify the transcriptome without cell-matched measures of related surface proteins due to technical limitations and financial constraints (Zhou et al., 2020; Du et al., 2022). The specific cell types and differentially abundant surface proteins are determined after thoroughly analyzing the transcriptome. This has led researchers to investigate how to reliably predict protein abundances in individual cells using their gene expressions. Specifically, Heckmann et al. (2018); Li et al. (2019); Xu et al. (2021) have illustrated the effectiveness of ensemble methods on the protein prediction problem. Yet, in practice, because of the lack of theoretical results and pragmatic guidelines, the ensemble and subsample sizes are generally determined by ad hoc criteria.

In this section, we apply the proposed method to real datasets in single-cell multi-omics (Hao et al., 2021) (see Appendix S5.4 for more details). Based on these real-world datasets, we compare three different cross-validation methods for tuning both the ensemble size and the subsample size of random forests: (1) K -fold CV: the K -fold CV ($K = 5$); (2) sample-split CV: sample-split or holdout CV (the ratio of training to validation observations is 5:1); and (3) ECV: the proposed extrapolated CV. The grid of subsample sizes \mathcal{K}_n is generated according to Algorithm 1. To ensure all the CV methods are comparable and fairly evaluated, we evaluate the three CV methods on the same grid $[M_{\max}] \times \mathcal{K}_n$ for $M_{\max} = 50$. Decision trees are used as the base predictors to predict the abundance of each protein based on the gene expressions of subsampled cells. After the tuning parameters $(\widehat{M}, \widehat{k})$ are obtained, we refit the ensemble on the entire training set and evaluate it on the test set. For each method, the M_{\max} base predictors are fitted once so that the training costs are almost the same for all three. The computational complexity of the three methods is discussed in Appendix S4. Our target is to select a δ -optimal random forest so that its prediction risk is no more than $\delta = 0.05$ away from the best random forest with 50 trees.

Because different proteins may have different variances, we measure the overall protein prediction accuracy by the normalized mean squared error (NMSE), which is the ratio of the mean squared error to the empirical variance on the test set. As shown in Figure 5, because sample splitting introduces additional randomness and the reduced sample size has significant finite sample effects, we see from Figure 5(a) that sample-split CV does not control the out-of-sample error within the specified tolerance of $\delta = 0.05$ away from the best. On the other hand, even though K -fold CV gives the valid error control as ECV, it costs extra computational time, which significantly increases as the sample size increases; see Figure 5(b). Overall, the distributions of tuned ensemble parameters $(\widehat{M}, \widehat{k})$ are similar between K -fold CV and ECV; see Figure 5(c)-(d).

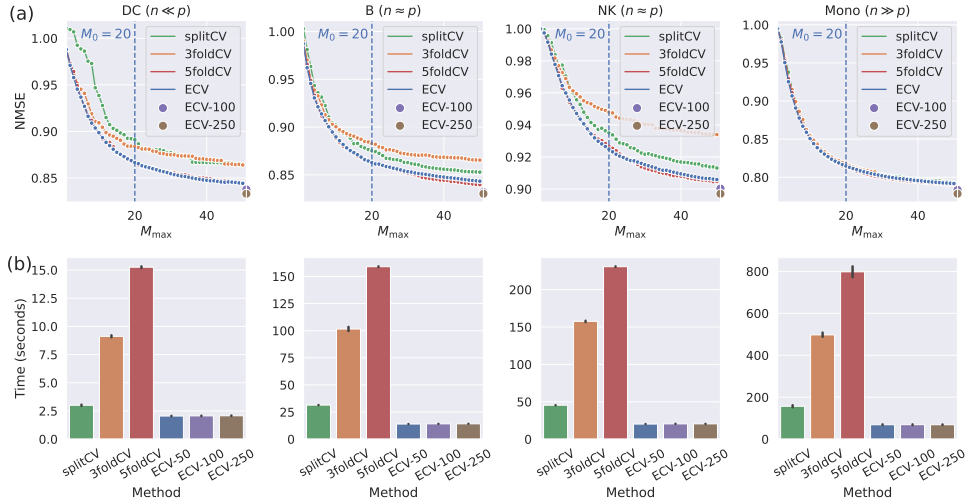


Figure 6: Performance of CV methods on predicting the protein abundances in different cell types. (a) The average NMSEs of the cross-validated predictors for different methods. ECV uses $M_0 = 20$ trees to extrapolate risk estimates, and the points correspond to $M_{\max} \in \{100, 250\}$. (b) The average CV time consumption in seconds.

Next, we compare the performance of different CV methods on various cell types. As shown in Figure 6(a), K -fold CV is very sensitive to the choice of the number of fold K . sample-split CV and K -fold CV with $K = 3$ have the worst out-of-sample performance among all methods. In the low-dimensional dataset of the Mono cell type, all methods have similar performance. However, ECV significantly improves upon sample-split CV with insufficient sample sizes, as in the DC, B, and NK cell types. In all cases, the out-of-sample NMSEs of ECV are comparable to K -fold CV with $K = 5$. Yet, ECV is more flexible to tuning large ensemble sizes, such as $M_{\max} = 100$ and 250. This suggests that the extrapolated risk estimates of ECV based on only $M_0 = 20$ trees are accurate for tuning ensemble parameters on these datasets.

Regarding time consumption, recall that the base predictors are only fitted once (Appendix S4) so that the comparison is fair for all methods. From Figure 6(b), we see that tuning by ECV is significantly faster than K -fold CV because we are extrapolating the risks from 20 trees rather than estimating them for every $M > 20$. Though ECV has similar time complexity as sample-split CV when the sample sizes are small, it uses less than 50% of the time used by sample-split CV as the sample size increases. Thus, ECV achieves better computational efficiency than the alternative CV methods in a variety of settings.

7 Conclusion

In this paper, we focus on the challenge posed by tuning the ensemble and subsample sizes for randomized ensemble learning. While much work has focused on the statistical properties of bagging and random forests, relatively little attention has been given to ensemble parameter tuning. Our proposed method efficiently provides δ -optimal ensemble parameters without enumerating all feasible alternatives, unlike typical CV methods. The risk estimate extrapolation succeeds because of squared risk decomposition and the consistent estimate of each component. It is also sample efficient by utilizing the OOB observations. Further, our algorithm establishes the δ -optimality of the tuned ensemble to the oracle ensemble. Finally, we demonstrate the utility of ECV on single-cell protein prediction tasks. For small sample sizes, ECV obtains smaller out-of-sample error without sample splitting compared to sample-split CV. On the other hand, it reduces the time complexity significantly compared to K -fold CV but maintains comparable accuracy without fitting numerous predictors. In summary, ECV obtains statistical and computational efficiency on the protein prediction tasks.

In concluding the paper, we point out some limitations and possible future directions for this work. First, our theory only works for squared error loss; however, one can sandwich the sub-optimality gap for any ensemble and smooth loss function (Patil et al., 2022a, Proposition 3.6). Second, the focus of the paper is on proving the consistency of the prediction risk estimates as the sample size tends to infinity; however, it is of great interest in practice to take into account the uncertainty of the estimates in finite samples. It is

possible to extend the idea of risk extrapolation to extrapolate the variance estimate of the risk as well. Such an extension would allow us to quantify the tuned model for performing model selection with confidence similar in spirit to doing CV with confidence as in [Lei \(2020\)](#).

References

- Allen, D. M. (1974). The relationship between variable selection and data augmentation and a method for prediction. *Technometrics*, 16(1):125–127.
- Arlot, S. and Celisse, A. (2010). A survey of cross-validation procedures for model selection. *Statistics Surveys*, 4:40–79.
- Austern, M. and Zhou, W. (2020). Asymptotics of cross-validation. *arXiv preprint arXiv:2001.11111*.
- Bates, S., Hastie, T., and Tibshirani, R. (2021). Cross-validation: what does it estimate and how well does it do it? *arXiv preprint arXiv:2104.00673*.
- Bayle, P., Bayle, A., Janson, L., and Mackey, L. (2020). Cross-validation confidence intervals for test error. *Advances in Neural Information Processing Systems*, 33:16339–16350.
- Bellec, P. C. (2018). Optimal bounds for aggregation of affine estimators. *The Annals of Statistics*, 46(1):30–59.
- Bickel, P. J., Götze, F., and van Zwet, W. R. (1997). Resampling fewer than n observations: gains, losses, and remedies for losses. *Statistica Sinica*, 7(1):1–31.
- Breiman, L. (1996). Bagging predictors. *Machine Learning*, 24(2):123–140.
- Breiman, L. (2001). Random forests. *Machine Learning*, 45(1):5–32.
- Bühlmann, P. and Yu, B. (2002). Analyzing bagging. *The Annals of Statistics*, 30(4):927–961.
- Celisse, A. and Guedj, B. (2016). Stability revisited: new generalisation bounds for the leave-one-out. *arXiv preprint arXiv:1608.06412*.
- Du, J.-H., Cai, Z., and Roeder, K. (2022). Robust probabilistic modeling for single-cell multimodal mosaic integration and imputation via scvaeit. *Proceedings of the National Academy of Sciences*, 119(49):e2214414119.
- Geisser, S. (1975). The predictive sample reuse method with applications. *Journal of the American Statistical Association*, 70(350):320–328.
- Greene, E. and Wellner, J. A. (2017). Exponential bounds for the hypergeometric distribution. *Bernoulli*, 23(3):1911.
- Grenander, U. and Szegő, G. (1958). *Toeplitz Forms and Their Applications*. University of California Press. First edition.
- Guo, X. and Peterson, J. (2019). Berry–esseen estimates for regenerative processes under weak moment assumptions. *Stochastic Processes and their Applications*, 129(4):1379–1412.
- Gut, A. (2005). *Probability: A Graduate Course*. Springer, New York.
- Hao, Y., Hao, S., Andersen-Nissen, E., Mauck, W. M., Zheng, S., Butler, A., Lee, M. J., Wilk, A. J., Darby, C., Zager, M., et al. (2021). Integrated analysis of multimodal single-cell data. *Cell*, 184(13):3573–3587.
- Hastie, T., Montanari, A., Rosset, S., and Tibshirani, R. J. (2022). Surprises in high-dimensional ridgeless least squares interpolation. *The Annals of Statistics*, 50(2):949–986.
- Hastie, T., Tibshirani, R., and Friedman, J. H. (2009). *The Elements of Statistical Learning: Data Mining, Inference, and Prediction*. Springer. Second edition.

- Heckmann, D., Lloyd, C. J., Mih, N., Ha, Y., Zielinski, D. C., Haiman, Z. B., Desouki, A. A., Lercher, M. J., and Palsson, B. O. (2018). Machine learning applied to enzyme turnover numbers reveals protein structural correlates and improves metabolic models. *Nature communications*, 9(1):1–10.
- Kale, S., Kumar, R., and Vassilvitskii, S. (2011). Cross-validation and mean-square stability. In *In Proceedings of the Second Symposium on Innovations in Computer Science*.
- Kumar, R., Lokshtanov, D., Vassilvitskii, S., and Vattani, A. (2013). Near-optimal bounds for cross-validation via loss stability. In *International Conference on Machine Learning*.
- Lee, A. J. (1990). *U-statistics: Theory and Practice*. Routledge. First edition.
- Lei, J. (2020). Cross-validation with confidence. *Journal of the American Statistical Association*, 115(532):1978–1997.
- Li, H., Siddiqui, O., Zhang, H., and Guan, Y. (2019). Joint learning improves protein abundance prediction in cancers. *BMC Biology*, 17(1):1–14.
- Liu, L., Chin, S. P., and Tran, T. D. (2019). Reducing sampling ratios and increasing number of estimates improve bagging in sparse regression. In *2019 53rd Annual Conference on Information Sciences and Systems (CISS)*, pages 1–5. IEEE.
- Lopes, M. E. (2019). Estimating the algorithmic variance of randomized ensembles via the bootstrap. *The Annals of Statistics*, 47(2):1088–1112.
- Lopes, M. E., Wu, S., and Lee, T. C. (2020). Measuring the algorithmic convergence of randomized ensembles: The regression setting. *SIAM Journal on Mathematics of Data Science*, 2(4):921–943.
- Lugosi, G. and Mendelson, S. (2019). Mean estimation and regression under heavy-tailed distributions: A survey. *Foundations of Computational Mathematics*, 19(5):1145–1190.
- Oshiro, T. M., Perez, P. S., and Baranauskas, J. A. (2012). How many trees in a random forest? In *International workshop on machine learning and data mining in pattern recognition*.
- Patil, P., Du, J.-H., and Kuchibhotla, A. K. (2022a). Bagging in overparameterized learning: Risk characterization and risk monotonicity. *arXiv preprint arXiv:2210.11445*.
- Patil, P., Kuchibhotla, A. K., Wei, Y., and Rinaldo, A. (2022b). Mitigating multiple descents: A model-agnostic framework for risk monotonicity. *arXiv preprint arXiv:2205.12937*.
- Politis, D. N. (2023). Scalable subsampling: computation, aggregation and inference. *Biometrika*. asad021.
- Politis, D. N. and Romano, J. P. (1994). Large sample confidence regions based on subsamples under minimal assumptions. *The Annals of Statistics*, pages 2031–2050.
- Pugh, C. C. (2002). *Real Mathematical Analysis*. Springer.
- Rad, K. R. and Maleki, A. (2020). A scalable estimate of the out-of-sample prediction error via approximate leave-one-out cross-validation. *Journal of the Royal Statistical Society: Series B (Statistical Methodology)*, 82(4):965–996.
- Rad, K. R., Zhou, W., and Maleki, A. (2020). Error bounds in estimating the out-of-sample prediction error using leave-one-out cross validation in high-dimensions. In *International Conference on Artificial Intelligence and Statistics*, pages 4067–4077. PMLR.
- Rio, E. (2017). About the constants in the Fuk-Nagaev inequalities. *Electronic Communications in Probability*, 22(28):12p.
- Stephenson, W. and Broderick, T. (2020). Approximate cross-validation in high dimensions with guarantees. In *International Conference on Artificial Intelligence and Statistics*.

- Stone, M. (1974). Cross-validatory choice and assessment of statistical predictions. *Journal of the Royal Statistical Society: Series B*, 36(2):111–133.
- Stone, M. (1977). Asymptotics for and against cross-validation. *Biometrika*, 64(1):29–35.
- Vershynin, R. (2018). *High-Dimensional Probability: An Introduction with Applications in Data Science*. Cambridge University Press.
- Wager, S., Hastie, T., and Efron, B. (2014). Confidence intervals for random forests: The jackknife and the infinitesimal jackknife. *The Journal of Machine Learning Research*, 15(1):1625–1651.
- Wang, S., Zhou, W., Lu, H., Maleki, A., and Mirrokni, V. (2018). Approximate leave-one-out for fast parameter tuning in high dimensions. In *International Conference on Machine Learning*.
- Wilson, A., Kasy, M., and Mackey, L. (2020). Approximate cross-validation: Guarantees for model assessment and selection. In *International Conference on Artificial Intelligence and Statistics*.
- Xu, F., Wang, S., Dai, X., Mundra, P. A., and Zheng, J. (2021). Ensemble learning models that predict surface protein abundance from single-cell multimodal omics data. *Methods*, 189:65–73.
- Zhang, Y. and Yang, Y. (2015). Cross-validation for selecting a model selection procedure. *Journal of Econometrics*, 187(1):95–112.
- Zhou, Z., Ye, C., Wang, J., and Zhang, N. R. (2020). Surface protein imputation from single cell transcripts by deep neural networks. *Nature communications*, 11(1):651.

Supplementary material for “Extrapolated cross-validation for randomized ensembles”

This document acts as a supplement to the paper “Extrapolated cross-validation for randomized ensembles.” The section numbers in this supplement begin with the letter “S” and the equation numbers begin with the letter “E” to differentiate them from those appearing in the main paper.

Notation and organization

Notation

Below we provide an overview of the notation used in the main paper and the supplement.

1. General notation: We denote scalars in non-bold lower or upper case (e.g., n , λ , C), vectors in lower case (e.g., \mathbf{x} , $\boldsymbol{\beta}$), and matrices in upper case (e.g., \mathbf{X}). For a real number x , $(x)_+$ denotes its positive part, $\lfloor x \rfloor$ its floor, and $\lceil x \rceil$ its ceiling. For a natural number n , $n! = \prod_{i=1}^n i$ denotes the n factorial. For a vector $\boldsymbol{\beta}$, $\|\boldsymbol{\beta}\|_2$ denotes its ℓ_2 norm. For a pair of vectors \mathbf{v} and \mathbf{w} , $\langle \mathbf{v}, \mathbf{w} \rangle$ denotes their inner product. For an event A , $\mathbf{1}_A$ denotes the associated indicator random variable. We use \mathcal{O}_p and o_p to denote probabilistic big-O and little-o notation, respectively.
2. Set notation: We denote sets using calligraphic letters (e.g., \mathcal{D}), and use blackboard letters to denote some special sets: \mathbb{N} denotes the set of positive integers, \mathbb{R} denotes the set of real numbers, $\mathbb{R}_{\geq 0}$ denotes the set of non-negative real numbers, and $\mathbb{R}_{> 0}$ denotes the set of positive real numbers. For a natural number n , we use $[n]$ to denote the set $\{1, \dots, n\}$.
3. Matrix notation: For a matrix $\mathbf{X} \in \mathbb{R}^{n \times p}$, $\mathbf{X}^\top \in \mathbb{R}^{p \times n}$ denotes its transpose. For a square matrix $\mathbf{A} \in \mathbb{R}^{p \times p}$, $\mathbf{A}^{-1} \in \mathbb{R}^{p \times p}$ denotes its inverse, provided it is invertible. For a positive semi-definite matrix $\boldsymbol{\Sigma}$, $\boldsymbol{\Sigma}^{1/2}$ denotes its principal square root. A $p \times p$ identity matrix is denoted \mathbf{I}_p , or simply by \mathbf{I} , when it is clear from the context.

Organization

Below we outline the structure of the rest of the supplement.

- In Appendix S1, we present proofs of results appearing in Section 3.
 - Appendix S1.1 proves Proposition 3.1.
 - Appendix S1.2 proves Proposition 3.2.
 - Appendix S1.3 proves Proposition 3.3, conditional on certain helper lemmas presented in the next section.
 - Appendix S1.4 provides intermediate concentration results used in the proof of Proposition 3.3.
- In Appendix S2, we present proof of results in Section 4.
 - Appendix S2.1 proves Theorem 4.1.
 - Appendix S2.2 extends additive optimality in Theorem 4.1 to multiplicative optimality stated in Remark 4.2.
 - Appendix S2.3 proves Proposition 4.3.
- In Appendix S3, we collect various technical helper lemmas related to concentrations and convergences along with their proofs that are used in proofs in Appendices S1 to S2.
- In Appendix S4, we compare the computational complexity of Algorithm 1 with other CV methods.
- In Appendix S5, we present additional numerical results for Section 5 and Section 6.

- Appendix S5.1 presents additional illustrations for subbagging and bagging in Section 5.1.
- Appendix S5.2 presents additional illustrations for subbagging and bagging in Section 5.2.
- Appendix S5.3 presents additional illustrations for bagging in Section 5.3.
- Appendix S5.4 presents additional illustrations for Section 6.

S1 Proofs of results in Section 3

S1.1 Proof of Proposition 3.1 (Squared risk decomposition)

Proof of Proposition 3.1. We start by expanding the squared risk as:

$$\begin{aligned}
& R(\tilde{f}_{M,k}; \mathcal{D}_n, \{I_\ell\}_{\ell=1}^M) \\
&= \int \left(y - \frac{1}{M} \sum_{\ell=1}^M \hat{f}(\mathbf{x}; \mathcal{D}_{I_\ell}) \right)^2 dP(\mathbf{x}, y) \\
&= \int \left(\frac{1}{M} \sum_{\ell=1}^M (y - \hat{f}(\mathbf{x}; \mathcal{D}_{I_\ell})) \right)^2 dP(\mathbf{x}, y) \\
&= \frac{1}{M^2} \sum_{\ell=1}^M \int (y - \hat{f}(\mathbf{x}; \mathcal{D}_{I_\ell}))^2 dP(\mathbf{x}, y) + \frac{1}{M^2} \sum_{i=1}^M \sum_{\substack{j=1 \\ j \neq i}}^M \int (y - \hat{f}(\mathbf{x}; \mathcal{D}_{I_i}))(y - \hat{f}(\mathbf{x}; \mathcal{D}_{I_j})) dP(\mathbf{x}, y) \\
&= \frac{1}{M^2} \sum_{\ell=1}^M R(\tilde{f}_{1,k}; \mathcal{D}_n, I_\ell) + \frac{1}{M^2} \sum_{i=1}^M \sum_{\substack{j=1 \\ j \neq i}}^M \int (y - \hat{f}(\mathbf{x}; \mathcal{D}_{I_i}))(y - \hat{f}(\mathbf{x}; \mathcal{D}_{I_j})) dP(\mathbf{x}, y) \\
&\stackrel{(i)}{=} \frac{1}{M^2} \sum_{\ell=1}^M R(\tilde{f}_{1,k}; \mathcal{D}_n, I_\ell) \\
&\quad + \frac{1}{M^2} \sum_{i=1}^M \sum_{\substack{j=1 \\ j \neq i}}^M \int \frac{1}{2} \left\{ 4 \left(y - \frac{1}{2} (\hat{f}(\mathbf{x}; \mathcal{D}_{I_i}) + \hat{f}(\mathbf{x}; \mathcal{D}_{I_j})) \right)^2 - (y - \hat{f}(\mathbf{x}; \mathcal{D}_{I_i}))^2 - (y - \hat{f}(\mathbf{x}; \mathcal{D}_{I_j}))^2 \right\} dP(\mathbf{x}, y) \\
&= \frac{1}{M^2} \sum_{\ell=1}^M R(\tilde{f}_{1,k}; \mathcal{D}_n, I_\ell) \\
&\quad + \frac{1}{M^2} \sum_{i=1}^M \sum_{\substack{j=1 \\ j \neq i}}^M \frac{1}{2} \left\{ 4R(\hat{f}_{2,k}; \mathcal{D}_n; I_i, I_j) - R(\tilde{f}_{1,k}; \mathcal{D}_n; I_i) - R(\tilde{f}_{1,k}; \mathcal{D}_n; I_j) \right\} \\
&= \frac{1}{M^2} \sum_{\ell=1}^M R(\tilde{f}_{1,k}; \mathcal{D}_n, I_\ell) \\
&\quad - \frac{1}{2M^2} \sum_{i=1}^M \sum_{\substack{j=1 \\ j \neq i}}^M R(\tilde{f}_{1,k}; I_i) - \frac{1}{2M^2} \sum_{i=1}^M \sum_{\substack{j=1 \\ j \neq i}}^M R(\tilde{f}_{1,k}; I_j) + \frac{1}{M^2} \sum_{i=1}^M \sum_{\substack{j=1 \\ j \neq i}}^M 2R(\hat{f}_{2,k}; \mathcal{D}_n; I_i, I_j) \\
&= \frac{1}{M^2} \sum_{\ell=1}^M R(\tilde{f}_{1,k}; \mathcal{D}_n; I_\ell) - \frac{1}{2M^2} \cdot 2 \cdot (M-1) \sum_{\ell=1}^M R(\tilde{f}_{1,k}; I_\ell) + \frac{2}{M^2} \sum_{\substack{i,j \in [M] \\ i \neq j}} R(\hat{f}_{2,k}; \mathcal{D}_n; I_i, I_j) \\
&= \left(\frac{1}{M^2} - \frac{(M-1)}{M^2} \right) \sum_{\ell=1}^M R(\tilde{f}_{1,k}; \mathcal{D}_n; I_\ell) + \frac{2}{M^2} \sum_{\substack{i,j \in [M] \\ i \neq j}} R(\hat{f}_{2,k}; \mathcal{D}_n; I_i, I_j)
\end{aligned}$$

$$= - \left(\frac{1}{M} - \frac{2}{M^2} \right) \sum_{\ell=1}^M R(\tilde{f}_{1,k}; \mathcal{D}_n, \{I_\ell\}) + \frac{2}{M^2} \sum_{\substack{i,j \in [M] \\ i \neq j}} R(\tilde{f}_{2,k}; \mathcal{D}_n, \{I_i, I_j\}).$$

In the expansion above, for equality (i), we used the fact that $ab = \{4(a/2 + b/2)^2 - a^2 - b^2\}/2$. \square

S1.2 Proof of Proposition 3.2 (Consistent component risk estimation)

Proof of Proposition 3.2. Let $\Delta_n = |\widehat{R}(f, \mathcal{D}_I) - R(\widehat{f}; \mathcal{D}_I)|$. We will view p , $|I|$, and $|I^c|$ as sequences indexed by n . Define $\widehat{\sigma}_I := \|(y_0 - \widehat{f}(\mathbf{x}_0; \mathcal{D}_I))^2\|_{\psi_1|_{\mathcal{D}_I}}$. From Patil et al. (2022a, Lemma 2.9, Lemma 2.10), we have

$$\mathbb{P} \left(\Delta_n \geq C \widehat{\sigma}_I \max \left\{ \sqrt{\frac{A \log n}{|I^c|}}, \frac{A \log n}{|I^c|} \right\} \right) \leq n^{-A}, \quad (\text{S1.1})$$

for some positive constant C . Let $\kappa_n = C \widehat{\sigma}_I \max \left\{ \sqrt{\frac{A \log n}{|I^c|}}, \frac{A \log n}{|I^c|} \right\}$.

Since $\widehat{\sigma}_I = o_p(\sqrt{|I^c|/\log n})$ as $n \rightarrow \infty$, we have that $\kappa_n = o_p(1)$. Let $A > 0$ be fixed, For all $\epsilon > 0$, we have that

$$\begin{aligned} \mathbb{P}(\Delta_n > \epsilon) &= \mathbb{P}(\Delta_n > \epsilon \geq \kappa_n) + \mathbb{P}(\Delta_n > \epsilon, \kappa_n > \epsilon) \\ &\leq n^{-A} + \mathbb{P}(\kappa_n > \epsilon) \rightarrow 0, \end{aligned}$$

which implies that $\Delta_n = o_p(1)$. The proof for $\|\cdot\|_{L_2|_{\mathcal{D}_I}}$ follows analogously. \square

S1.3 Proof of Proposition 3.3 (Uniform risk estimation over (M, k))

Proof of Proposition 3.3. Before we prove Proposition 3.3, we present the proof strategy in Figure S1. In Figure S1, four important auxiliary lemmas and propositions are deferred to the next section. For the asymptotic results, we will let k, p be sequences of integers $\{k_n\}_{n=1}^\infty, \{p_n\}_{n=1}^\infty$ indexed by n but drop the subscripts n .

From Lemma S1.4 we have

$$\sup_{M \in \mathbb{N}, k \in \mathcal{K}_n} |R_{M,k} - \mathfrak{R}_{M,k}| = \mathcal{O}_p(n^\epsilon(\gamma_{1,n} + \gamma_{2,n})).$$

On the other hand, from Proposition S1.2 we have

$$\sup_{M \in \mathbb{N}, k \in \mathcal{K}_n} |\widehat{R}_{M,k}^{\text{ECV}} - \mathfrak{R}_{M,k}| = \mathcal{O}_p(\widehat{\sigma}_n \log n / n^{1/2} + n^\epsilon(\gamma_{1,n} + \gamma_{2,n})),$$

where $\widehat{\sigma}_n = \max_{m, \ell \in [M_0], k \in \mathcal{K}_n} \widehat{\sigma}_{I_{k, \ell} \cup I_{k, m}}$. By the triangle inequality, we have

$$\sup_{M \in \mathbb{N}, k \in \mathcal{K}_n} |\widehat{R}_{M,k}^{\text{ECV}} - R_{M,k}| = \mathcal{O}_p(\widehat{\sigma}_n \log n / n^{1/2} + n^\epsilon(\gamma_{1,n} + \gamma_{2,n})),$$

which completes the proof. \square

S1.4 Intermediate concentration results for Proposition 3.3

In this section, we show the concentration of conditional prediction risks to their limits. Proposition S1.1 derives the uniform consistency over $k \in \mathcal{K}_n$ of the cross-validated risk estimates to the risk $R_{M,k}$ for $M = 1, 2$. Proposition S1.2 derives the uniform consistency over $(M, k) \in \mathbb{N} \times \mathcal{K}_n$ of the cross-validated risk estimates to the deterministic limits $\mathfrak{R}_{M,k}$. Lemma S1.3 establishes the concentration for the expected (with respect to sampling) conditional risk over $k \in \mathcal{K}_n$. Lemma S1.4 establishes the concentration for subsample conditional risks over $M \in \mathbb{N}$ and $k \in \mathcal{K}_n$.

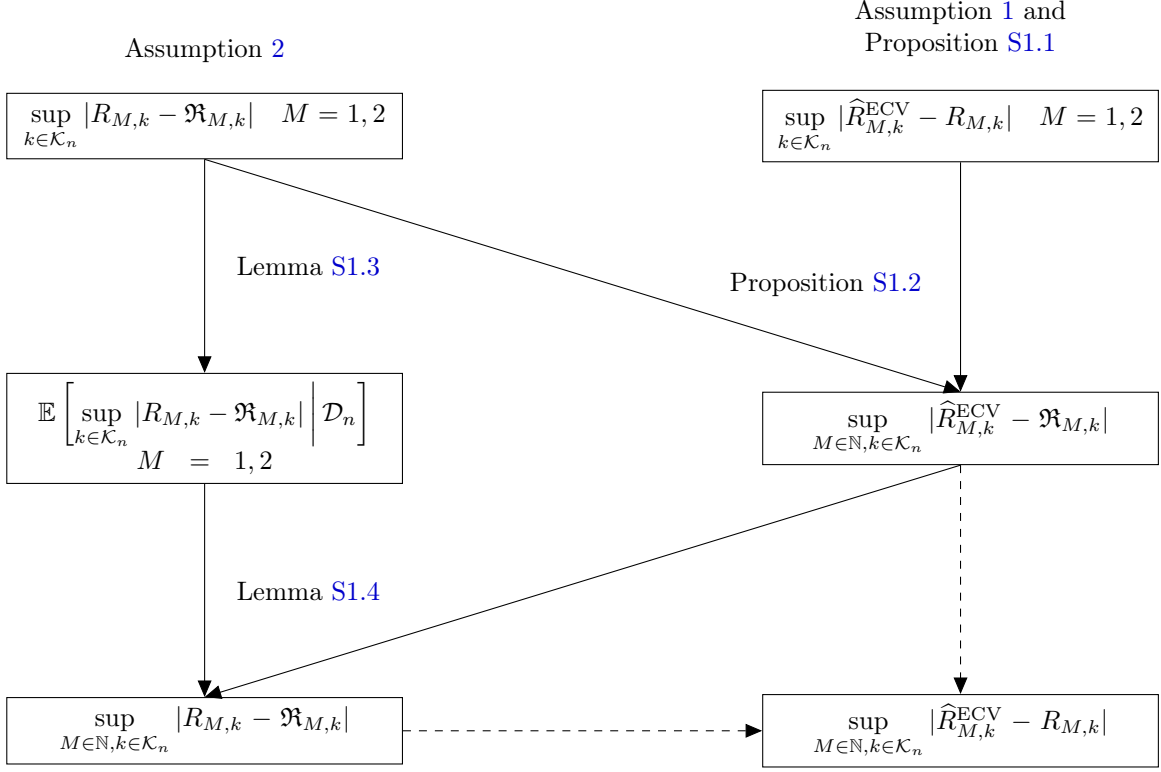


Figure S1: Reduction strategy for obtaining concentration results in Proposition 3.3. The solid lines indicate basic components presented later in Appendix S1.4 and the dashed lines indicate the proof strategy in Appendix S1.3. Here, $\mathfrak{R}_{M,k} = 2\mathfrak{R}_{2,k} - \mathfrak{R}_{1,k} + 2(\mathfrak{R}_{1,k} - \mathfrak{R}_{2,k})/M$.

S1.4.1 Uniform consistency of cross-validated risk over k for $M = 1, 2$

In what follows, we derive the uniform consistency over $k \in \mathcal{K}_n$ of the cross-validated risk estimates for $M = 1, 2$ in Appendix S1.4.1.

Proposition S1.1 (Uniform consistency over k for $M = 1, 2$). *Suppose that Assumption 2 holds, then the ECV estimates defined in (3.3) satisfy that for $M = 1, 2$,*

$$\sup_{k \in \mathcal{K}_n} \left| \widehat{R}_{M,k}^{\text{ECV}} - R_{M,k} \right| = \mathcal{O}_p(\widehat{\sigma}_n \log(n)n^{-1/2} + n^\epsilon(\gamma_{1,n} + \gamma_{2,n})),$$

where $\widehat{\sigma}_n = \max_{m, \ell \in [M_0], k \in \mathcal{K}_n} \widehat{\sigma}_{I_{k,\ell} \cup I_{k,m}}$ and $R_{M,k} = R_{M,k}(\widetilde{f}_{M,k}; \mathcal{D}_n, \{I_{k,\ell}\}_{\ell=1}^M)$ for $\{I_{k,\ell}\}_{\ell=1}^M \stackrel{\text{SRS}}{\sim} \mathcal{I}_k$.

Proof of Proposition S1.1. Note that

$$\begin{aligned} \widehat{R}_{1,k}^{\text{ECV}} &= \frac{1}{M_0} \sum_{\ell=1}^{M_0} \widehat{R}(\widehat{f}(\cdot; \{\mathcal{D}_{I_{k,\ell}}\}), \mathcal{D}_{I_{k,\ell}^c}) \\ \widehat{R}_{2,k}^{\text{ECV}} &= \frac{1}{M_0(M_0-1)} \sum_{\substack{\ell, m \in [M_0] \\ \ell \neq m}} \widehat{R}(\widehat{f}(\cdot; \{\mathcal{D}_{I_{k,\ell}}, \mathcal{D}_{I_{k,m}}\}), \mathcal{D}_{(I_{k,\ell} \cup I_{k,m})^c}). \end{aligned}$$

Define $\widehat{\sigma}_I := \|(y_0 - \widehat{f}(\mathbf{x}_0; \mathcal{D}_I))^2\|_{\psi_1 | \mathcal{D}_I}$ and recall $\Delta_{M,k}$ for $M = 1, 2$ are defined as follows:

$$\begin{aligned} \Delta_{1,k} &= \widehat{R}_{1,k}^{\text{ECV}} - \frac{1}{M_0} \sum_{\ell=1}^{M_0} R_{1,k}(\widehat{f}; \mathcal{D}_n, \{I_{k,\ell}\}) \\ \Delta_{2,k} &= \widehat{R}_{2,k}^{\text{ECV}} - \frac{1}{M_0(M_0-1)} \sum_{\substack{\ell, m \in [M_0] \\ \ell \neq m}} R_{2,k}(\widehat{f}_{2,k}; \mathcal{D}_n, \{I_{k,\ell}, I_{k,m}\}). \end{aligned} \tag{S1.2}$$

By the triangle inequality, for $M = 1, 2$, it holds that

$$\sup_{k \in \mathcal{K}_n} |\widehat{R}_{1,k}^{\text{ECV}} - \mathfrak{R}_{1,k}| \leq \sup_{k \in \mathcal{K}_n} |\Delta_{1,k}| + \sup_{k \in \mathcal{K}_n, \ell \in [M_0]} |R_{1,k}(\widehat{f}; \mathcal{D}_n, \{I_{k,\ell}\}) - \mathfrak{R}_{1,k}| \quad (\text{S1.3})$$

$$\sup_{k \in \mathcal{K}_n} |\widehat{R}_{2,k}^{\text{ECV}} - \mathfrak{R}_{1,k}| \leq \sup_{k \in \mathcal{K}_n} |\Delta_{2,k}| + \sup_{k \in \mathcal{K}_n, m, \ell \in [M_0]} |R_{2,k}(\widehat{f}; \mathcal{D}_n, \{I_{k,m}, I_{k,\ell}\}) - \mathfrak{R}_{1,k}| \quad (\text{S1.4})$$

where $\Delta_{M,k}$ are defined in (S1.2). Next we analyze each term separately for $M = 1, 2$.

Part (1) For the first term, from (S1.1) in Proposition 3.2 and applying union bound over $k \in \mathcal{K}_n$, we have that

$$\begin{aligned} \mathbb{P} \left(\sup_{k \in \mathcal{K}_n} |\Delta_{1,k}| \geq C \max_{k \in \mathcal{K}_n, \ell \in [M_0]} \widehat{\sigma}_{I_{k,\ell}} \max \left\{ \sqrt{\frac{\log(M_0 |\mathcal{K}_n| \eta)}{n / \log n}}, \frac{\log(M_0 |\mathcal{K}_n| \eta)}{n / \log n} \right\} \right) &\leq \frac{1}{\eta}, \\ \mathbb{P} \left(\sup_{k \in \mathcal{K}_n} |\Delta_{2,k}| \geq C \max_{k \in \mathcal{K}_n, \ell \neq m \in [M_0]} \widehat{\sigma}_{I_{k,\ell} \cup I_{k,m}} \max \left\{ \sqrt{\frac{\log(M_0 |\mathcal{K}_n| \eta)}{n / \log n}}, \frac{\log(M_0 |\mathcal{K}_n| \eta)}{n / \log n} \right\} \right) &\leq \frac{1}{\eta}, \end{aligned} \quad (\text{S1.5})$$

for some constant $C > 0$. This implies that

$$\begin{aligned} \sup_{k \in \mathcal{K}_n} |\Delta_{1,k}| &= \mathcal{O}_p \left(\max_{k \in \mathcal{K}_n, \ell \in [M_0]} \widehat{\sigma}_{I_{k,\ell}} \sqrt{\frac{\log(|\mathcal{K}_n|) \log n}{n}} \right) \\ \sup_{k \in \mathcal{K}_n} |\Delta_{2,k}| &= \mathcal{O}_p \left(\max_{k \in \mathcal{K}_n, \ell \neq m \in [M_0]} \widehat{\sigma}_{I_{k,\ell} \cup I_{k,m}} \sqrt{\frac{\log(|\mathcal{K}_n|) \log n}{n}} \right). \end{aligned}$$

To summarize, $\sup_{k \in \mathcal{K}_n} |\Delta_{M,k}|$ for $M = 1, 2$ can be bounded as:

$$\sup_{k \in \mathcal{K}_n} |\Delta_{M,k}| = \mathcal{O}_p \left(\widehat{\sigma}_n \sqrt{\frac{\log^2 n}{n}} \right), \quad (\text{S1.6})$$

where $\widehat{\sigma}_n = \max_{m, \ell \in [M_0], k \in \mathcal{K}_n} \widehat{\sigma}_{I_{k,\ell} \cup I_{k,m}}$.

Part (2) For the second term, from (3.5) in Assumption 2 we have that when n is large enough, for all $\eta \geq 1$,

$$\mathbb{P} \left(n^{-\epsilon} \gamma_{1,n}^{-1} |R(\widetilde{f}_{1,k}; \mathcal{D}_{I_{k,\ell}}) - \mathfrak{R}_{1,k}| \geq \eta \right) \leq \frac{C_0}{n \eta^{1/\epsilon}}.$$

Let $\gamma'_{1,n} := n^\epsilon \gamma_{1,n}$. Taking a union bound over $k \in \mathcal{K}_n$ and $\ell \in [M_0]$, we have

$$\mathbb{P} \left(\gamma'^{-1}_{1,n} \sup_{k \in \mathcal{K}_n, \ell \in [M_0]} |R_{1,k}(\widehat{f}; \mathcal{D}_n, \{I_{k,\ell}\}) - \mathfrak{R}_{1,k}| \geq \eta \right) \leq \frac{C_0 M_0}{\eta^{1/\epsilon}},$$

which implies that

$$\sup_{k \in \mathcal{K}_n, \ell \in [M_0]} |R_{1,k}(\widehat{f}; \mathcal{D}_n, \{I_{k,\ell}\}) - \mathfrak{R}_{1,k}| = \mathcal{O}_p(n^\epsilon \gamma_{1,n}). \quad (\text{S1.7})$$

Analogously, for $M = 2$, we also have

$$\sup_{k \in \mathcal{K}_n, m \neq \ell \in [M_0]} |R_{2,k}(\widehat{f}; \mathcal{D}_n, \{I_{k,m}, I_{k,\ell}\}) - \mathfrak{R}_{1,k}| = \mathcal{O}_p(n^\epsilon \gamma_{2,n}). \quad (\text{S1.8})$$

Part (3) Combining (S1.4), (S1.6), (S1.7) and (S1.8) yields that

$$\sup_{k \in \mathcal{K}_n} |\widehat{R}_{M,k}^{\text{ECV}} - \mathfrak{R}_{M,k}| = \mathcal{O}_p \left(\widehat{\sigma}_n \sqrt{\frac{\log^2 n}{n}} + n^\epsilon \gamma_{M,n} \right), \quad M = 1, 2,$$

ignoring constant factors. \square

S1.4.2 Uniform consistency of cross-validated risk to $\mathfrak{R}_{M,k}$ over (M, k)

Proposition S1.2 (Uniform consistency to $\mathfrak{R}_{M,k}$ over (M, k)). *Suppose that Assumptions 1 and 2 hold, then the ECV estimates defined in (3.3) satisfy that*

$$\sup_{M \in \mathbb{N}, k \in \mathcal{K}_n} \left| \widehat{R}_{M,k}^{\text{ECV}} - \mathfrak{R}_{M,k} \right| = \mathcal{O}_p(\widehat{\sigma}_n \log(n) n^{-\frac{1}{2}} + n^\epsilon (\gamma_{1,n} + \gamma_{2,n})),$$

where $\widehat{\sigma}_n = \max_{m, \ell \in [M_0], k \in \mathcal{K}_n} \widehat{\sigma}_{I_{k,\ell} \cup I_{k,m}}$.

Proof of Proposition S1.2. Note that $\widehat{R}_{M,k}^{\text{ECV}}$ satisfies the squared risk decomposition and the randomness of $\widehat{R}_{M,k}^{\text{ECV}}$ also due to both the full data \mathcal{D}_n and random sampling.

From Proposition S1.1, we have

$$\sup_{k \in \mathcal{K}_n} |\widehat{R}_{M,k}^{\text{ECV}} - \mathfrak{R}_{M,k}| = \mathcal{O}_p \left(\widehat{\sigma}_n \sqrt{\frac{\log^2 n}{n}} + n^\epsilon \gamma_{M,n} \right), \quad M = 1, 2.$$

On the other hand, by the definition of $\widehat{R}_{M,k}^{\text{ECV}}$ for $M \in \mathbb{N}$ in (3.4), taking the supremum over both M and k yields that

$$\begin{aligned} \sup_{M \in \mathbb{N}, k \in \mathcal{K}_n} \left| \widehat{R}_{M,k}^{\text{ECV}} - \mathfrak{R}_{M,k} \right| &\leq \sup_{k \in \mathcal{K}_n} \left| \widehat{R}_{1,k}^{\text{ECV}} - \mathfrak{R}_{1,k} \right| + 2 \sup_{k \in \mathcal{K}_n} \left| \widehat{R}_{2,k}^{\text{ECV}} - \mathfrak{R}_{2,k} \right| \\ &= \mathcal{O}_p(\zeta_n), \end{aligned}$$

where $\zeta_n = \widehat{\sigma}_n \sqrt{\log^2 n/n} + n^\epsilon (\gamma_{1,n} + \gamma_{2,n})$. □

S1.4.3 Proof of Lemma S1.3 (Concentration of expected risk over $k \in \mathcal{K}_n$)

To obtain tail bounds for the subsample conditional risk defined in (2.3), we need to analyze its conditional expectation. Here the expectation is taken with respect to only the randomness due to sampling and conditioned on \mathcal{D}_n . For example, we define the data conditional (on \mathcal{D}_n) risks as:

$$R(\widetilde{f}_{M,k}(\cdot; \{\mathcal{D}_{I_\ell}\}_{\ell=1}^M); \mathcal{D}_n) := \int \mathbb{E} \left[\left(y - \widetilde{f}_{M,k}(\mathbf{x}; \{\mathcal{D}_{I_{k,\ell}}\}_{\ell=1}^M) \right)^2 \mid \mathcal{D}_n \right] dP(\mathbf{x}, y). \quad (\text{S1.9})$$

Observe that the conditional (on \mathcal{D}_n) risk of the bagged predictor $\widetilde{f}_{M,k}(\cdot; \{\mathcal{D}_{I_{k,\ell}}\}_{\ell=1}^M)$ integrates over the randomness of the future observation (\mathbf{x}, y) as well as the randomness due to the simple random sampling of $I_{k,\ell}$, $\ell = 1, \dots, M$. Nevertheless, the subsample conditional risk ignores the expectation over the simple random sample. Considering a more general setup, when we need to obtain tail bounds for $\sup_{k \in \mathcal{K}} |R(\widetilde{f}_M; \mathcal{D}_n, \{I_{k,\ell}\}_{\ell=1}^M) - \mathfrak{R}_{M,k}|$, we again need to control its expectation conditional on \mathcal{D}_n . The result is summarized as in the following lemma. Note that when $|\mathcal{K}_n| = 1$, it simply reduces to controlling the data conditional risk.

Lemma S1.3 (Concentration of expected risk). *Consider a dataset \mathcal{D}_n with n observations, a subsample grid $\mathcal{K}_n \subset [n]$, and a base predictor \widehat{f} . Suppose Assumptions 1 and 2 hold, then it holds for $M = 1, 2$ that*

$$\mathbb{E} \left[\sup_{k \in \mathcal{K}_n} |R(\widetilde{f}_M; \mathcal{D}_n, \{I_{k,\ell}\}_{\ell=1}^M) - \mathfrak{R}_{M,k}| \right] = \mathcal{O}(n^\epsilon \gamma_{M,n}),$$

where $\{I_{k,\ell}\}_{\ell=1}^M \stackrel{\text{SRS}}{\sim} \mathcal{I}_k$.

Proof of Lemma S1.3. Define

$$B_{1,n} := \sup_{k \in \mathcal{K}_n} |R(\widetilde{f}_{1,k}; \mathcal{D}_n, \{I_{k,1}\}) - \mathfrak{R}_{1,k}|. \quad (\text{S1.10})$$

$$B_{2,n} := \sup_{k \in \mathcal{K}_n} |R(\widetilde{f}_{2,k}; \mathcal{D}_n, \{I_{k,1}, I_{k,2}\}) - \mathfrak{R}_{2,k}|. \quad (\text{S1.11})$$

We start with the $M = 1$ case by bounding the expectation of (S1.10). Note that from (3.5), we have that for all $\eta \geq \eta_0$,

$$\mathbb{P}\left(n^{-\epsilon}\gamma_{1,n}^{-1}|R(\tilde{f}_{1,k}; \mathcal{D}_{I_1}) - \mathfrak{R}_{1,k}| \geq \eta\right) \leq \frac{1}{n\eta^{1/\epsilon}}$$

Let $\gamma'_{1,n} := n^\epsilon \gamma_{1,n}$. Taking a union bound over $k \in \mathcal{K}_n$, we have

$$\mathbb{P}(\gamma'_{1,n} B_{1,n} \geq \eta) \leq \frac{1}{\eta^{1/\epsilon}}. \quad (\text{S1.12})$$

Then, it follows that

$$\begin{aligned} \mathbb{E}[B_{1,n}] &= \gamma'_{1,n} \int_0^\infty \mathbb{P}(\gamma'_{1,n} B_{1,n} \geq \eta) d\eta \\ &\leq \gamma'_{1,n} \left(\int_0^{\eta_0} 1 d\epsilon + \int_{\eta_0}^\infty \frac{C_0}{\eta^{1/\epsilon}} d\epsilon \right) \\ &\leq \gamma'_{1,n} \left(\eta_0 - C_0 \frac{\epsilon - 1}{\epsilon} \eta^{1-1/\epsilon} \Big|_{\eta_0}^\infty \right) \\ &= \left(\eta_0 + C_0 \frac{\epsilon - 1}{\epsilon} \eta_0^{1-1/\epsilon} \right) \gamma'_{1,n}. \end{aligned}$$

The proof for $M = 2$ follows analogously. \square

S1.4.4 Proof of Lemma S1.4 (Concentration of conditional risk)

Lemma S1.4 (Concentration of conditional risk). *Consider a dataset \mathcal{D}_n with n observations and a base predictor \hat{f} . Under Assumption 2, it holds that,*

$$\sup_{M \in \mathbb{N}, k \in \mathcal{K}_n} |R_{M,k} - \mathfrak{R}_{M,k}| = \mathcal{O}_p(C_1(|\mathcal{K}_n|)\gamma_{1,n} + C_2(|\mathcal{K}_n|)\gamma_{1,n}), \quad (\text{S1.13})$$

where $\mathfrak{R}_{M,k} := 2\mathfrak{R}_{2,k} - \mathfrak{R}_{1,k} + 2(\mathfrak{R}_{1,k} - \mathfrak{R}_{2,k})/M$.

Proof of Lemma S1.4. By Proposition 3.1, we have for $\{I_{k,\ell}\}_{\ell=1}^M \stackrel{\text{SRS}}{\sim} \mathcal{I}_k$

$$\begin{aligned} &\left| R(\tilde{f}_{M,k}; \mathcal{D}_n, \{I_{k,\ell}\}_{\ell=1}^M) - \mathfrak{R}_{M,k} \right| \\ &= \left| R(\tilde{f}_{M,k}; \mathcal{D}_n, \{I_{k,\ell}\}_{\ell=1}^M) - \left[(2\mathfrak{R}_{2,k} - \mathfrak{R}_{1,k}) + \frac{2(\mathfrak{R}_{1,k} - \mathfrak{R}_{2,k})}{M} \right] \right| \\ &= \left| -\left(\frac{1}{M} - \frac{2}{M^2} \right) \sum_{\ell=1}^M \left(R(\tilde{f}_{1,k}; \mathcal{D}_n, \{I_{k,\ell}\}) - \mathfrak{R}_{1,k} \right) \right| + \left| \frac{2}{M^2} \sum_{\substack{i,j \in [M] \\ i \neq j}} \left(R(\tilde{f}_{2,k}; \mathcal{D}_n, \{I_{k,i}, I_{k,j}\}) - \mathfrak{R}_{2,k} \right) \right|. \end{aligned}$$

Then, it follows that

$$\begin{aligned} &\sup_{M \in \mathbb{N}, k \in \mathcal{K}_n} \left| R(\tilde{f}_{M,k}; \mathcal{D}_n, \{I_{k,\ell}\}_{\ell=1}^M) - \mathfrak{R}_{M,k} \right| \\ &\leq \left| 1 - \frac{2}{M} \right| \sup_{M \geq 1} \left| \frac{1}{M} \sum_{\ell \in [M]} \sup_{k \in \mathcal{K}_n} |R(\tilde{f}_{1,k}; \mathcal{D}_n, \{I_{k,\ell}\}) - \mathfrak{R}_{1,k}| \right| \\ &\quad + 2 \sup_{M \geq 2} \left| \frac{1}{M(M-1)} \sum_{i,j \in [M], i \neq j} \sup_{k \in \mathcal{K}_n} |R(\tilde{f}_{2,k}; \mathcal{D}_n, \{I_{k,i}, I_{k,j}\}) - \mathfrak{R}_{2,k}| \right| \end{aligned}$$

$$\begin{aligned}
&\leq \sup_{M \geq 1} \left| \frac{1}{M} \sum_{\ell \in [M]} \sup_{k \in \mathcal{K}_n} |R(\tilde{f}_{1,k}; \mathcal{D}_n, \{I_{k,\ell}\}) - \mathfrak{R}_{1,k}| \right| \\
&\quad + 2 \sup_{M \geq 2} \left| \frac{1}{M(M-1)} \sum_{i,j \in [M], i \neq j} \sup_{k \in \mathcal{K}_n} |R(\tilde{f}_{2,k}; \mathcal{D}_n, \{I_{k,i}, I_{k,j}\}) - \mathfrak{R}_{2,k}| \right|. \tag{S1.14}
\end{aligned}$$

We start by observing that the two terms

$$\begin{aligned}
U_M &= \frac{1}{M} \sum_{\ell \in [M]} \sup_{k \in \mathcal{K}_n} |R(\tilde{f}_{1,k}; \mathcal{D}_n, \{I_{k,\ell}\}) - \mathfrak{R}_{1,k}|, \\
U'_M &= \frac{1}{M(M-1)} \sum_{i,j \in [M], i \neq j} \sup_{k \in \mathcal{K}_n} |R(\tilde{f}_{2,k}; \mathcal{D}_n, \{I_{k,i}, I_{k,j}\}) - \mathfrak{R}_{2,k}|
\end{aligned}$$

are U -statistics based on sample $\mathcal{D}_{I_1}, \dots, \mathcal{D}_{I_M}$. Theorem 2 in Section 3.4.2 of Lee (1990) implies that $\{U_M\}_{M \geq 1}$ and $\{U'_M\}_{M \geq 2}$ are a reverse martingale conditional on \mathcal{D}_n with respect to some filtration. This combined with Theorem 3 (maximal inequality for reverse martingales) in Section 3.4.1 of Lee (1990) (for $r = 1$) yields

$$\mathbb{P} \left(\sup_{M \geq 1} |U_M| \geq \delta \right) \leq \frac{1}{\delta} \mathbb{E} [|U_1|] = \frac{1}{\delta} \mathbb{E} \left[\sup_{k \in \mathcal{K}_n} |R(\tilde{f}_{1,k}; \mathcal{D}_n, \{I_{k,1}\}) - \mathfrak{R}_{1,k}| \right].$$

On the other hand, from Lemma S1.3, the expectations are bounded as

$$\mathbb{E} \left[\sup_{k \in \mathcal{K}_n} |R(\tilde{f}_{1,k}; \mathcal{D}_n, \{I_{k,1}\}) - \mathfrak{R}_{1,k}| \right] = \mathcal{O}(n^\epsilon \gamma_{1,n}).$$

It follows that

$$\sup_{M \geq 1} |U_M| = \mathcal{O}_p(n^\epsilon \gamma_{1,n}).$$

Analogously, for the second U -statistic we also have

$$\sup_{M \geq 2} |U'_M| = \mathcal{O}_p(n^\epsilon \gamma_{2,n}).$$

From (S1.14), it follows that

$$\begin{aligned}
&\sup_{M \in \mathbb{N}, k \in \mathcal{K}_n} |R(\tilde{f}_M; \mathcal{D}_n, \{I_{k,\ell}\}_{\ell=1}^M) - \mathfrak{R}_{M,k}| \\
&= \sup_{M \geq 1} |U_M| + 2 \sup_{M \geq 2} |U'_M| \\
&= \mathcal{O}_p(n^\epsilon (\gamma_{1,n} + \gamma_{2,n})). \tag{S1.15}
\end{aligned}$$

□

S2 Proofs of results in Section 4

S2.1 Proof of Theorem 4.1 (δ -optimality of ECV)

Proof of Theorem 4.1. For simplicity, we denote $R(\tilde{f}_{M,k}; \mathcal{D}_n, \{I_{k,\ell}\}_{\ell=1}^M)$ by $R_{M,k}$ as a function of M and k . We split the proof for the two parts below.

Part (1) Error bound on the estimated risk. From Proposition 3.3, we have

$$\sup_{M \in \mathbb{N}, k \in \mathcal{K}_n} |\widehat{R}_{M,k}^{\text{ECV}} - R_{M,k}| = \mathcal{O}_p(\zeta_n),$$

where $\zeta_n = \widehat{\sigma}_n \log n/n^{1/2} + n^\epsilon(\gamma_{1,n} + \gamma_{2,n})$ and $\widehat{\sigma}_n = \max_{m, \ell \in [M_0], k \in \mathcal{K}_n} \widehat{\sigma}_{I_{k,\ell} \cup I_{k,m}}$. Then the conditional risk of the ECV-tuned predictor $R_{\widehat{M}, \widehat{k}}$ admits

$$|\widehat{R}_{\widehat{M}, \widehat{k}}^{\text{ECV}} - R_{\widehat{M}, \widehat{k}}| \leq \sup_{M \in \mathbb{N}, k \in \mathcal{K}_n} |\widehat{R}_{M,k}^{\text{ECV}} - R_{M,k}| = \mathcal{O}_p(\zeta_n).$$

Part (2) Additive suboptimality. The proof proceeds in two steps.

Step 1: Bounding the difference between $\widehat{R}_{\infty}^{\text{ECV}}(\widetilde{f}_{M_0, \widehat{k}})$ and the oracle-tuned risk. Let

$$(M^*, k^*) \in \underset{M \in \mathbb{N}, k \in \mathcal{K}_n}{\operatorname{arginf}} R(\widetilde{f}_{M,k}; \mathcal{D}_n, \{I_\ell\}_{\ell=1}^M),$$

which is a tuple of random variables and also functions of n . For any $k \in \mathcal{K}_n$, by the risk decomposition (3.1) we have that

$$\inf_{M \in \mathbb{N}} R_{M,k} = R_{\infty,k}.$$

That is, $M^* = \infty$ is one minimizer for any $k \in \mathcal{K}_n$. Then it follows that

$$\widehat{R}_{\infty, \widehat{k}}^{\text{ECV}} = \inf_{k \in \mathcal{K}_n} R_{\infty,k} + \mathcal{O}_p(\zeta_n) = \inf_{M \in \mathbb{N}, k \in \mathcal{K}_n} R_{M,k} + \mathcal{O}_p(\zeta_n) \quad (\text{S2.1})$$

where the first equality is due to Proposition 3.3.

Step 2: δ optimality. Next, we bound the suboptimality by the triangle inequality:

$$\begin{aligned} & |R_{\widehat{M}, \widehat{k}} - \inf_{M \in \mathbb{N}, k \in \mathcal{K}_n} R_{M,k}| \\ &= |R_{\widehat{M}, \widehat{k}} - \widehat{R}_{\widehat{M}, \widehat{k}}^{\text{ECV}} + \widehat{R}_{\widehat{M}, \widehat{k}}^{\text{ECV}} - \widehat{R}_{\infty, \widehat{k}}^{\text{ECV}} + \widehat{R}_{\infty, \widehat{k}}^{\text{ECV}} - R_{\infty, k^*}| \\ &\leq |R_{\widehat{M}, \widehat{k}} - \widehat{R}_{\widehat{M}, \widehat{k}}^{\text{ECV}}| + |\widehat{R}_{\widehat{M}, \widehat{k}}^{\text{ECV}} - \widehat{R}_{\infty, \widehat{k}}^{\text{ECV}}| + |\widehat{R}_{\infty, \widehat{k}}^{\text{ECV}} - R_{\infty, k^*}|. \end{aligned} \quad (\text{S2.2})$$

From Part (1) we know that the first term in (S2.2) can be bounded as $|R_{\widehat{M}, \widehat{k}} - \widehat{R}_{\widehat{M}, \widehat{k}}^{\text{ECV}}| = \mathcal{O}_p(\zeta_n)$. From (S2.1) we know that the last term in (S2.2) can also be bounded as $|\widehat{R}_{\infty, \widehat{k}}^{\text{ECV}} - R_{\infty, k^*}| = \mathcal{O}_p(\zeta_n)$. It remains to bound the second term in (S2.2). By the definition of $\widehat{R}_{M,k}^{\text{ECV}}$ in (3.4), we have that

$$\widehat{R}_{\infty, k}^{\text{ECV}} = 2\widehat{R}_{2,k}^{\text{ECV}} - \widehat{R}_{1,k}^{\text{ECV}}.$$

Since $\widehat{M} = \lceil 2/\delta \cdot \widehat{R}_{1, \widehat{k}}^{\text{ECV}} - \widehat{R}_{2, \widehat{k}}^{\text{ECV}} \rceil \geq 2/\delta \cdot \widehat{R}_{1, \widehat{k}}^{\text{ECV}} - \widehat{R}_{2, \widehat{k}}^{\text{ECV}}$, the second term in (S2.2) is bounded by

$$|\widehat{R}_{\widehat{M}, \widehat{k}}^{\text{ECV}} - \widehat{R}_{\infty, \widehat{k}}^{\text{ECV}}| = \frac{2}{\widehat{M}} \left| \widehat{R}_{1, \widehat{k}}^{\text{ECV}} - \widehat{R}_{2, \widehat{k}}^{\text{ECV}} \right| \leq \delta. \quad (\text{S2.3})$$

Therefore, the δ -optimality conclusion on $\widehat{R}_{M,k}^{\text{ECV}}$ follows. \square

S2.2 Proof of multiplicative optimality

Proposition S2.1 (Multiplicative optimality). *Under the same conditions in Theorem 4.1, if $\int (y - \mathbb{E}[y | \mathbf{x}])^2 dP(\mathbf{x}, y)$ is lower bounded away from zero and $(\widehat{M}, \widehat{k})$ is defined for relative optimality such that*

$$\widehat{R}_{\widehat{M}, \widehat{k}}^{\text{ECV}} \leq (1 + \delta) \inf_{M \in \mathbb{N}, k \in \mathcal{K}_n} \widehat{R}_{M,k}^{\text{ECV}}, \quad (\text{S2.4})$$

then it holds that

$$R_{\widehat{M}, \widehat{k}} \leq (1 + \delta) \inf_{M \in \mathbb{N}, k \in \mathcal{K}_n} R_{M,k} (1 + \mathcal{O}_p(\zeta_n)).$$

Proof of Proposition S2.1. By definition of (S2.4), we have

$$\begin{aligned}\widehat{R}_{\widehat{M},\widehat{k}}^{\text{ECV}} &= (1 + \delta) \inf_{M \in \mathbb{N}, k \in \mathcal{K}_n} \widehat{R}_{M,k}^{\text{ECV}} \\ &\leq (1 + \delta) \left(\inf_{M \in \mathbb{N}, k \in \mathcal{K}_n} R_{M,k} + \mathcal{O}_p(\zeta_n) \right) \\ &= (1 + \delta) \inf_{M \in \mathbb{N}, k \in \mathcal{K}_n} R_{M,k} (1 + \mathcal{O}_p(\zeta_n)).\end{aligned}$$

where the inequality is from Theorem 4.1 and the last equality is from the assumption that the risks are lower bounded. Further, since from Proposition 3.3, $\sup_{M \in \mathbb{N}, k \in \mathcal{K}_n} |R_{M,k} - \widehat{R}_{M,k}^{\text{ECV}}| = \mathcal{O}_p(\zeta_n)$, we have

$$R_{\widehat{M},\widehat{k}} \leq \widehat{R}_{\widehat{M},\widehat{k}}^{\text{ECV}} + \mathcal{O}_p(\zeta_n) \leq (1 + \delta) \inf_{M \in \mathbb{N}, k \in \mathcal{K}_n} R_{M,k} (1 + \mathcal{O}_p(\zeta_n)).$$

□

S2.3 Proof of Proposition 4.3 (ECV for ridge predictors)

We consider Assumptions A1-A2 on the dataset \mathcal{D}_n to characterize the risk, which are standard in the study of the ridge and ridgeless regression under proportional asymptotics; see, e.g., Hastie et al. (2022); Patil et al. (2022a).

Assumption A1 (Feature model). The feature vectors $\mathbf{x}_i \in \mathbb{R}^p$, $i = 1, \dots, n$, multiplicatively decompose as $\mathbf{x}_i = \mathbf{\Sigma}^{1/2} \mathbf{z}_i$, where $\mathbf{\Sigma} \in \mathbb{R}^{p \times p}$ is a positive semi-definite matrix and $\mathbf{z}_i \in \mathbb{R}^p$ is a random vector containing i.i.d. entries with mean 0, variance 1, and bounded k th moment for $k \geq 2$. Let $\mathbf{\Sigma} = \mathbf{W} \mathbf{R} \mathbf{W}^\top$ denote the eigenvalue decomposition of the covariance matrix $\mathbf{\Sigma}$, where $\mathbf{R} \in \mathbb{R}^{p \times p}$ is a diagonal matrix containing eigenvalues (in non-increasing order) $r_1 \geq r_2 \geq \dots \geq r_p \geq 0$, and $\mathbf{W} \in \mathbb{R}^{p \times p}$ is an orthonormal matrix containing the associated eigenvectors $\mathbf{w}_1, \mathbf{w}_2, \dots, \mathbf{w}_p \in \mathbb{R}^p$. Let H_p denote the empirical spectral distribution of $\mathbf{\Sigma}$ (supported on $\mathbb{R}_{>0}$) whose value at any $r \in \mathbb{R}$ is given by

$$H_p(r) = \frac{1}{p} \sum_{i=1}^p \mathbb{1}_{\{r_i \leq r\}}.$$

Assume there exists $0 < r_{\min} \leq r_{\max} < \infty$ such that $r_{\min} \leq r_1 \leq r_p \leq r_{\max}$, and there exists a fixed distribution H such that $H_p \xrightarrow{d} H$ as $p \rightarrow \infty$.

Assumption A2 (Response model). The response variables $y_i \in \mathbb{R}$, $i = 1, \dots, n$, additively decompose as $y_i = \mathbf{x}_i^\top \boldsymbol{\beta}_0 + \varepsilon_i$, where $\boldsymbol{\beta}_0 \in \mathbb{R}^p$ is an unknown signal vector and ε_i is an unobserved error that is assumed to be independent of \mathbf{x}_i with mean 0, variance σ^2 , and bounded moment of order $4 + \delta$ for some $\delta > 0$. The ℓ_2 -norm of the signal vector $\|\boldsymbol{\beta}_0\|_2$ is uniformly bounded in p , and $\lim_{p \rightarrow \infty} \|\boldsymbol{\beta}_0\|_2^2 = \rho^2 < \infty$. Let G_p denote a certain distribution (supported on $\mathbb{R}_{>0}$) that encodes the components of the signal vector $\boldsymbol{\beta}_0$ in the eigenbasis of $\mathbf{\Sigma}$ via the distribution of (squared) projection of $\boldsymbol{\beta}_0$ along the eigenvectors \mathbf{w}_j , $1 \leq j \leq p$, whose value at any $r \in \mathbb{R}$ is given by

$$G_p(r) = \frac{1}{\|\boldsymbol{\beta}_0\|_2^2} \sum_{i=1}^p (\boldsymbol{\beta}_0^\top \mathbf{w}_i)^2 \mathbb{1}_{\{r_i \leq r\}}.$$

Assume there exists a fixed distribution G such that $G_p \xrightarrow{d} G$ as $p \rightarrow \infty$.

Under Assumptions A1-A2, we will show that $\widehat{\sigma}_n = o(1)$ when using with MOM. To prove the result for MEAN, we need the modified assumptions by replacing the bounded moment conditions on z_{ij} in Assumption A1 and ε_i in Assumption A1 by bounded ψ_2 -norm conditions.

We will analyze the bagged predictors (with M bags) in the proportional asymptotics regime, where the original data aspect ratio (p/n) converges to $\phi \in (0, \infty)$ as $n, p \rightarrow \infty$, and the subsample data aspect ratio (p/k) converges to ϕ_s as $k, p \rightarrow \infty$. Because $k \leq n$, ϕ_s is always no less than ϕ .

Proof of Proposition 4.3. We split the proof into different parts.

Part (1) Bounded moments of the risk for $M = 1$. For $I \in \mathcal{I}_k$, define \mathbf{L}_I be the diagonal matrix whose i th diagonal entry is one if $i \in I$ and zero otherwise, let $\widehat{\boldsymbol{\Sigma}}_I = \mathbf{X}^\top \mathbf{L}_I \mathbf{X} / |I|$. We begin with analyzing the risk for $M = 1$:

$$\begin{aligned} R(\widetilde{f}_{1,k}; \mathcal{D}_I) &= \mathbb{E}[(y_0 - \mathbf{x}_0^\top \boldsymbol{\beta}_0)^2] + \|\widehat{\boldsymbol{\beta}}_1(\mathcal{D}_I) - \boldsymbol{\beta}_0\|_{\widehat{\boldsymbol{\Sigma}}_I}^2 \\ &= \mathbb{E}[(y_0 - \mathbf{x}_0^\top \boldsymbol{\beta}_0)^2] + \boldsymbol{\beta}_0^\top \widehat{\boldsymbol{\Sigma}}_I (\widehat{\boldsymbol{\Sigma}}_I + \lambda \mathbf{I}_p)^{-2} \widehat{\boldsymbol{\Sigma}}_I \boldsymbol{\beta}_0 + \frac{1}{k^2} \boldsymbol{\varepsilon}^\top \mathbf{L}_I \mathbf{X} (\widehat{\boldsymbol{\Sigma}}_I + \lambda \mathbf{I}_p)^{-2} \mathbf{X}^\top \mathbf{L}_I \boldsymbol{\varepsilon}. \end{aligned} \quad (\text{S2.5})$$

Note that the first term is just a constant, and the last two terms can be bounded as:

$$\begin{aligned} \boldsymbol{\beta}_0^\top \widehat{\boldsymbol{\Sigma}}_I (\widehat{\boldsymbol{\Sigma}}_I + \lambda \mathbf{I}_p)^{-2} \widehat{\boldsymbol{\Sigma}}_I \boldsymbol{\beta}_0 &\leq \|\widehat{\boldsymbol{\Sigma}}_I (\widehat{\boldsymbol{\Sigma}}_I + \lambda \mathbf{I}_p)^{-2} \widehat{\boldsymbol{\Sigma}}_I\|_{\text{op}} \|\boldsymbol{\beta}_0\|_2^2 \\ &\leq \rho^2 \max_{j \in [p]} \frac{s_j(\widehat{\boldsymbol{\Sigma}}_I)^2}{(\lambda + s_j(\widehat{\boldsymbol{\Sigma}}_I))^2} \\ &\leq \rho^2 \\ \frac{1}{k^2} \boldsymbol{\varepsilon}^\top \mathbf{L}_I \mathbf{X} (\widehat{\boldsymbol{\Sigma}}_I + \lambda \mathbf{I}_p)^{-2} \mathbf{X}^\top \mathbf{L}_I \boldsymbol{\varepsilon} &\leq \frac{1}{k^2} \|\mathbf{L}_I \mathbf{X} (\widehat{\boldsymbol{\Sigma}}_I + \lambda \mathbf{I}_p)^{-2} \mathbf{X}^\top \mathbf{L}_I\|_{\text{op}} \|\mathbf{L}_I \boldsymbol{\varepsilon}\|_2^2 \\ &\leq \frac{\|\mathbf{L}_I \boldsymbol{\varepsilon}\|_2^2}{k} \max_{j \in [p]} \frac{s_j(\widehat{\boldsymbol{\Sigma}}_I)}{(\lambda + s_j(\widehat{\boldsymbol{\Sigma}}_I))^2} \\ &\leq \frac{\|\mathbf{L}_I \boldsymbol{\varepsilon}\|_2^2}{k\lambda}, \end{aligned}$$

where $s_j(\widehat{\boldsymbol{\Sigma}}_I) \geq 0$ is the j th eigenvalue of $\widehat{\boldsymbol{\Sigma}}_I$. For all $q \leq 2 + \delta/2$, it follows that

$$\begin{aligned} \|R(\widetilde{f}_{1,k}; \mathcal{D}_I)\|_{L_q} &\leq \mathbb{E}[(y_0 - \mathbf{x}_0^\top \boldsymbol{\beta}_0)^2] + \rho^2 + \frac{1}{k\lambda} \|\|\mathbf{L}_I \boldsymbol{\varepsilon}\|_2^2\|_{L_q} \\ &\leq \mathbb{E}[(y_0 - \mathbf{x}_0^\top \boldsymbol{\beta}_0)^2] + \rho^2 + \frac{1}{\lambda} \max_{j \in [n]} \|\epsilon_j^2\|_{L_q} =: C_{0,q}. \end{aligned}$$

From the bounded moment assumption [A2](#), we know that $\|\epsilon_j^2\|_{L_q} < \infty$ for all j . Thus, $\|R(\widetilde{f}_{1,k}; \mathcal{D}_I)\|_{L_q}$ is upper bounded by constant $C_{0,q}$ for all $n \in \mathbb{N}$.

Part (2) Uniform integrability of the risk for $M = 1$. Under Assumptions [A1-A2](#), from [Patil et al. \(2022a, Theorem 4.1\)](#) we have that there exist deterministic functions \mathfrak{R}_1 and \mathfrak{R}_2 such that, for all $I \in \mathcal{I}_k$ and $\{I_1, I_2\} \stackrel{\text{SRS}}{\sim} \mathcal{I}_k$,

$$R(\widetilde{f}_{1,k}; \mathcal{D}_I) - \mathfrak{R}_1(\phi, \phi_s) \xrightarrow{\text{a.s.}} 0, \quad R(\widetilde{f}_{2,k}; \mathcal{D}_n, \{I_1, I_2\}) - \mathfrak{R}_2(\phi, \phi_s) \xrightarrow{\text{a.s.}} 0, \quad (\text{S2.6})$$

as $k, n, p \rightarrow \infty$, $p/n \rightarrow \phi \in [\psi, \psi^{-1}]$ and $p/k \rightarrow \phi_s \in [\phi, \psi^{-1}]$. Furthermore, \mathfrak{R}_1 and \mathfrak{R}_2 are continuous function on ϕ_s for any ϕ , which are bounded in the domain. To verify the tail bound condition for $M = 1$, [Hastie et al. \(2022, Theorem 5\)](#) shows that

$$\mathbb{P}(n^{(1-\epsilon')/2} |R(\widetilde{f}_{1,k}; \mathcal{D}_I) - \mathfrak{R}_1(\phi, \phi_s)| \geq C_1) \leq Cn^{-D},$$

where $C_1 = C(\rho^2 + \lambda^{-1})\lambda^{-1}$ for any $D, \epsilon' > 0$ and the constant C depends on ϵ' , D and other model parameters. For all $q \leq 1 + \delta/4$, let $\gamma_{1,n} = n^{-(1-\epsilon')/(2q)}$ and $Z_n = \gamma_{1,n}^{-1} |R(\widetilde{f}_{1,k}; \mathcal{D}_I) - \mathfrak{R}_1(\phi, \phi_s)|$. Then, we have $\mathbb{P}(Z_n^q \geq C_1^q) \leq 1 - Cn^{-D}$, and

$$\begin{aligned} \mathbb{E}[Z_n^q] &= \mathbb{E}[Z_n^q \mathbf{1}\{Z_n < C_1\}] + \mathbb{E}[Z_n^q \mathbf{1}\{Z_n \geq C_1\}] \\ &\leq C_1^q + (\mathbb{E}[Z_n^{2q}])^{\frac{1}{2}} \mathbb{P}(Z_n \geq C_1)^{\frac{1}{2}} \\ &\leq C_1^q + (C_{0,2q}^q + \mathfrak{R}_1(\phi, \phi_s)^{\frac{q}{2}}) \gamma_{1,n}^{-q} 2^{q-1} C^{\frac{1}{2}} n^{-\frac{D}{2}}, \end{aligned}$$

where the first inequality is from Hölder's inequality. For $\epsilon' \in (0, 1)$ fixed, setting $D = (1 - \epsilon')/2$ yields that

$$\mathbb{E}[Z_n^q] \leq C_1^q + (C_{0,2q}^q + \mathfrak{R}_1(\phi, \phi_s)^{\frac{q}{2}})2^{q-1}C^{\frac{1}{2}},$$

Therefore, Z_n^q is uniformly integrable. By Chebyshev's inequality, we further have

$$\limsup_{n \rightarrow \infty} \sup_{\eta > 0} \eta^q \mathbb{P}(Z_n \geq \eta) \leq C_1^q + (C_{0,2q}^q + \mathfrak{R}_1(\phi, \phi_s)^{\frac{q}{2}})2^{q-1}C^{\frac{1}{2}}, \quad (\text{S2.7})$$

which implies Assumption 2 for $\gamma_{1,n} = n^{-(1-\epsilon')/2}$ and for any $\epsilon = 1/q$ where $q \leq 1 + \delta/4$.

Part (3) Concentration of the risk for $M = 2$. To show the existence of $\gamma_{2,n}$, from Patil et al. (2022a, Lemma 3.8.), we have that

$$R(\tilde{f}_{2,k}; \mathcal{D}_n, \{I_1, I_2\}) - \mathfrak{R}_2(\phi, \phi_s) \xrightarrow{\text{a.s.}} 0.$$

By convexity, we have

$$0 \leq R(\tilde{f}_{2,k}; \mathcal{D}_n, \{I_1, I_2\}) \leq 2^{-1}(R(\tilde{f}_{1,k}; \mathcal{D}_n, \{I_1\}) + R(\tilde{f}_{1,k}; \mathcal{D}_n, \{I_2\})),$$

which implies that

$$0 \leq R(\tilde{f}_{2,k}; \mathcal{D}_n, \{I_1, I_2\})^{1/\epsilon} \leq 2^{-1/\epsilon}(R(\tilde{f}_{1,k}; \mathcal{D}_n, \{I_1\}) + R(\tilde{f}_{1,k}; \mathcal{D}_n, \{I_2\}))^{1/\epsilon}. \quad (\text{S2.8})$$

We next apply Pratt's lemma to show $L^{1/\epsilon}$ -convergence for $M = 2$. Note that the tail bound condition (S2.7) implies $L^{1/\epsilon}$ -convergence:

$$\gamma_{1,n}^{-1/\epsilon} \mathbb{E}[(R(\tilde{f}_{1,k}; \mathcal{D}_n, \{I_j\}) - \mathfrak{R}_1(\phi, \phi_s))^{1/\epsilon}] \rightarrow 0, \quad j = 1, 2$$

and the $1/\epsilon$ -th moment converges:

$$\gamma_{1,n}^{-1/\epsilon} \mathbb{E}[R(\tilde{f}_{1,k}; \mathcal{D}_n, \{I_j\})^{1/\epsilon} - \mathfrak{R}_1(\phi, \phi_s)^{1/\epsilon}] \rightarrow 0, \quad j = 1, 2.$$

By Pratt's lemma (see, e.g., Gut, 2005, Theorem 5.5), we have the $1/\epsilon$ -th moment for $M = 2$ also converges:

$$\gamma_{1,n}^{-1/\epsilon} \mathbb{E}[R(\tilde{f}_{2,k}; \mathcal{D}_n, \{I_1, I_2\})^{1/\epsilon} - \mathfrak{R}_2(\phi, \phi_s)^{1/\epsilon}] \rightarrow 0.$$

From Gut (2005, Theorem 5.2), we further have $L^{1/\epsilon}$ -convergence for $M = 2$:

$$\gamma_{1,n}^{-1/\epsilon} \mathbb{E}[(R(\tilde{f}_{2,k}; \mathcal{D}_n, \{I_1, I_2\}) - \mathfrak{R}_2(\phi, \phi_s))^{1/\epsilon}] \rightarrow 0.$$

This implies that there exists a constant sequence of $\gamma'_{2,n}$ such that $\mathbb{E}[(R(\tilde{f}_{2,k}; \mathcal{D}_n, \{I_1, I_2\}) - \mathfrak{R}_2(\phi, \phi_s))^{1/\epsilon}] \leq \gamma'_{2,n}$ and $\gamma'_{2,n} \geq \gamma_{1,n}^{1/\epsilon}$. Hence, we can simply pick $\gamma'_{2,n} = \gamma_{1,n}^{1/\epsilon}$. Then, by Markov's inequality, we have that for all $\eta' > 0$

$$\mathbb{P}(|R(\tilde{f}_{2,k}; \mathcal{D}_n, \{I_1, I_2\}) - \mathfrak{R}_2(\phi, \phi_s)|^{1/\epsilon} > \eta') \leq \gamma'_{2,n}/\eta',$$

or equivalently for all $\eta > 1$,

$$\mathbb{P}(|R(\tilde{f}_{2,k}; \mathcal{D}_n, \{I_1, I_2\}) - \mathfrak{R}_2(\phi, \phi_s)| > \eta\gamma_{2,n}) \leq 1/\eta^{1/\epsilon},$$

where $\gamma_{2,n} = \gamma_{2,n}^{\epsilon}$ and $\gamma_{2,n} = o(n^{-\epsilon})$. Thus, Assumption 2 is satisfied under proportional asymptotics.

Part (4) Bounded variance proxy for CV estimates. From results by Patil et al. (2022b, Remark 2.19), Assumption A1 in random matrix theory implies $L_4 - L_2$ norm equivalence, since the components of \mathbf{Z} are independent and have bounded kurtosis. Invoking Proposition 2.16 of Patil et al. (2022b), there exists $\tau > 0$ such that

$$\hat{\sigma}_I \leq \tau \inf_{\boldsymbol{\beta} \in \mathbb{R}^p} (\|y_0 - \mathbf{x}_0^\top \boldsymbol{\beta}\|_{L_2} + \|\boldsymbol{\beta} - \hat{\boldsymbol{\beta}}_\lambda(\mathcal{D}_I)\|_{\Sigma})^2.$$

When $\boldsymbol{\beta} = \boldsymbol{\beta}_0$, $\|y_0 - \mathbf{x}_0^\top \boldsymbol{\beta}_0\|_{L_2} = \sigma$ and $\|\boldsymbol{\beta}_0 - \hat{\boldsymbol{\beta}}_\lambda(\mathcal{D}_I)\|_{\Sigma} \xrightarrow{\text{a.s.}} \mathfrak{R}_1(\phi, \phi_s)$, which is continuous and bounded in $\phi \in [\psi, \psi^{-1}]$ and $\phi_s \in [\phi, \psi^{-1}]$. This implies that $\hat{\sigma}_I = \mathcal{O}_p(1)$. Analogously, $\hat{\sigma}_{I_1 \cup I_2} = \mathcal{O}_p(1)$ and hence it holds for EST = MOM.

Combining the parts above finishes the proof. \square

S3 Helper concentration results

S3.1 Size of the intersection of randomly sampled datasets

In this section, we collect a helper result concerned with convergences that are used in the proofs of Theorem 4.1. Before stating the lemma, we recall the definition of a hypergeometric random variable below, along with its mean and variance. See, e.g., [Greene and Wellner \(2017\)](#) for more related details.

Definition S3.1 (Hypergeometric random variable). *A random variable X follows the hypergeometric distribution $X \sim \text{Hypergeometric}(n, K, N)$ if its probability mass function is given by*

$$\mathbb{P}(X = k) = \frac{\binom{K}{k} \binom{N-K}{n-k}}{\binom{N}{n}}, \quad \max\{0, n + K - N\} \leq k \leq \min\{n, K\}.$$

The expectation and variance of X are given by

$$\mathbb{E}[X] = \frac{nK}{N}, \quad \text{Var}(X) = \frac{nK(N-K)(N-n)}{N^2(N-1)}.$$

The following lemma characterizes the limiting proportions of shared observations in two simple random samples under proportional asymptotics when both the subsample size k and the full data size n tend to infinity.

Lemma S3.2 (Asymptotic proportions of shared observations, adapted from [Patil et al. \(2022a\)](#)). *For $n \in \mathbb{N}$, define $\mathcal{I}_k := \{\{i_1, i_2, \dots, i_k\} : 1 \leq i_1 < i_2 < \dots < i_k \leq n\}$. Let $I_1, I_2 \stackrel{\text{SRSWR}}{\sim} \mathcal{I}_k$, define the random variable $i_0^{\text{SRSWR}} := |I_1 \cap I_2|$ to be the number of shared samples, and define i_0^{SRSWOR} accordingly. Then $i_0^{\text{SRSWR}} \sim \text{Binomial}(k, k/n)$ and $i_0^{\text{SRSWOR}} \sim \text{Hypergeometric}(k, k, n)$. Let $\{k_m\}_{m=1}^\infty$ and $\{n_m\}_{m=1}^\infty$ be two sequences of positive integers such that n_m is strictly increasing in m , $n_m^\nu \leq k_m \leq n_m$ for some constant $\nu \in (0, 1)$. Then, $i_0^{\text{SRSWR}}/k_m - k_m/n_m \xrightarrow{\text{a.s.}} 0$, and $i_0^{\text{SRSWOR}}/k_m - k_m/n_m \xrightarrow{\text{a.s.}} 0$.*

S4 Computational complexity of Algorithm 1

For each $k \in \mathcal{K}_n$, suppose the computational complexity of fitting one base predictor on k subsampled observations and obtain their predicted values on $n - k$ OOB observations is $\mathcal{O}(C_n)$ (ignoring k). We analyze the computational complexity of estimating \widehat{M} and \widehat{k} for all three validation methods as below:

- **ECV**: For each $k \in \mathcal{K}_n$, we need to fit M_0 base predictors. Then we estimate $R_{1,k}$ and $R_{2,k}$ in $\mathcal{O}(M_0(n - k))$ and $\mathcal{O}(M_0^2(n - 2k + i_0))$, respectively, where $i_0 = k^2/n$ is the intersect observations between two indices of a simple random sample. The computational complexity of risk extrapolation is negligible compared to the above time consumption. All in all, it takes $\mathcal{O}(C_n(|\mathcal{K}_n|M_0 + M_{\max}))$ to obtain tuned bagging parameter by ECV.
- **splitCV**: Suppose the ratio of training data is $\alpha \in (0, 1)$. Similar to ECV, each base predictor is fitted and evaluated on $\lceil n\alpha \rceil$ observations and we need to fit M_{\max} base predictors. We then compute the moving average of the predicted values for M varying from 1 to M_{\max} , which gives the predicted values of the M -bagged predictors, which takes $\mathcal{O}(M_{\max})$ operations. We note that one can alternatively fit one bagged predictor for each k and each M ; however, this will cause much more time consumption compared to the simple matrix computation operations we used above. All in all, it takes $\mathcal{O}(|\mathcal{K}_n|M_{\max}(C_{n\alpha} + n))$ to obtain the tuned parameter.
- **KfoldCV**: We follow the same strategy for fitting base predictors so that KfoldCV has roughly K times of complexity as splitCV. Specifically, it takes $\mathcal{O}(K|\mathcal{K}_n|M_{\max}(C_{n/K} + n))$ to obtain the tuned parameter.

In general, we would expect C_n to grow much faster than n , because fitting one base predictor may involve matrix multiplication operation, which takes $\mathcal{O}(n^2)$. Therefore, the computational complexity of the three methods has the ordering: $\text{ECV} \leq \text{splitCV} \leq \text{KfoldCV}$, provided that M_0 is much smaller than M_{\max} .

S5 Additional experimental results

S5.1 Risk estimation and extrapolation in Section 5.1

Subbagging

$\phi = p/n$	Predictors					
	ridgeless	ridge	lassoless	lasso	logistic	kNN
0.1 (underparameterized)	Fig. S2	Fig. 2	Fig. S3	Fig. S4	Fig. S5	Fig. S6
1.1 (overparameterized)	Fig. S7	Fig. S8	Fig. S9	Fig. S10	Fig. S11	Fig. S12

Table S1: Summary of experimental results in Section 4

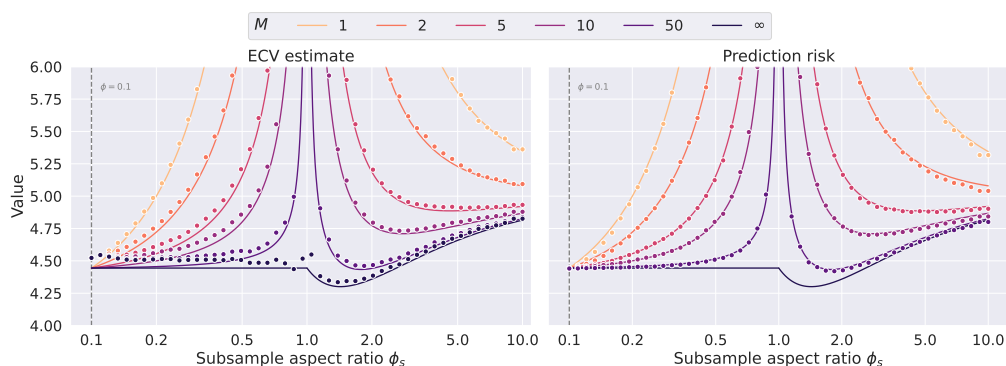


Figure S2: Finite-sample ECV estimate (left panel) and prediction risk (right panel) for ridgeless predictors ($\lambda = 0$), under model (M-ISO-LI) when $\rho^2 = 1$ and $\sigma^2 = 0.01$ for varying bag size $k = \lfloor p/\phi_s \rfloor$, and number of bags M . The lines denote the theoretical asymptotic prediction risk curves. For each value of M , the points denote the finite-sample ECV cross-validation estimates (3.4) computed on $M_0 = 10$ bags or the out-of-sample prediction error computed on $n_{te} = 1,000$ samples, averaged over 100 dataset repetitions, with $n = 1,000$ and $p = \lfloor n\phi \rfloor$, and $\phi = 0.1$ ($p < n$).

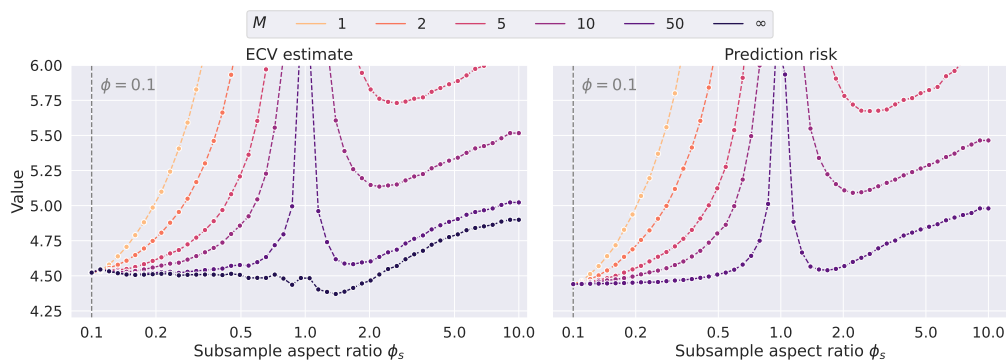


Figure S3: Finite-sample ECV estimate (left panel) and prediction risk (right panel) for lassoless predictors ($\lambda = 0$), under model (M-ISO-LI) when $\rho^2 = 1$ and $\sigma^2 = 0.25$ for varying bag size $k = \lfloor p/\phi_s \rfloor$, and number of bags M . For each value of M , the points denote the finite-sample ECV cross-validation estimates (3.4) computed on $M_0 = 10$ bags or the out-of-sample prediction error computed on $n_{te} = 1,000$ samples, averaged over 100 dataset repetitions, with $n = 1,000$ and $p = \lfloor n\phi \rfloor$, and $\phi = 0.1$ ($p < n$).

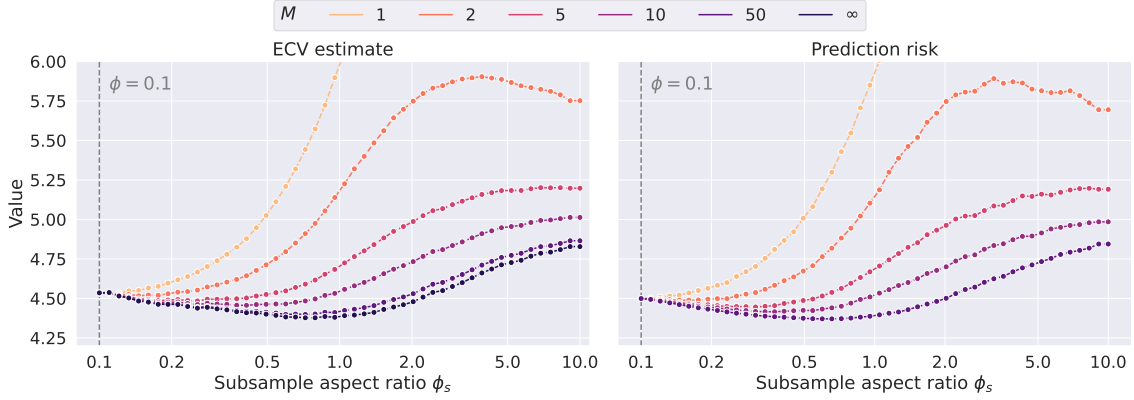


Figure S4: Finite-sample ECV estimate (left panel) and prediction risk (right panel) for lasso predictors ($\lambda = 0.1$), under model (M-ISO-LI) when $\rho^2 = 1$ and $\sigma^2 = 0.25$ for varying bag size $k = \lfloor p/\phi_s \rfloor$, and number of bags M . For each value of M , the points denote the finite-sample ECV cross-validation estimates (3.4) computed on $M_0 = 10$ bags or the out-of-sample prediction error computed on $n_{te} = 1,000$ samples, averaged over 100 dataset repetitions, with $n = 1,000$ and $p = \lfloor n\phi \rfloor$, and $\phi = 0.1$ ($p < n$).

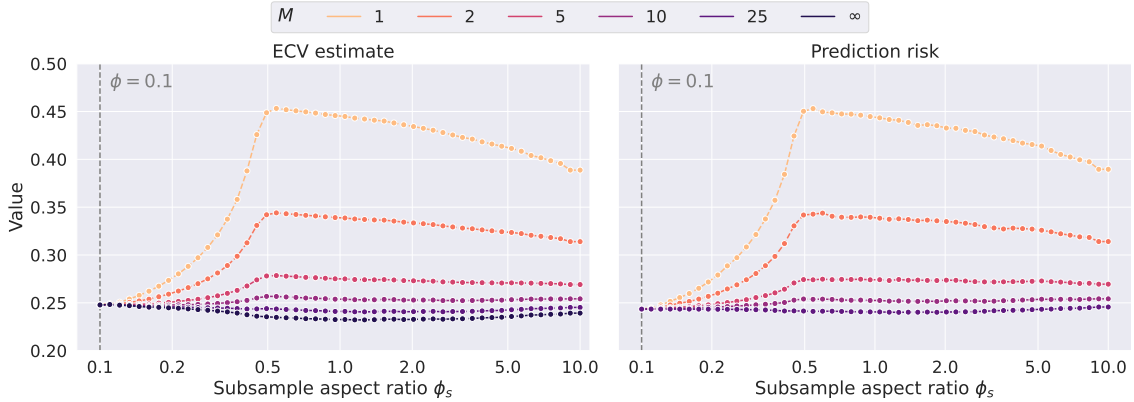


Figure S5: Finite-sample ECV estimate (left panel) and prediction risk (right panel) for Logistic predictors, under model (M-ISO-LI) when $\rho^2 = 1$ and $\sigma^2 = 0.25$ for varying bag size $k = \lfloor p/\phi_s \rfloor$, and number of bags M . For each value of M , the points denote the finite-sample ECV cross-validation estimates (3.4) computed on $M_0 = 10$ bags or the out-of-sample prediction error computed on $n_{te} = 1,000$ samples, averaged over 100 dataset repetitions, with $n = 1,000$ and $p = \lfloor n\phi \rfloor$, and $\phi = 0.1$ ($p < n$).

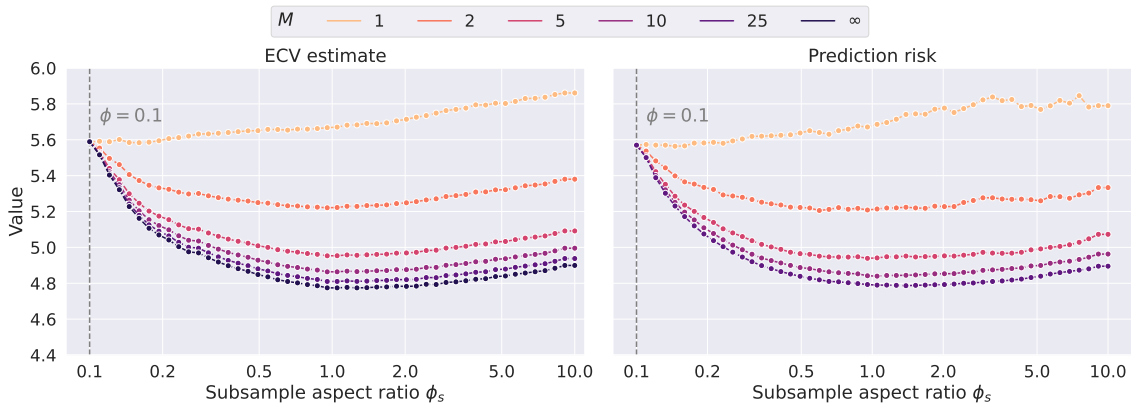


Figure S6: Finite-sample ECV estimate (left panel) and prediction risk (right panel) for K-nearest neighbors predictors, under model (M-ISO-LI) when $\rho^2 = 1$ and $\sigma^2 = 0.25$ for varying bag size $k = \lfloor p/\phi_s \rfloor$, and number of bags M . For each value of M , the points denote the finite-sample ECV cross-validation estimates (3.4) computed on $M_0 = 10$ bags or the out-of-sample prediction error computed on $n_{te} = 1,000$ samples, averaged over 100 dataset repetitions, with $n = 1,000$ and $p = \lfloor n\phi \rfloor$, and $\phi = 0.1$ ($p < n$).

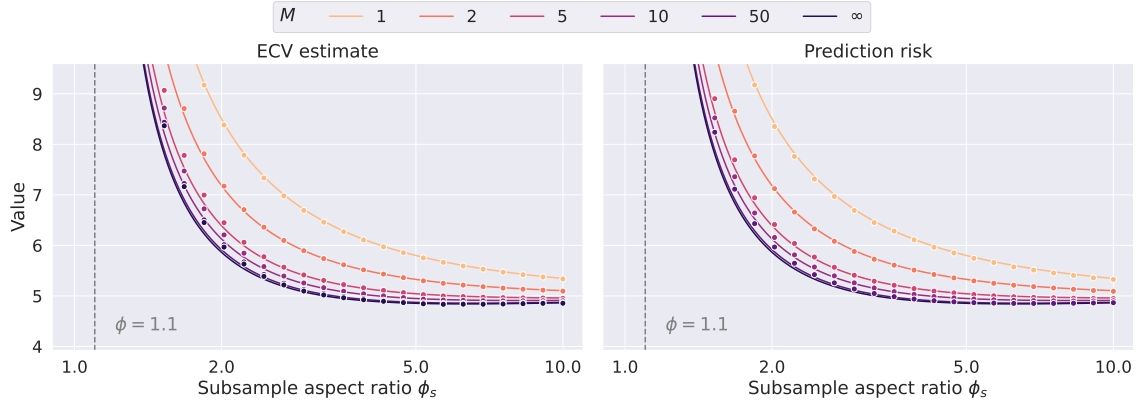


Figure S7: Finite-sample ECV estimate (left panel) and prediction risk (right panel) for ridgeless predictors ($\lambda = 0$), under model (M-ISO-LI) when $\rho^2 = 1$ and $\sigma^2 = 0.01$ for varying bag size $k = \lfloor p/\phi_s \rfloor$, and number of bags M . The lines denote the theoretical asymptotic prediction risk curves. For each value of M , the points denote the finite-sample ECV cross-validation estimates (3.4) computed on $M_0 = 10$ bags or the out-of-sample prediction error computed on $n_{te} = 1,000$ samples, averaged over 100 dataset repetitions, with $n = 1,000$ and $p = \lfloor n\phi \rfloor$, and $\phi = 1.1$ ($p > n$).

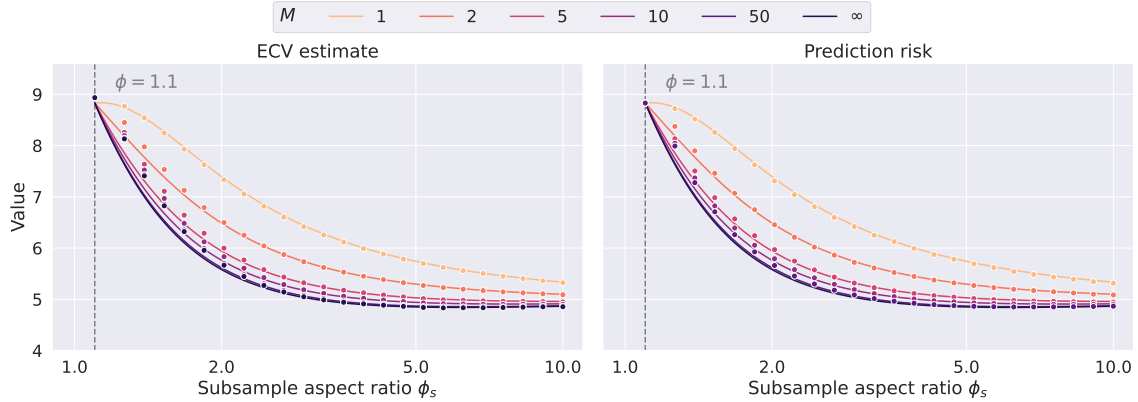


Figure S8: Finite-sample ECV estimate (left panel) and prediction risk (right panel) for ridge predictors ($\lambda = 0.1$), under model (M-ISO-LI) when $\rho^2 = 1$ and $\sigma^2 = 0.01$ for varying bag size $k = \lfloor p/\phi_s \rfloor$, and number of bags M . The lines denote the theoretical asymptotic prediction risk curves. For each value of M , the points denote the finite-sample ECV cross-validation estimates (3.4) computed on $M_0 = 10$ bags or the out-of-sample prediction error computed on $n_{te} = 1,000$ samples, averaged over 100 dataset repetitions, with $n = 1,000$ and $p = \lfloor n\phi \rfloor$, and $\phi = 1.1$ ($p > n$).

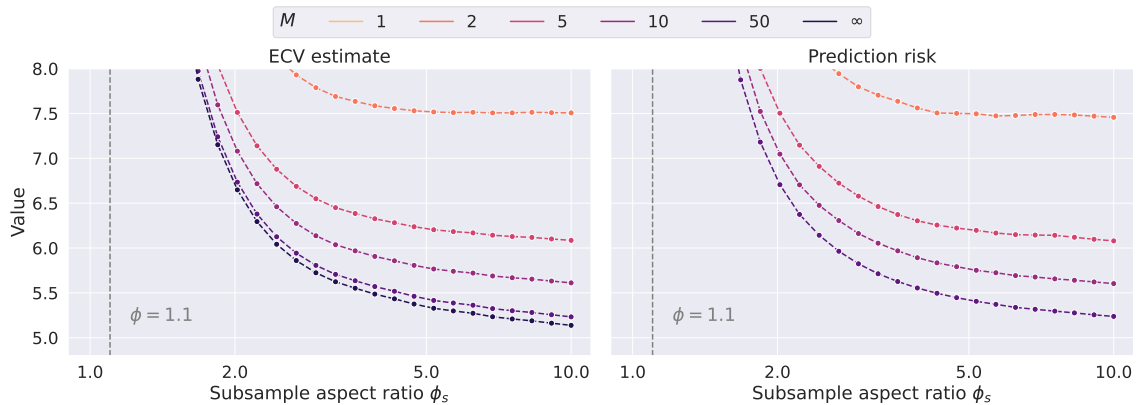


Figure S9: Finite-sample ECV estimate (left panel) and prediction risk (right panel) for lassoless predictors ($\lambda = 0$), under model (M-ISO-LI) when $\rho^2 = 1$ and $\sigma^2 = 0.25$ for varying bag size $k = \lfloor p/\phi_s \rfloor$, and number of bags M . For each value of M , the points denote the finite-sample ECV cross-validation estimates (3.4) computed on $M_0 = 10$ bags or the out-of-sample prediction error computed on $n_{te} = 1,000$ samples, averaged over 100 dataset repetitions, with $n = 1,000$ and $p = \lfloor n\phi \rfloor$, and $\phi = 1.1$ ($p > n$).

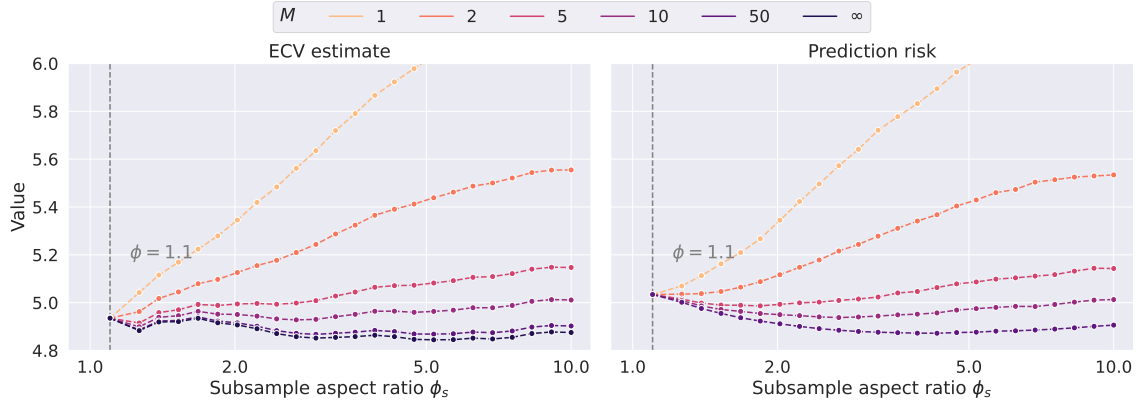


Figure S10: Finite-sample ECV estimate (left panel) and prediction risk (right panel) for lasso predictors ($\lambda = 0.1$), under model (M-ISO-LI) when $\rho^2 = 1$ and $\sigma^2 = 0.25$ for varying bag size $k = \lfloor p/\phi_s \rfloor$, and number of bags M . For each value of M , the points denote the finite-sample ECV cross-validation estimates (3.4) computed on $M_0 = 10$ bags or the out-of-sample prediction error computed on $n_{te} = 1,000$ samples, averaged over 100 dataset repetitions, with $n = 1,000$ and $p = \lfloor n\phi \rfloor$, and $\phi = 1.1$ ($p > n$).

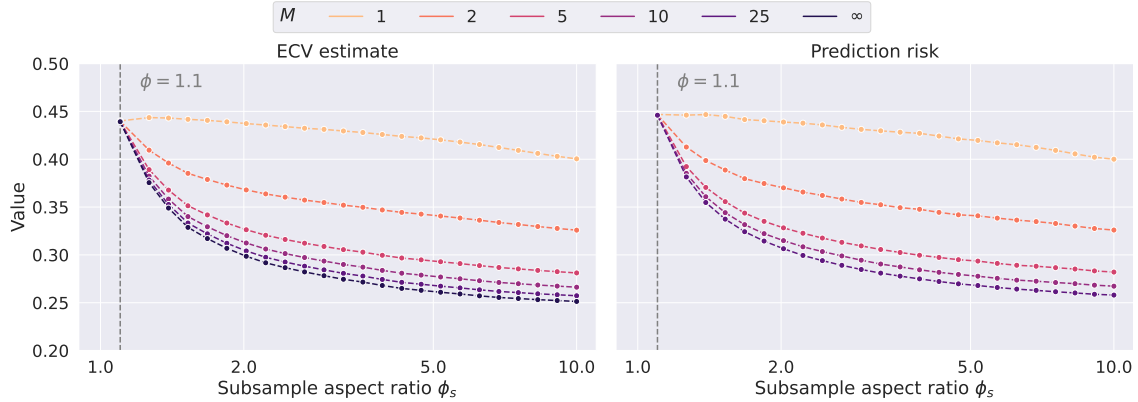


Figure S11: Finite-sample ECV estimate (left panel) and prediction risk (right panel) for Logistic predictors, under model (M-ISO-LI) when $\rho^2 = 1$ and $\sigma^2 = 0.25$ for varying bag size $k = \lfloor p/\phi_s \rfloor$, and number of bags M . For each value of M , the points denote the finite-sample ECV cross-validation estimates (3.4) computed on $M_0 = 10$ bags or the out-of-sample prediction error computed on $n_{te} = 1,000$ samples, averaged over 100 dataset repetitions, with $n = 1,000$ and $p = \lfloor n\phi \rfloor$, and $\phi = 1.1$ ($p > n$).

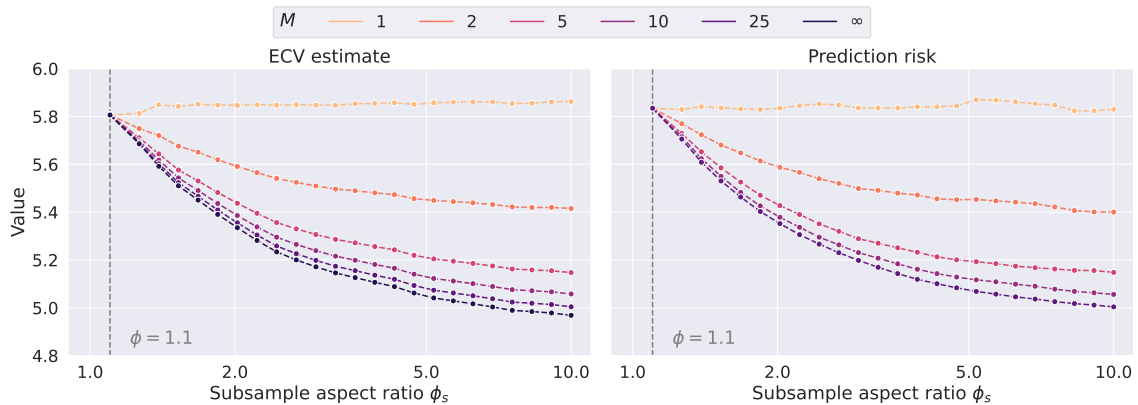


Figure S12: Finite-sample ECV estimate (left panel) and prediction risk (right panel) for k-nearest neighbors predictors, under model (M-ISO-LI) when $\rho^2 = 1$ and $\sigma^2 = 0.25$ for varying bag size $k = \lfloor p/\phi_s \rfloor$, and the number of bags M . For each value of M , the points denote the finite-sample ECV cross-validation estimates (3.4) computed on $M_0 = 10$ bags or the out-of-sample prediction error computed on $n_{te} = 1,000$ samples, averaged over 100 dataset repetitions, with $n = 1,000$ and $p = \lfloor n\phi \rfloor$, and $\phi = 1.1$ ($p > n$).

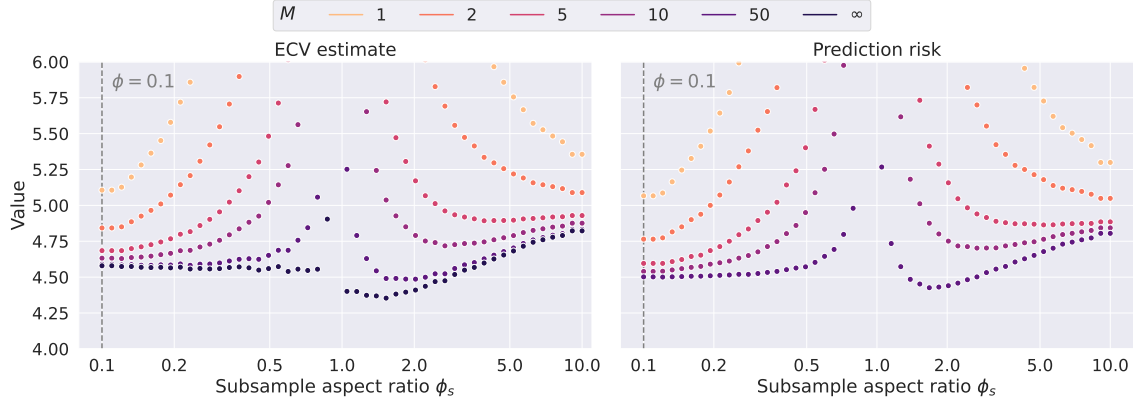


Figure S13: Finite-sample ECV estimate (left panel) and prediction risk (right panel) for ridgeless predictors ($\lambda = 0$), under model (M-ISO-LI) when $\rho^2 = 1$ and $\sigma^2 = 0.01$ for varying bag size $k = \lfloor p/\phi_s \rfloor$, and number of bags M . The lines denote the theoretical asymptotic prediction risk curves. For each value of M , the points denote the finite-sample ECV cross-validation estimates (3.4) computed on $M_0 = 10$ bags or the out-of-sample prediction error computed on $n_{te} = 1,000$ samples, averaged over 100 dataset repetitions, with $n = 1,000$ and $p = \lfloor n\phi \rfloor$, and $\phi = 0.1$ ($p < n$).

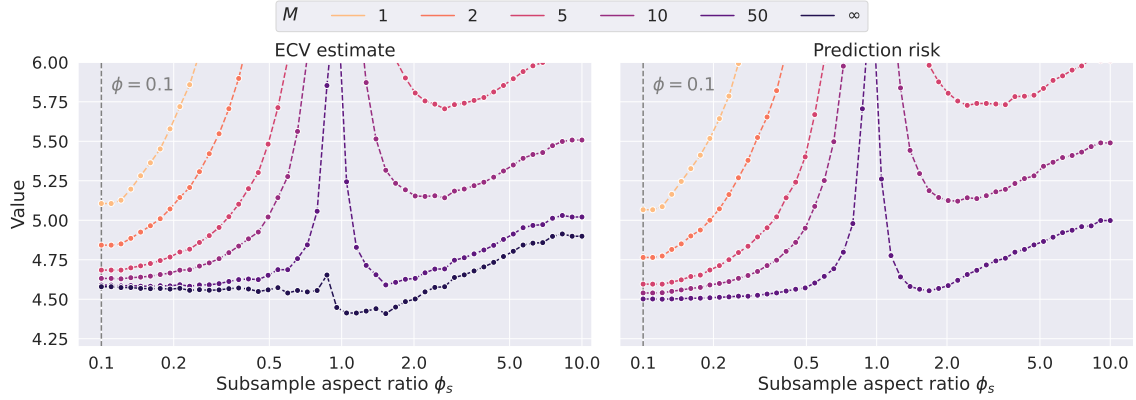


Figure S14: Finite-sample ECV estimate (left panel) and prediction risk (right panel) for lassoless predictors ($\lambda = 0$), under model (M-ISO-LI) when $\rho^2 = 1$ and $\sigma^2 = 0.25$ for varying bag size $k = \lfloor p/\phi_s \rfloor$, and number of bags M . For each value of M , the points denote the finite-sample ECV cross-validation estimates (3.4) computed on $M_0 = 10$ bags or the out-of-sample prediction error computed on $n_{te} = 1,000$ samples, averaged over 100 dataset repetitions, with $n = 1,000$ and $p = \lfloor n\phi \rfloor$, and $\phi = 0.1$ ($p < n$).

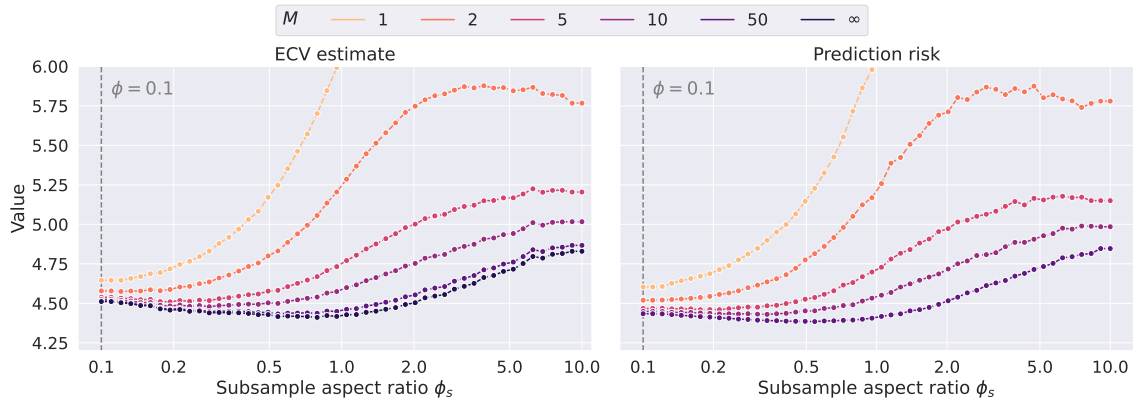


Figure S15: Finite-sample ECV estimate (left panel) and prediction risk (right panel) for lasso predictors ($\lambda = 0.1$), under model (M-ISO-LI) when $\rho^2 = 1$ and $\sigma^2 = 0.25$ for varying bag size $k = \lfloor p/\phi_s \rfloor$, and number of bags M . For each value of M , the points denote the finite-sample ECV cross-validation estimates (3.4) computed on $M_0 = 10$ bags or the out-of-sample prediction error computed on $n_{te} = 1,000$ samples, averaged over 100 dataset repetitions, with $n = 1,000$ and $p = \lfloor n\phi \rfloor$, and $\phi = 0.1$ ($p < n$).

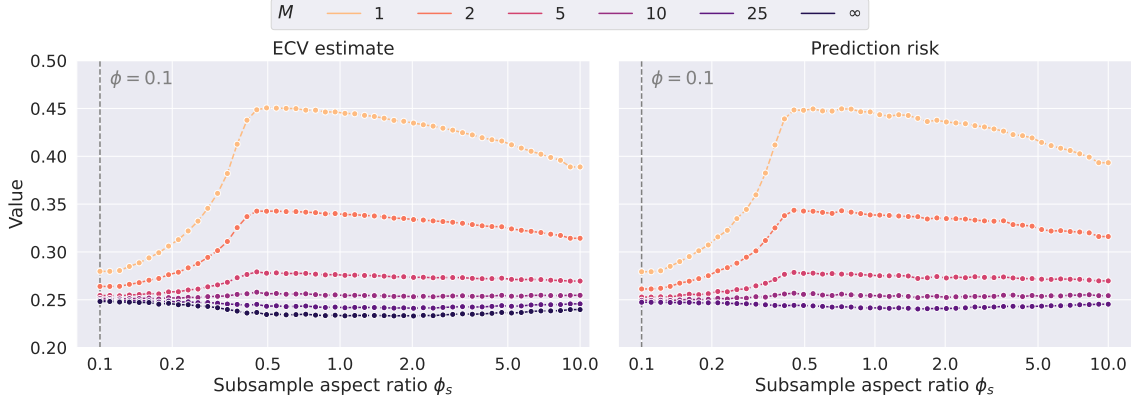


Figure S16: Finite-sample ECV estimate (left panel) and prediction risk (right panel) for Logistic predictors, under model (M-ISO-LI) when $\rho^2 = 1$ and $\sigma^2 = 0.25$ for varying bag size $k = \lfloor p/\phi_s \rfloor$, and number of bags M . For each value of M , the points denote the finite-sample ECV cross-validation estimates (3.4) computed on $M_0 = 10$ bags or the out-of-sample prediction error computed on $n_{te} = 1,000$ samples, averaged over 100 dataset repetitions, with $n = 1,000$ and $p = \lfloor n\phi \rfloor$, and $\phi = 0.1$ ($p < n$).

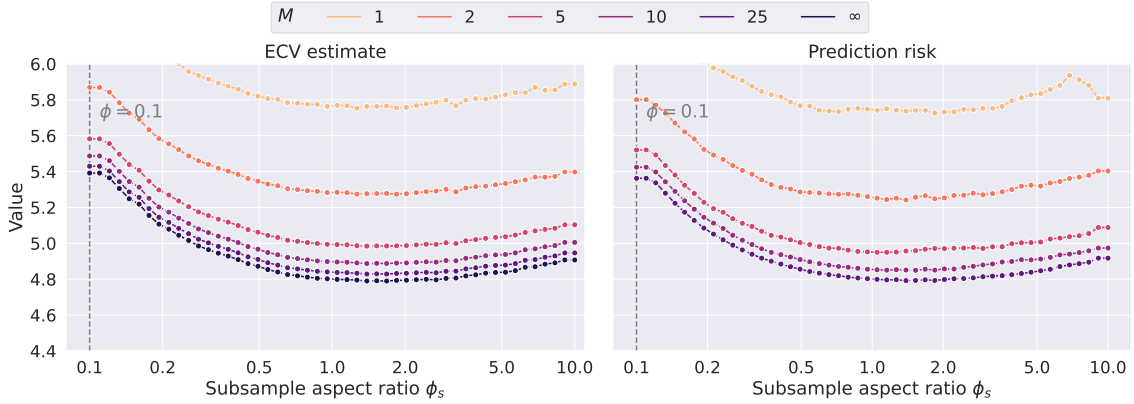


Figure S17: Finite-sample ECV estimate (left panel) and prediction risk (right panel) for K-nearest neighbors predictors, under model (M-ISO-LI) when $\rho^2 = 1$ and $\sigma^2 = 0.25$ for varying bag size $k = \lfloor p/\phi_s \rfloor$, and number of bags M . For each value of M , the points denote the finite-sample ECV cross-validation estimates (3.4) computed on $M_0 = 10$ bags or the out-of-sample prediction error computed on $n_{te} = 1,000$ samples, averaged over 100 dataset repetitions, with $n = 1,000$ and $p = \lfloor n\phi \rfloor$, and $\phi = 0.1$ ($p < n$).

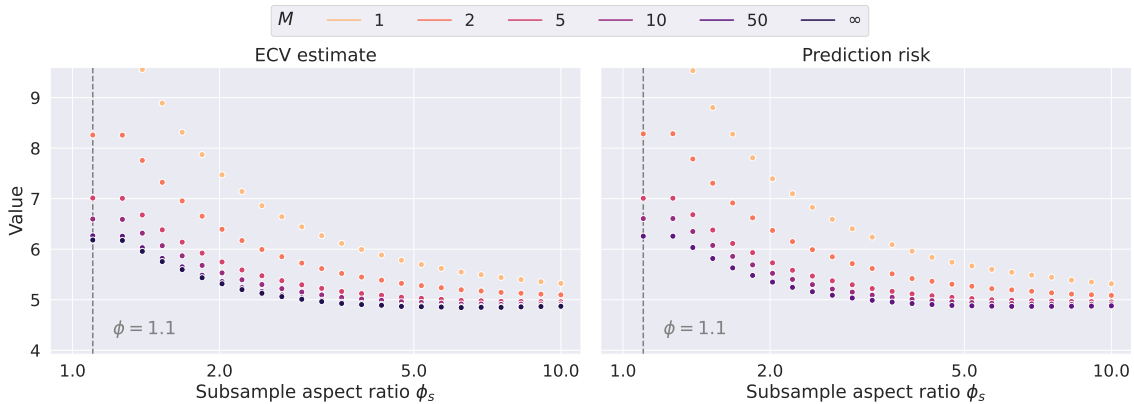


Figure S18: Finite-sample ECV estimate (left panel) and prediction risk (right panel) for ridgeless predictors ($\lambda = 0$), under model (M-ISO-LI) when $\rho^2 = 1$ and $\sigma^2 = 0.01$ for varying bag size $k = \lfloor p/\phi_s \rfloor$, and number of bags M . The lines denote the theoretical asymptotic prediction risk curves. For each value of M , the points denote the finite-sample ECV cross-validation estimates (3.4) computed on $M_0 = 10$ bags or the out-of-sample prediction error computed on $n_{te} = 1,000$ samples, averaged over 100 dataset repetitions, with $n = 1,000$ and $p = \lfloor n\phi \rfloor$, and $\phi = 1.1$ ($p > n$).

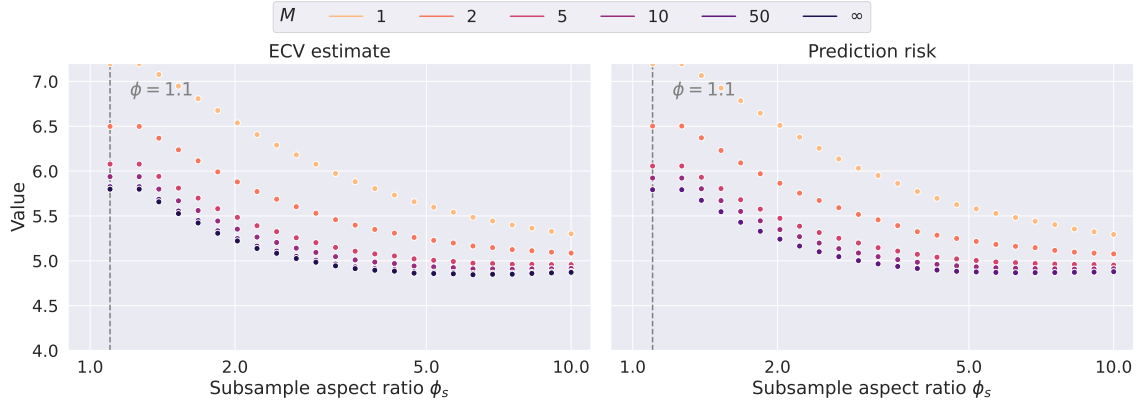


Figure S19: Finite-sample ECV estimate (left panel) and prediction risk (right panel) for ridge predictors ($\lambda = 0.1$), under model (M-ISO-LI) when $\rho^2 = 1$ and $\sigma^2 = 0.01$ for varying bag size $k = \lfloor p/\phi_s \rfloor$, and number of bags M . The lines denote the theoretical asymptotic prediction risk curves. For each value of M , the points denote the finite-sample ECV cross-validation estimates (3.4) computed on $M_0 = 10$ bags or the out-of-sample prediction error computed on $n_{te} = 1,000$ samples, averaged over 100 dataset repetitions, with $n = 1,000$ and $p = \lfloor n\phi \rfloor$, and $\phi = 1.1$ ($p > n$).

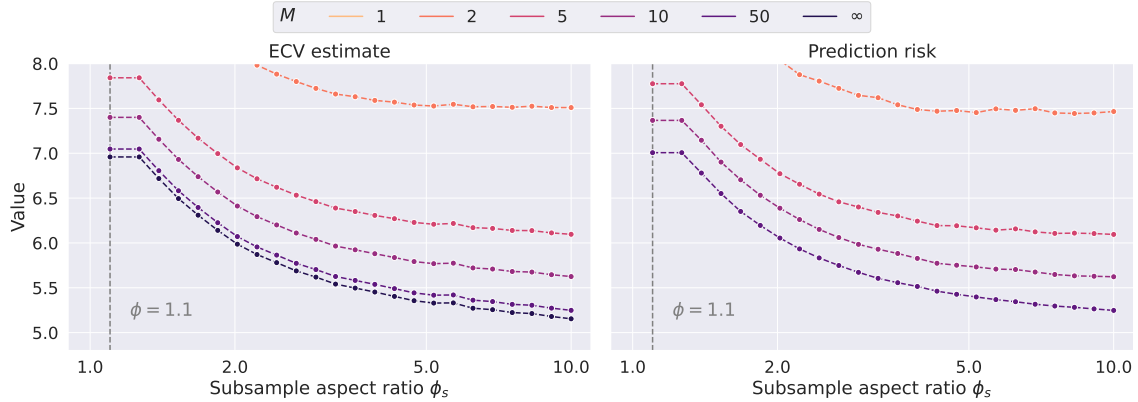


Figure S20: Finite-sample ECV estimate (left panel) and prediction risk (right panel) for lassless predictors ($\lambda = 0$), under model (M-ISO-LI) when $\rho^2 = 1$ and $\sigma^2 = 0.25$ for varying bag size $k = \lfloor p/\phi_s \rfloor$, and number of bags M . For each value of M , the points denote the finite-sample ECV cross-validation estimates (3.4) computed on $M_0 = 10$ bags or the out-of-sample prediction error computed on $n_{te} = 1,000$ samples, averaged over 100 dataset repetitions, with $n = 1,000$ and $p = \lfloor n\phi \rfloor$, and $\phi = 1.1$ ($p > n$).

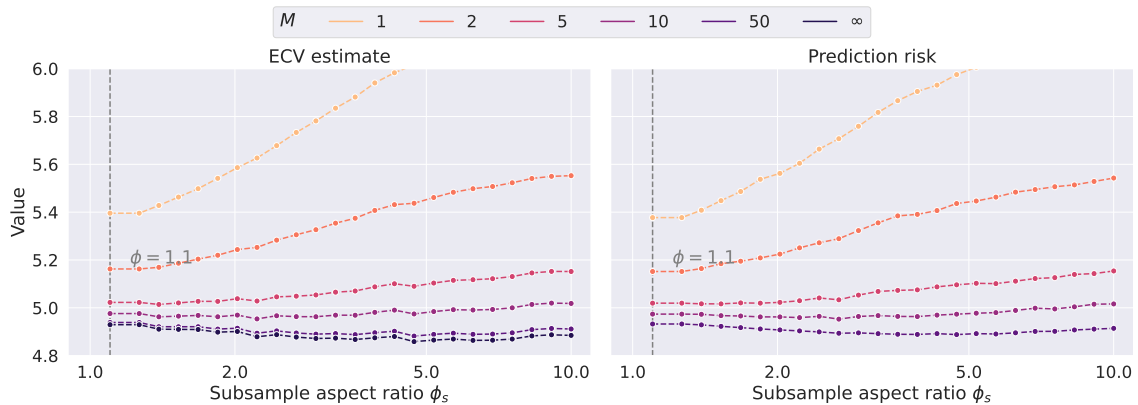


Figure S21: Finite-sample ECV estimate (left panel) and prediction risk (right panel) for lasso predictors ($\lambda = 0.1$), under model (M-ISO-LI) when $\rho^2 = 1$ and $\sigma^2 = 0.25$ for varying bag size $k = \lfloor p/\phi_s \rfloor$, and number of bags M . For each value of M , the points denote the finite-sample ECV cross-validation estimates (3.4) computed on $M_0 = 10$ bags or the out-of-sample prediction error computed on $n_{te} = 1,000$ samples, averaged over 100 dataset repetitions, with $n = 1,000$ and $p = \lfloor n\phi \rfloor$, and $\phi = 1.1$ ($p > n$).

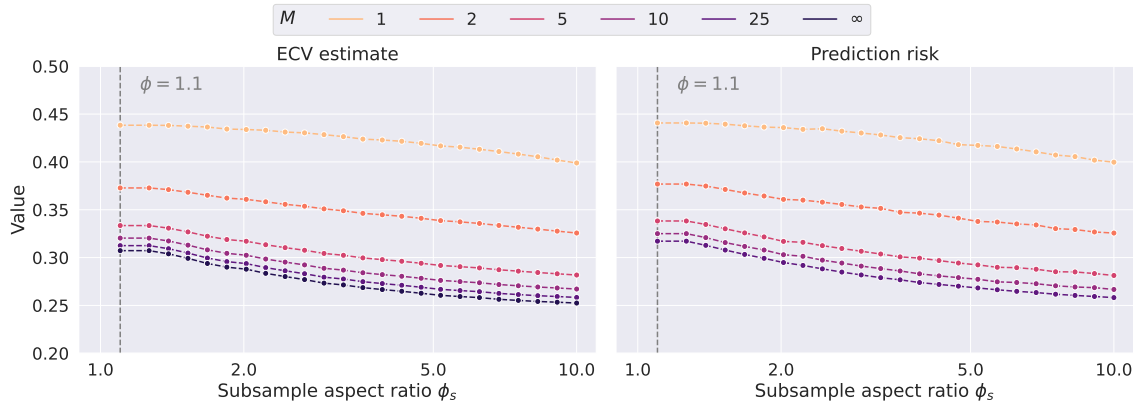


Figure S22: Finite-sample ECV estimate (left panel) and prediction risk (right panel) for Logistic predictors, under model (M-ISO-LI) when $\rho^2 = 1$ and $\sigma^2 = 0.25$ for varying bag size $k = \lfloor p/\phi_s \rfloor$, and number of bags M . For each value of M , the points denote the finite-sample ECV cross-validation estimates (3.4) computed on $M_0 = 10$ bags or the out-of-sample prediction error computed on $n_{te} = 1,000$ samples, averaged over 100 dataset repetitions, with $n = 1,000$ and $p = \lfloor n\phi \rfloor$, and $\phi = 1.1$ ($p > n$).

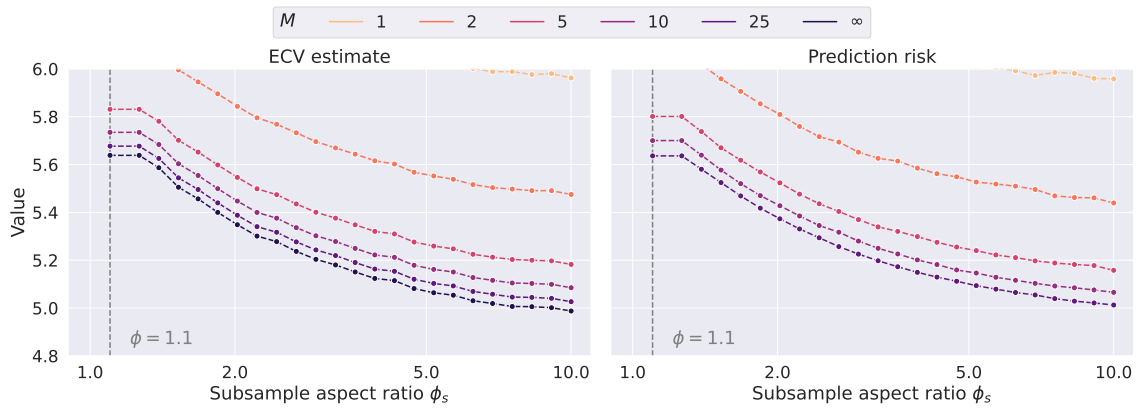


Figure S23: Finite-sample ECV estimate (left panel) and prediction risk (right panel) for k-nearest neighbors predictors, under model (M-ISO-LI) when $\rho^2 = 1$ and $\sigma^2 = 0.25$ for varying bag size $k = \lfloor p/\phi_s \rfloor$, and the number of bags M . For each value of M , the points denote the finite-sample ECV cross-validation estimates (3.4) computed on $M_0 = 10$ bags or the out-of-sample prediction error computed on $n_{te} = 1,000$ samples, averaged over 100 dataset repetitions, with $n = 1,000$ and $p = \lfloor n\phi \rfloor$, and $\phi = 1.1$ ($p > n$).

S5.2 Tuning ensemble and subsample sizes in Section 5.2

Subbagging

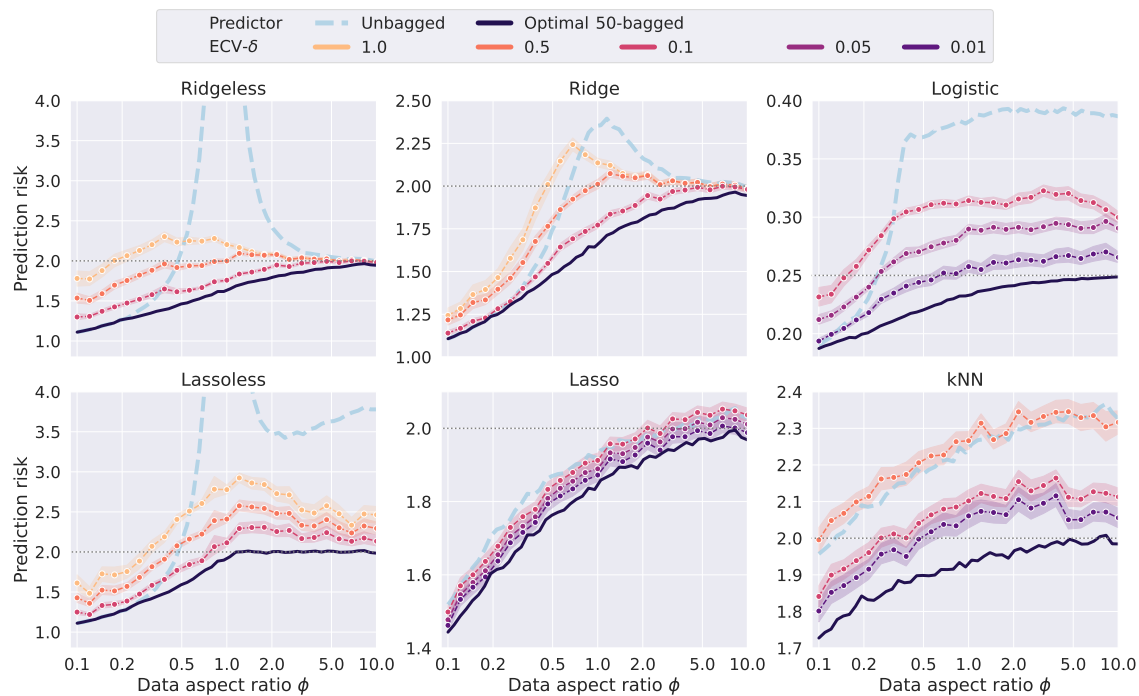


Figure S24: Prediction risk for different bagged predictors by ECV, under model (M-ISO-LI) with $\sigma^2 = 1$, $\rho^2 = 1$, $M_0 = 10$, and $M_{\max} = 50$, for varying data aspect ratio ϕ and tolerance threshold δ . The null risks and the risks for the unbagged predictors are marked as dotted lines and dashed lines, respectively. The points denote finite-sample risks averaged over 100 dataset repetitions and the shaded regions denote the values within one standard deviation, with $n = 1,000$ and $p = \lfloor n\phi \rfloor$.

Bagging

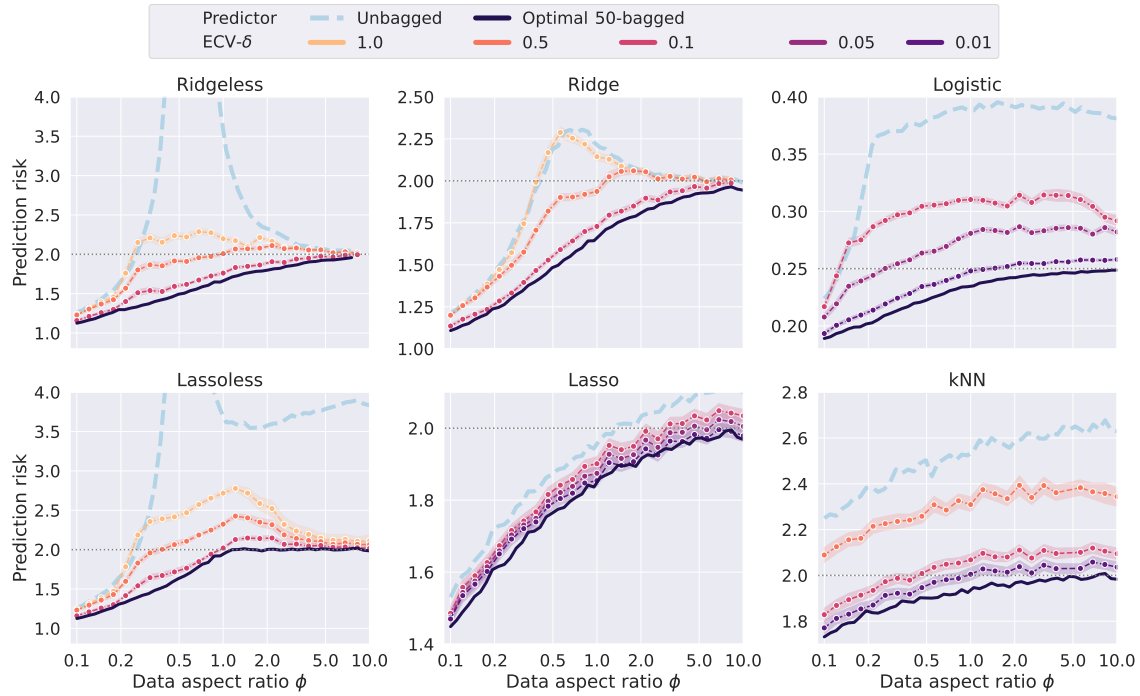


Figure S25: Prediction risk for different bagged predictors by ECV, under model (M-ISO-LI) with $\sigma^2 = 1$, $\rho^2 = 1$, $M_0 = 10$, and $M_{\max} = 50$, for varying data aspect ratio ϕ and tolerance threshold δ . An ensemble is fitted when (4.4) in Section 4.2 is satisfied with $\zeta = 5$. The null risks and the risks for the non-ensemble predictors are marked as gray dotted lines and blue dashed lines, respectively. The points denote finite-sample risks averaged over 100 dataset repetitions, and the shaded regions denote the values within one standard deviation, with $n = 1,000$ and $p = \lfloor n\phi \rfloor$.

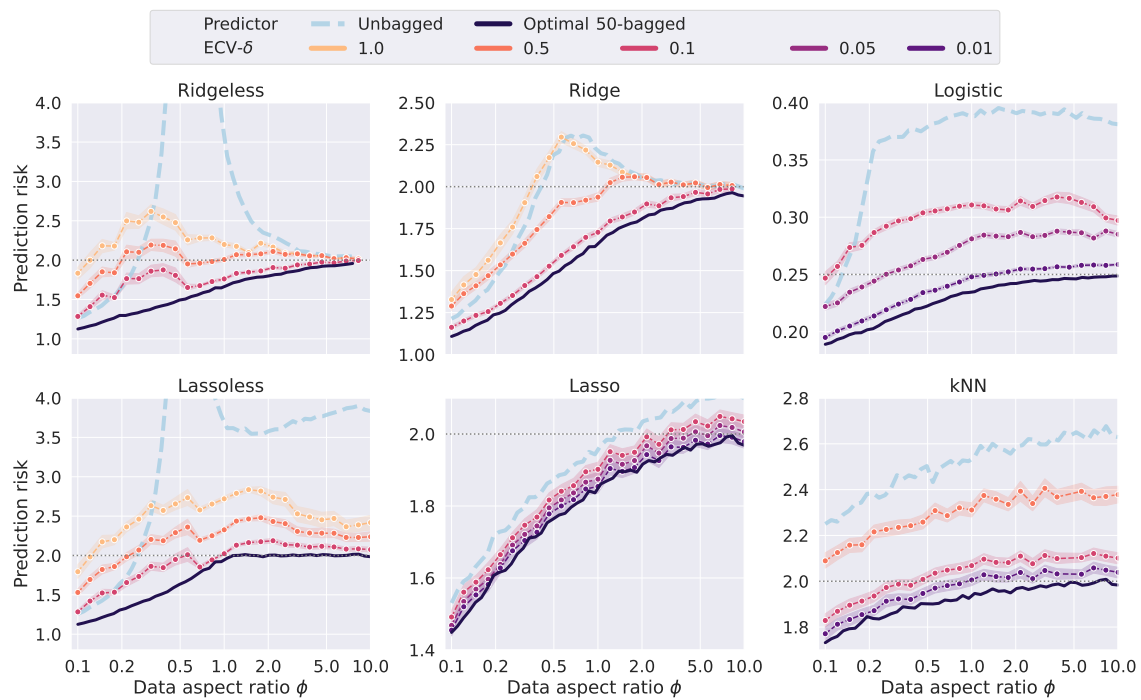


Figure S26: Prediction risk for different bagged predictors by ECV, under model (M-ISO-LI) with $\sigma^2 = 1$, $\rho^2 = 1$, $M_0 = 10$, and $M_{\max} = 50$, for varying data aspect ratio ϕ and tolerance threshold δ . The null risks and the risks for the non-ensemble predictors are marked as gray dotted lines and blue dashed lines, respectively. The points denote finite-sample risks averaged over 100 dataset repetitions, and the shaded regions denote the values within one standard deviation, with $n = 1,000$ and $p = \lfloor n\phi \rfloor$.

S5.3 Risk extrapolation in Section 5.3 (bagging)

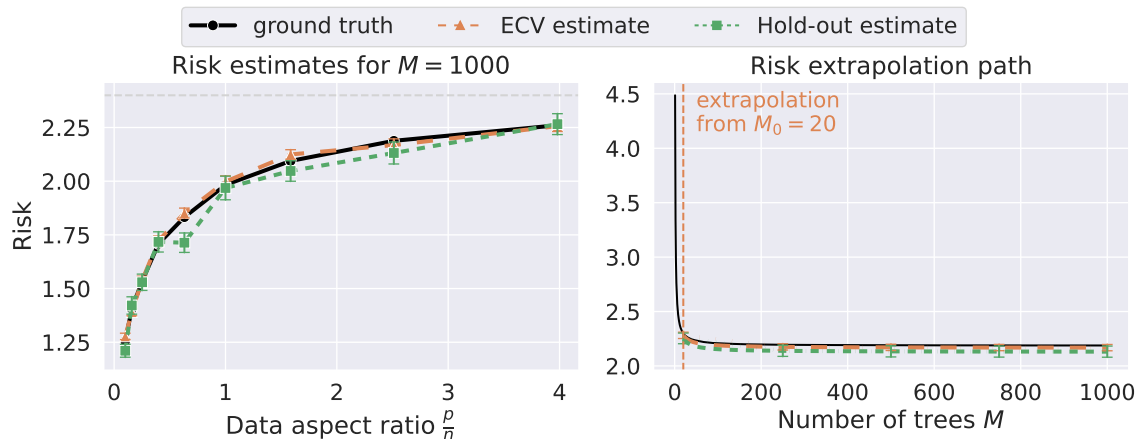


Figure S27: Risk extrapolation for random forest based on the first $M_0 = 20$ trees, under model (M-AR1-LI) with $\sigma^2 = 1$ and $\rho_{\text{ar1}} = 0.75$. The left panel shows the risk estimates for random forests with $M = 1,000$ trees and varying data aspect ratios, and the gray dash line $y = 2.4$ denotes the risk of the null predictor; the right panel shows the full risk extrapolation path in M when $p/n = 4$. The error bar denotes one standard deviation across 100 simulations, and the ground truth is estimated from 5,000 test observations, with $n = 1,000$.

S5.4 Risk profile in Section 6

Hao et al. (2021) collected samples of 50,781 human peripheral blood mononuclear cells (PBMCs) originating from eight volunteers post-vaccination (day 3) of an HIV vaccine. This single-cell CITE-seq dataset simultaneously measures 20,729 genes and 228 proteins in individual cells. As most genes are not variable across the dataset, we further subset the top 5,000 highly variable genes that exhibit high cell-to-cell variation in the dataset and the top 50 highly abundant surface proteins. Then the genes and proteins are size-normalized to have total counts 10^4 and log-normalized. In Figure S28, we visualize the low-dimensional cell embeddings as well as the histograms of gene expressions and protein abundances in the Mono cell type. Overall, the gene expressions are extraordinarily sparse and zero-inflated distributed. On the contrary, the distribution of protein abundances is close to normal distributions. As there is the most outstanding level of heterogeneity within T cell subsets, we only consider the non-T cell types for the experiments and randomly split cells in each cell type into the training and test sets with equal probability. Different cell types consist of different numbers of cells and have various data aspect ratios. As summarized in Table S2, the four cell types cover both low-dimensional ($n > p$) and high-dimensional ($n < p$) datasets. Because the gene expressions exhibit high dimensionality, sparsity, and heterogeneity, predicting the protein abundances based on the transcriptome is thus a challenging problem.

To illustrate our proposed method, we visualize the prediction risk estimate and out-of-sample error for surface protein CD103 in fig. S29. Because the response is centered, the empirical variance of the response serves as an estimate of the null risk, i.e., the risk of the null predictor that always outputs zeros. A value of NMSE less than one indicates that the predictor performs better than the null risk. From fig. S29, we see that the ECV extrapolated estimates in the left panel are largely consistent with the actual prediction errors in the right panel. Specifically, the risk can be more sizable than the null risk if the ensemble size is small or if we do not use ensemble learning (fig. S30). The out-of-sample error can still be considerable when $M = 10$ as shown in fig. S29. As the ensemble size M increases, both become more stable for various subsample sizes. Further, we observe that the tuned ensemble and subsample sizes are close to the optimal ones on the test dataset in finite samples. The tune subsample size k is much smaller than the total sample size n . This indicates that our proposed method tracks the out-of-sample optimal parameter well.

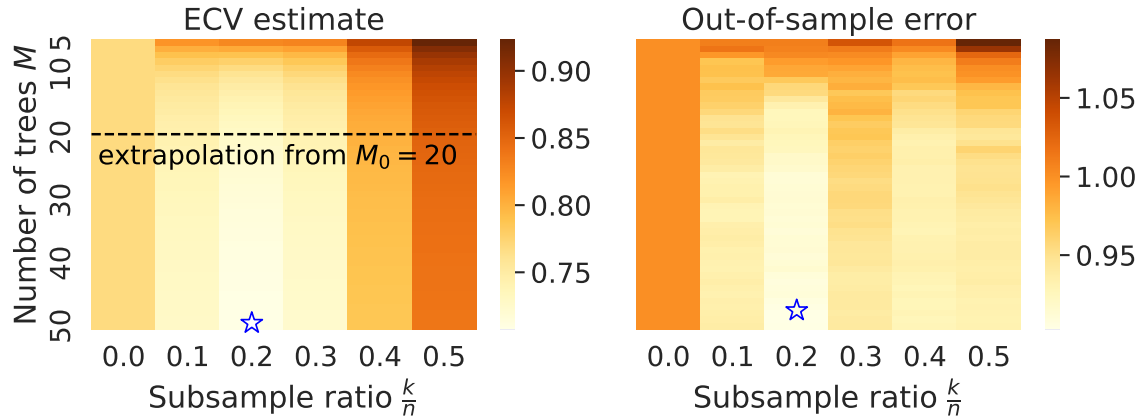


Figure S29: Heatmap of ECV performance on predicting the abundances of surface protein CD103 in the DC cell type by random forests (subbagging). The left and right panels show the NMSEs of OOB risk estimates and out-of-sample prediction risk, respectively. The values are normalized by the empirical variance of the response estimated from the test set; the darker, the larger the value of NMSE. The extrapolated risk estimates are based on $M_0 = 20$ trees.

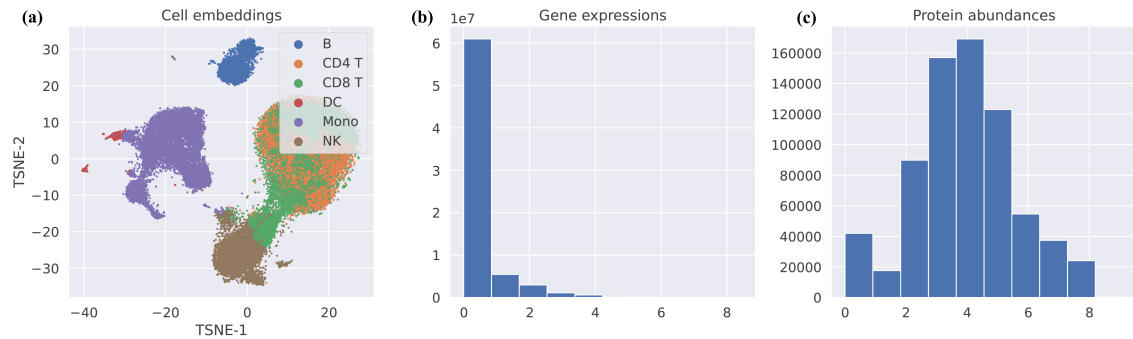


Figure S28: Overview of the single-cell CITE-seq dataset from Hao et al. (2021). (a) The 2-dimensional tSNE cell embeddings. (b-c) The histogram of overall log-normalized gene expressions and protein abundances in the Mono cell type.

Table S2: Description of different cell types in the CITE-seq dataset (Hao et al., 2021). The samples of PBMCs originate from eight volunteers post-vaccination (day 3) of an HIV vaccine

Cell type	Training size n	Test size n_{te}	Data aspect ratio p/n
DC	516	515	9.71
B	2279	2279	2.19
NK	3152	3152	1.59
Mono	7156	7156	0.70

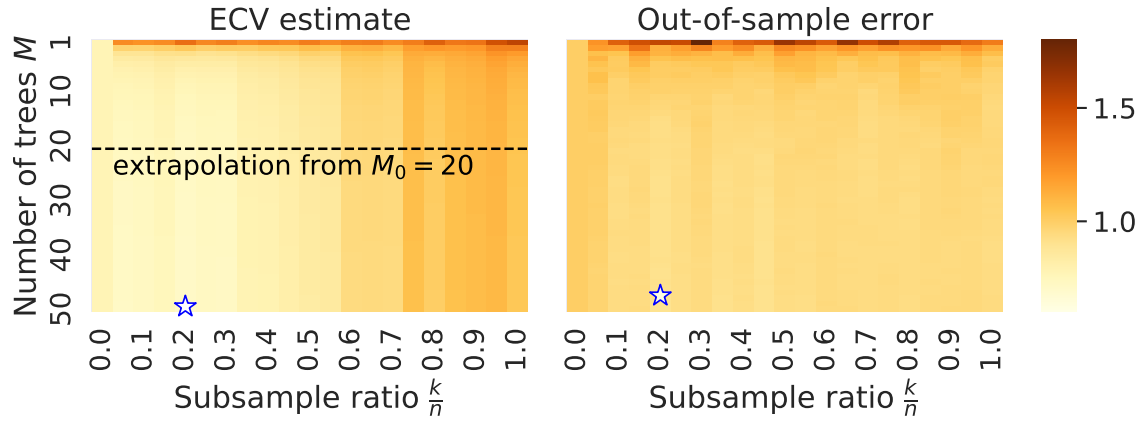


Figure S30: Heatmap of ECV performance on predicting the abundances of surface protein CD103 in the DC cell type by random forests (subbagging) as in fig. S29 with $M \in \{1, \dots, 50\}$ and p/k ranging from 0 to 1 displayed.

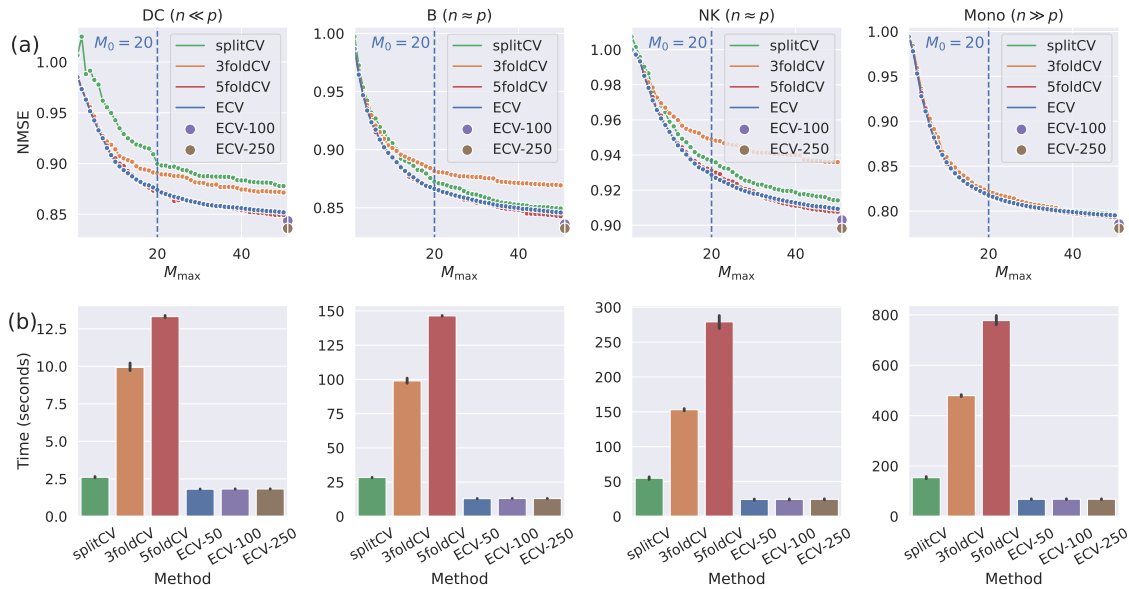


Figure S31: Performance of cross-validation methods on predicting the protein abundances in different cell types. (a) The average normalized mean squared error (NMSE) of the cross-validated predictors for different methods. ECV (bagging) uses $M_0 = 20$ trees to extrapolate risk estimates, and the dashed lines represent the performance using $M_{\max} \in \{100, 250\}$. (b) The average time consumption for cross-validation in seconds.